Helena Catarina Teixeira Meireles

Refining thymic epithelial cell differentiation: from progenitor cell isolation to the identification of discrete mature lineages

Tese de Candidatura ao grau de Doutor em Biologia Molecular e Celular submetida ao Instituto de Ciências Biomédicas Abel Salazar da Universidade do Porto.

Orientador – Doutor Nuno Miguel de Oliveira Lages Alves

Categoria – Investigador Principal

Afiliação – Instituto de Investigação e Inovação em Saúde (i3S); Instituto de Biologia Molecular e Celular (IBMC)

Coorientador – Prof. Doutor Manuel João Rua Vilanova

Categoria – Professor Associado

Afiliação – Instituto de Ciências Biomédicas Abel Salazar da Universidade do Porto; Instituto de Investigação e Inovação em Saúde, Universidade do Porto e Instituto de Biologia Molecular e Celular, Universidade do Porto

De acordo com o disposto no Decreto Lei no 74/2006 de 24 de Março, esclarece-se ser da nossa responsabilidade a execução das experiências que estiveram na origem dos resultados apresentados, assim como a sua interpretação, discussão e redacção.

Nesta tese foram utilizados os resultados dos artigos publicados ou submetidos para publicação abaixo indicados:

Ribeiro AR, Meireles C, Rodrigues PM and Alves NL, *The intermediate expression of CCRL1 reveals novel subpopulations of medullary thymic epithelial cells that emerge in the postnatal thymus*. European Journal of Immunology, 2014. 44(10):2918-2924.

Meireles C, Ribeiro AR, Pinto RD, Leitão C, Rodrigues PM, Alves NL, *Thymic crosstalk restrains the pool of cortical thymic epithelial cells with progenitor properties.* European Journal of Immunology, 2017. 47(6):958-969

ACKNOWLEDGMENTS

The work presented here represents the culmination of a long path during which I had the opportunity and the pleasure to contact and meet several people who have helped me to progress and develop my abilities. Thus, I have to thank:

First of all, to my supervisor Nuno Alves, to give me this opportunity and to believe on me to achieve this purpose. I learnt so much with you and all this thesis and the current achievements were not possible without all your help. Thank you so much for everything!

To the people directly involved in this work: Ana Rosalina Ribeiro for all the knowledge that you shared with me and the friendship in and outside of the lab (an huge thanks); to Pedro Mendes Rodrigues; Rute Pinto; Leonor Araújo; my dearest Chiara and Gema (friends in and out of the institute); and also, to the recent expanded team: Pedro Ferreirinha (also known as: Avô or Ferreiripedia), Laura and Camila.

This work was not possible without the IBMC/I3S platforms. A special thanks to Catarina Leitão (Translational Cytometry platform) for all the scientific help and to listen all my silly stories. I would like to thank all the people from the Animal Facility (specially Sofia Lamas). To Paula Sampaio (Advance Light Microscopy platform) and André Maia (Biosciences Screening platform), thanks for all the technical help.

To the people from CAGE, headed by Alexandre do Carmo, for homing us in their lab. CAGE was a place of lot of conversations and laughs that I won't forget. Special thanks to Liliana ("**A** post-doc") and Rita ("uma força da natureza").

To Emília Cardoso for all the help and long talks in our TraCy rooms.

To my friends outside the lab, gigantic thanks! You cannot imagine how lucky I feel to have all of you in my life. To Pedro (Tarza), Lenita, Anita (Ferrão), Ghafa, Sófia, Dário, Tiago (Tweety) and Carvalhal. Thanks for all the walks, dinners, nights out, road trips and conversations.

To Diogo Tildes for having been on my side in such struggling moments during this path. Our trips and music chats were crucial to keep my sanity.

To Pedro Sousa, my Rock'n Roll live concerts partner, for all the chats and music sharing.

To my favorite bass guitar professors: Bruno Macedo, Carl Minneman and João Paulo Rosado for the all the music and private conversations.

À Tamara e à Glória por toda a ajuda e conselhos preciosos.

Aos meus companheiros, Lupi e Rita!

Por ultimo, mas nada menos importante, à minha família: Mãe, Pai, Sandra, Pedro e Agostinho. Obrigada por todo o apoio, não só por este momento da minha vida, mas por todos os passos que dei. Vocês são o meu pilar e as pessoas mais importante na minha vida. Nunca haverão palavras suficientes para vos agradecer.

Apesar de ser uma tagarela, é nestas alturas que me faltam as palavras. Obrigada por estarem presentes em momentos importantes e também nos que não parecem relevantes, mas que são tão precisos. Obrigada por tudo!

"You can't always get what you want. But if you try sometimes, you just might find you get what you need!"
Rolling Stones

TABLE OF CONTENTS

ABSTRACT

Thymic epithelial cells (TECs) provide crucial instructive signals for T cell differentiation. TECs are subdivided into functionally distinct cortical (cTECs) and medullary (mTECs) specialized microenvironments and its appropriate development is essential for the selection of a diverse and self-tolerant T cell pool. Importantly, cTEC and mTEC microenvironments derive from common bipotent TEC progenitors (TEPs) that emerge during early thymic organogenesis and persists during postnatal life. However, the nature and maintenance of TEPs, as well as the cellular and molecular mechanisms underlying TEC differentiation pathways downstream of TEPs are still poorly understood.

In this thesis, taking advantage of CCRL1-reporter mice, we unravel a novel mTEC subset that appears specifically in the postnatal thymus and shares cTEC traits, suggesting that mTEC differentiation might follow distinct routes in embryonic and postnatal thymus. Moreover, we show that purified CCRL1^{+}-cTEC are able to generate both cTEC and mTEC, indicating that the cortical compartment harbors a pool of TEC progenitors. To test this possibility, we employ TEC clonogenic assays as a tool to monitor TEP activity. We describe that a fraction of cTECs generates specialized clonal-derived colonies, which contain cells with continual colony-forming potential (*Clono*TECs). *Clono*TECs present evidence of bipotent capacity upon integration within thymic microenvironments, as shown by their capacity to form TECs with cortical and medullary properties *in vivo.* Strikingly, we document that the abundance cTEC with clonogenic potential decrease with age as a result of continual interactions between TEC and developing thymocytes across life.

Altogether, our results indicate that a specialized TEP subset reside within the cortical compartment in the postnatal thymus and its bioavailability declines throughout life. Understanding the mechanisms that balance the maintenance of TEPs across life and their differentiation into cTEC/mTEC lineages is of great value to design strategies aimed to repair or regenerate thymus function through TEC therapy.

RESUMO

As células epiteliais do timo (TECs) providenciam sinais instrutivos para a diferenciação das células T. As TECs subdividem-se em microambientes especializados, cortical (cTEC) e medula (mTEC), e o seu desenvolvimento apropriado é essencial para a seleção de uma população diversa e auto-tolerante de células T. As cTEC e as mTEC derivam de um progenitor de TECs (TEP) bipotente comum que surge cedo na organogénese tímica e persistem durante a vida pós-natal. No entanto, a identidade e a manutenção das TEPs, bem como os mecanismos celulares e moleculares subjacentes às vias de diferenciação TEC a jusante doa TEPs ainda são mal compreendidos.

Nesta tese, utilizando o modelo de ratinho repórter para CCRL1, descobrimos um novo subpopulação de mTEC que aparece especificamente no timo pós-natal e compartilha características de cTEC, sugerindo que a diferenciação de mTEC pode seguir percursos distintos no timo embrionário e pós-natal. Adicionalmente, nós mostramos que células cTEC-CCRL1^{+} isoladas são capazes de gerar cTEC e mTEC, indicando que o compartimento cortical alberga um grupo de progenitores TEC. Para testar esta hipótese, usamos ensaios clonogênicos com TECs como uma ferramenta para monitorizar a atividade das TEPs. Dessa forma, descrevemos que uma fração de cTECs gera colônias especializadas derivadas de clones contendo células com potencial contínuo de formação de colônias (*Clono*TECs). As *Clono*TECs apresentam evidências de capacidade bipotente após a integração em microambientes tímicos, demonstrando capacidade de formar TECs com propriedades corticais e medulares in vivo. Surpreendentemente, comprovamos que a abundância de cTEC com potencial clonogênico diminui com a idade como resultado de interações contínuas entre TEC e timócitos em desenvolvimento ao longo da vida.

Em suma, os nossos resultados indicam que um subconjunto TEPs especializados residem no compartimento cortical do timo pós-natal e sua biodisponibilidade diminui ao longo da vida. A compreensão dos mecanismos que equilibram a manutenção das TEPs durante a vida e a sua diferenciação em linhagens cTEC / mTEC é de grande valor para delinear estratégias destinadas a reparar ou regenerar a função do timo através de terapia com TEC.

LIST OF ABBREVIATIONS

β5t – Proteasome subunit β5t

γc – common cytokine receptor gamma chain family

Aire – Autoimmune Regulator

APC – Antigen Presenting Cell

BAC – Bacterial Artificial Chromossome

CCL – CC-motif chemokine ligand

CCR – CC-motif chemokine receptor

CCRL – CC-motif chemokine receptor ligand

CD – cluster of differentiation

Cld - Claudin CMJ – Cortico-Medullary Junction

cTEC – Cortical Thymic Epithelial Cell

CTSL – Cathepsin L

CTSS – Cathepsin S

CXCL – C-XC-motif chemokine ligand

DC – Dendritic cell

dGuo - 2-deoxyguanosine

DLL4 – Delta-like Ligand 4

DN – Double Negative

DP – Double Positive

E – Embryonic day

EGF – Epidermal Growth Factor

EpCAM – Epithelial Cell Adhesion Molecule

Fezf2 – FEZ family Zink Finger 2 FGF – Fibroblast Growth Factor

Foxn1 – Forkhead box protein N1

FTOC – Fetal Thymic Organ Culture

GFP – Green Fluorescent Protein

HSC – Hematopoietic Stem Cell

HSCT – Hematopoietic Stem Cell Transplantation

IL – Interleukin

LTβR – Lymphotoxin β Receptor

Lti – Lymphoid Tissue Inducer

MHC – Major Histocompatibility Complex

mTEC – Medullary Thymic Epithelial Cell

MTS – Mouse Thymic Stromal

Nb - Newborn

NCC – Neural Crest Cell

NK – Natural Killer

OPG – Osteoprotegerin

PDPN – Podoplanin

Plet-1 – Placenta Expressed Transcript 1

RAG – Recombination-activating Genes

RANK – Receptor Activator of NF-κB

RANKL – Receptor Activator of NF-κB Ligand

RFP – Red Fluorescent Protein

RTOC – Reaggregate Thymic Organ Culture

Sema3E – Semaphorin

SP – Single Positive

SSEA-1 – Stage-specific Embryonic Antigen 1

TCR – T cell receptor

TEC – Thymic Epithelial Cell

TEP – Thymic Epithelial Progenitor

Tg - Transgenic

TNFRSF – Tumour Necrosis Factor Receptor Superfamily

TRA – Tissue-restricted Antigen

TRAF6 – Tumour Necrosis Factor Receptor Activator Factor 6

Treg – Regulatory T cell

TSSP – Thymus-specific serine protease

UEA-1 – Ulex Europaeus Agglutinin 1

YFP – Yellow Fluorescent Protein

INTRODUCTION

The immune system evolved to detect and respond to a wide variety of pathogens, such as bacteria, parasites and virus, while distinguishing them from the host own tissues. In this way, the immune system can activate protective responses to infections, suppress the development of spontaneous malignancies and avoid autoimmunity. Although classically divided in innate and adaptive immune system, these two arms actively collaborate during the course of immune responses. While the innate immunity represents the first line of protection, the adaptive immune system relies on highly specialized T and B cells that respond specifically to pathogen-derived antigens and confer long-term memory to those previously exposed infectious agents [1].

Accordingly, when pathogens invade our physical barriers, such the skin, microbe-derived conserved structures are initially recognized by cells of innate immune system through pattern-recognition receptors (PRRs), which detect pathogen-associated molecular patterns (PAMPs), such as bacterial and fungal cell-wall components or viral nucleic acids [2]. Recognition of PAMPs by PRRs leads to the induction of inflammatory responses and other innate host defenses such the activation of proteins of the complement system, maturation of professional phagocytes, or the activation of natural killer (NK) cells [1]. On the other hand, adaptive immune responses have evolved to permit the ability to recognize more specific and unique components of different pathogens (antigens), through the participation of responses coordinated by B and T cells. Despite their common origin, B and T cells develop and mature in distinct specialized lymphoid tissues, known as primary lymphoid organs. While B cells typically develop in the bone marrow (BM), T cells arise also from BM hematopoietic precursors but complete their development in the thymus [3]. This thesis is dedicated to the study of the thymus and I will discuss in the following sections the principles and actors that regulate the function of this specialized organ.

The thymus represents a critical component of the adaptive immune system, as an exclusive site for differentiation and selection of T cells, prior to their export into the systemic circulation and colonization of peripheral lymphoid organs. T cells express a unique membrane-bound antigen-recognizing T cell receptor (TCR), which typically

recognizes peptides presented in the context of major histocompatibility complex (MHC) molecule on the surface of antigen-presenting cell (APC). Once T cells complete their development in the thymus, naïve T cells start to patrol the secondary lymphoid organs waiting for the moment they become activated upon recognition of their cognate antigen in the context of MHC molecules and in presence of co-stimulatory signals expressed by APCs. Upon activation, T cells proliferate and acquire the potential to differentiate into distinct multifunctional effector cells. Interestingly, the basic roles that coordinate T cell immune responses are established during early stages of T cell development in the thymus.

In the following sections, I will cover the development and function of the thymus. In particular, I will detail how this organ provides the essential microenvironments for the generation of T cells. I will discuss with special interest the development and function of thymic epithelial cells (TECs), which comprise a population of resident thymic stromal cells with a non-redundant role in T cell development. I will further describe how TECs differentiate from their progenitors into fully functional cortical (cTEC) and medullary (mTEC) subsets and detail the specific roles of these subsets in coordinating different stages of T cell development and selection.

The importance of the thymus in the establishment of T cell responses

The thymus is a bilobed primary lymphoid organ located in the anterior mediastinum and its sole function is to support the differentiation and selection of T cells [4]. The immunological role of the thymus was only recognized in 1961, through the analysis of thymectomized young mice. Those studies revealed that thymectomy during neonatal life caused deficiency of lymphocytes in blood and lymphoid tissues and subsequent liver lesions such hepatitis virus infection. Additionally, those mice failed to reject engraftments of skin from other mice [5, 6].

The development of T cells within the thymus is a sequential process that requires the entry of BM-derived hematopoietic progenitors into the thymus, their commitment into

developing T cells, also known as thymocytes, and their migration within distinct thymic microenvironments, prior to the egress of T cells into the circulation [4]. Importantly, intrathymic T cell development is not a cell-autonomous process, as developing T cell precursors requiring a constant input from cells that make up thymic microenvironments. For this purpose, the stromal component of the thymus provides a highly specialized matrix that permits the development of T cells from BM-derived hematopoietic stem cells (HSC). The thymic stroma creates an organized three-dimensional cellular network, mainly composed of TECs, but includes also mesenchymal and endothelial cells, and other APCs such as macrophages and dendritic cells (DCs) [4, 7] (**Figure 1A**).

TECs are subdivided into two major compartments, cortex and medulla, which are anatomically, phenotypically and functionally distinct between each other (**Figure 1A**). While cTECs occupied the outer cortex of the thymus, mTECs reside in inner medullary areas, being this spatial organization more notorious in the postnatal and adult thymus. This thymic architecture defines the division of labour of the TEC lineages in thymopoiesis. While cTECs supports early stages of T cell differentiation, including the commitment of HSCs into T cell lineage and positive selection [4, 8, 9], mTECs control later stages of thymopoiesis that are important in the induction of T cell tolerance, including negative selection (also known as clonal deletion) of potentially harmful autoreactive T cells and/or their deviation into natural regulatory T (nTreg) cells. [4, 10-13].

The production of T cells by the thymus is not constant during life. In mice, thymic function reaches its peak of activity during adolescence, declines gradually during adulthood and becomes marginal in the elderly, a process known as thymic involution [14]. Thus, under physiological conditions, thymic involution represents a premature hallmark of aging in vertebrates and affects both thymocytes and TECs [15]. Specifically, TEC cellularity and cTEC/mTEC ratio decrease with age, with a loss of the compartmentalization between cortical and medullary areas [16, 17]. These alterations are associated with less efficient T cell production, leading to a decrease emigration of

naïve T cells to the periphery [14]. While of minimal consequences in healthy individuals, the degeneration of thymic activity restricts the immune recovery of patients undergoing hematopoietic stem cell transplantation (HSCT) to treat congenital immune deficiencies or malignancies [18], and is linked to their increased susceptibility to opportunistic infections and autoimmunity [14]. Thus, the study of TEC biology is of fundamental and clinical importance to develop strategies to repair and regenerate thymic activity, with the aim to physiologically restore the numbers and function of T lymphocytes in the periphery.

The entry of BM-derived early thymic T cell progenitors (ETPs) in the thymus is suggested to be an intermittent process, occurring in waves of colonization [19]. The first seeding of HSC precursors occurs in mice between embryonic day (E) 10.5 and E12.5, prior to the vascularization of the thymic primordium, through interaction of ETPs with the surrounding mesenchymal layer [20, 21]. Subsequent wave of fetal ETP seed the thymus through the vascularization, and continues to do so throughout life [22]. In the postnatal thymus, ETPs enter the thymus via endothelial vessels, which are strategically located in the cortico-medullary junction (CMJ). At this early stages, ETPs are multipotent in the sense that they still have the potential to differentiate into other non-T cell lineages, such as myeloid, NK and B cells [4]. Once the ETPs commit to the T cell lineage in the cortex, these precursors undergo distinct stages of maturation as they migrate from the CMJ to the subcapsular cortex, and then through the cortex back to the medulla, before exiting as mature T cells into the peripheral circulation through blood vessels located at CMJ/medulla (**Figure 1B**).

The majority of T cells in circulation are $CD4^+$ or $CD8^+$ αβ T cells, but in addition to those, there are other “non-conventional” T cells, such γδ T and NKT cells, which are also of thymic origin but develop through alternative differentiation programs not extensively detailed in this thesis (**Figure 1B**). Briefly, NKT cells share with NK cells some properties of cells of the innate immune system, although expressing invariant αβ TCRs. However, in contrast to the αβ “conventional” T cells, which have a diverse TCR repertoire, the repertoire of NKT receptors is limited. In addition, the TCR of NKT cells recognize lipid antigens presented by non-classical MHC class I molecules CD1d, instead of peptides presented by MHC class I or II molecules [23]. Like NKT cells, γδ T cells are also located

in the interface of innate and adaptive immunity and arise from T cell progenitors that differentiate into this lineage early during T cell development. The antigenic molecules that select them remain largely unknown, and they do not seem to require MHC presentation of peptide antigens. Although of rare abundance in the thymus, they are abundant in other peripheral sites, such as the gut mucosa wherein they play important role of defense [24]. In the subsequent sections of this introduction, I will focus in discussing the role of TECs during αβ T cell development, which represents the dominant T cell differentiation pathway in the thymus.

The time between the entry of a T cell progenitor into the thymus and egress of its mature T cell progeny is estimated to take around 3 weeks in the mouse [25]. During this period, thymocytes interact with distinct populations of thymic stroma [26]. In particular, the development of mature T cells within the thymus is dependent of intact cortical and medullary microenvironments. In turn, the establishment of thymic microenvironments is reciprocally reliant on thymocytes to maintain their integrity [27], a phenomenon designated as “thymic crosstalk”. In this context, TECs play a non-redundant role expressing a series of cell surface ligands and providing chemokines and cytokines essential to guide the differentiation, selection and migration of developing T cells, which express the receptors for those microenvironmental cues [4].

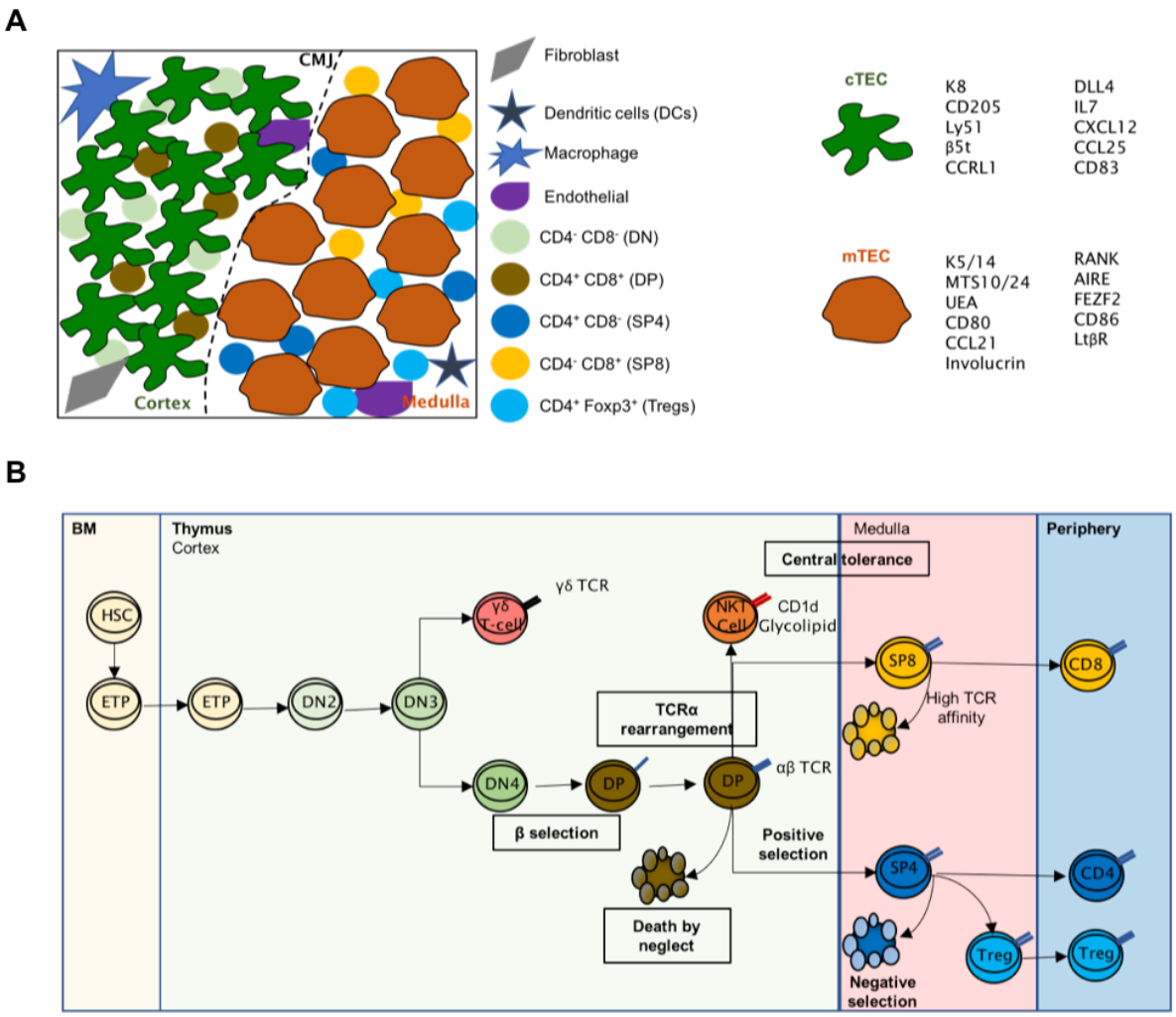

Figure 1 – An overall view of TEC anatomical compartmentalization and detailed T cell developmental stages taking place within distinct thymic microenvironments. **A)** Schematic illustration of postnatal cellular composition of the postnatal thymus with the representation of distinct hematopoietic (DNs, DPs, SPs, DCs and macrophages) and non-hematopoietic (TECs, fibroblasts and endothelial) cells. The thymic organization of these different subsets between the cortical and medullary areas, displays the requirement for specialized intrathymic microenvironments that support the step-wise development of T cells. The phenotypic characteristics of cTECs and mTECs are indicated on the right. Adapted from [28]. **B)** An overview of thymocyte developmental stages. The BM-derived hematopoietic stem cells (HSCs) give rise to early T cell progenitors (ETPs) that enter in the thymus and migrate to the cortical area. In this region, the ETPs are DNs without expressing the T cell receptor (TCR) or the co-receptors CD4 and CD8, and they start the rearrangement of TCR genes. Later, DP cells arise with expression of TCRβ and both CD4 and CD8 co-receptors and posterior rearrangement of TCR α-chain locus leads to expression of αβ TCR. At this stage, the DPs expressing a TCR that have intermediate affinity for self-peptide-MHC complexes are induced to survive and differentiate into single positive $CD4^+$

(SP4) or $CD8^+$ (SP8) cells, a process called positive selection. Positively selected SP thymocytes continue their migration into in the medulla, where they will predominantly interact with mTECs presenting an array of tissue restricted antigens. If the avidity of binding of the TCR expressed by thymocytes to MHC–peptide ligands presented by mTECs exceeds a certain threshold, the cells are deleted by negative selection or converted, in the case of CD4 T cells into $CD4^+Foxp3^+$ T regulatory cells (Tregs). After maturation, the thymocytes egress to periphery. Also, within the thymus, the γδ T cells are originated at the DN3 stage, from cells that have not undergone β-selection. The selection of natural killer T (NKT) cells is promoted by $CD1d^+$ DP thymocytes. Adapted from [29].

Cortical thymic microenvironment: A site for T cell lineage commitment and positive selection

The compartmentalization of TECs into cTEC and mTEC subsets starts concomitantly with thymic colonization by the first hematopoietic cells. Immature TEC expressing cortical-associated markers ($Ly51^+CD205^+β5t^+$) can be found in mice already at E12 of gestation in mice [30-33], suggesting that the commitment into cTEC lineage occurs early in thymus ontogeny. The ETPs start seeding the thymus already at E11.5 in mice and at 8-weeks of gestation in humans, and continued throughout adulthood [4] and are attracted into the thymus as a result of an interplay of receptor-ligands and a series of chemotactic factors produced by TECs, fibroblasts and thymic endothelial cells. For instance, intrathymic fibroblasts and endothelium express the FMS-like tyrosine kinase-3 (Flt3) ligand [34] and P-selectin [35] respectively, which interacting with Flt3 receptor and P-selectin ligand (PSGL-1) presented by ETPs, promote the homing of these cells to the thymus. On the other hand, TECs express chemokine CC ligand (CCL) 21, CCL25 and chemokine CXC ligand (CXCL) 12 that bind to CCR7, CCR9 and CXCR4 expressed on ETPs, mediating their entry to the thymus [36].

In the postnatal thymus, circulating ETPs migrate into the thymus through CMJ area. The ETPs proceed into T cell differentiation initially as double negative (DN) cells that lack CD4, CD8 and TCR. Cells at DN stage pass through 4 transitional stages of development (DN1-DN4) defined based on the combination of CD25 and CD44 surface markers. T cell-lineage commitment occurs at DN1-DN2 stage transition upon triggering

of Notch receptor in ETPs, mediated by the cTEC-derived Notch ligand Delta-like 4 (DLL4) [37-40]. Furthermore, during this early phase of T cell development, cTECs provide cytokines, such as interleukin-7 (IL-7), which are important for the survival and proliferation of DN thymocytes [41-43]. Subsequently, at DN2/3 stage, T cells begin activating recombination-activating genes (RAG) enzymes and undergo crucial rearrangements of TCRβ- (*Tcrb*) or γ- (*Tcrg*) and δ- (*Tcrd*) chain genes, based on DNA recombination of variable (V), diversity (D), and joining (J) gene segments, to initiate the process of generating TCR with diverse antigen-recognition potential [44]. (**Figure 1B**).

The commitment to αβ T cell lineage constitutes the major pathway of T cell differentiation. Therefore, for αβ T cell precursors, the β-selection checkpoint probes for successful in-frame TCRβ gene rearrangement. This requires signaling through a pre-TCR consisting of the product of a productive rearrangement of TCRβ gene, CD3 invariant chains and pre-Tα chain, assembling a pre-TCR complex [45]. This is followed by subsequent rearrangement of the TCR α-chain locus and the expression of a mature TCRαβ in DP thymocytes, which then audit for the ability of their TCR to recognize self-MHC molecules expressed by cTECs [46]. While the TCR of αβ T cells are selected by MHCI or MHCII molecules, the TCR of γδ T cells are not MHC-restricted [47]. At this stage, for αβ T cells development, cTECs play a key role during positive selection of thymocytes that express TCRs that bind with intermediate affinity for self-peptide-MHC complexes, inducing their differentiation into mature CD4 or CD8 single positive (SP) thymocytes [48]. In contrast, thymocytes expressing TCR without or low affinity for peptide–MHC complexes die by neglect. Although the process of lineage determination into CD4 and CD8 T cells is not yet fully understood, positively selected cells with TCRs with affinity to MHC class I molecules commit to CD8 lineage, retaining the expression of CD8 and losing the expression of CD4 (SP8), while cells expressing TCR that bind to MHC class II molecules commit to the CD4 lineage, through the retention of expression of CD4 molecule and down-regulation of CD8 co-receptor (SP4) [49]. Crucial to the function of cTECs during positive selection is their ability to express a unique set of selecting self-peptides generated by the particular action of several intracellular proteolytic enzymes. Among those, β5t (*Psmb11*) is a cTEC-restricted catalytic

proteasome subunit, which assembly to form the unique cTEC thymoimmunoproteasome; β5t is responsible for the production of specific MHCI-associated peptides that select SP8 [31, 50, 51]. Moreover, the thymus-specific serine protease (TSSP) (*Prss16*) and cathepsin L participate in the generation of peptides that contribute to positive selection of MHCII-restricted $CD4^+$ T cells [52-55].

The organization of thymic medulla and its role in T cell tolerance induction

Following positive selection, SP4 and SP8 cells migrate to the medulla to complete their final stages of differentiation by being exposed to a diverse set of self-antigens presented by mTECs and DCs. Positively selected thymocytes acquire the expression of CCR7, which makes them responsive to gradients of their ligands (CCL19 and CCL21) produced within the medulla by mTECs [56, 57]. Once in the medulla, thymocytes expressing TCRs that bind with high affinity to peptide-MHC complexes are eliminated by clonal deletion, a process also known as negative selection, to eliminate potential autoreactive T cells [30, 49]. Nevertheless, some developing SP4 thymocytes that have TCR specificities for self-antigens are rescued of clonal deletion and redirected into $CD4^+CD25^+FoxP3^+$ regulatory T cells (Tregs), which impose peripheral tolerance by regulating extrathymic immune responses [58-60]. These two processes, negative selection and Tregs differentiation, are critical for tolerance induction and depend on the coordinate action of mTECs and DCs [4, 30, 48] (**Figure 1B**).

To ensure the success of negative selection, mTECs express virtually all protein-coding genes of the genome, including tissue-restricted antigens (TRAs), through a promiscuous gene expression process that depends in part on autoimmune regulator (Aire) and the recently described FEZ family finger 2 (Fezf2) [61-63]. Consequently, the expression of proteins as Aire [62] and Fezf2 [63] is crucial for the transcriptional regulation of a large set of TRAs in mTECs and therefore for the establishment of self-tolerance [64]. Thus, the disruption of the medulla function, or mTECs impairing the migration of positive selected thymocytes, negative selection and Tregs differentiation, lead to defects in self-tolerance which often results in the development of autoimmunity

[49]. For example, genetic mutations that disrupt Aire function result in development of autoimmune-polyendocrinopathy-candidiasis-ectodermal dystrophy (APECED) syndrome in human [65, 66].

In this regard, important studies identified several molecules that mediate thymocyte-driven TEC differentiation, with the majority of them engaging the NF-kB signaling pathway in mTEC. As such, the NF-kB pathway is a critical regulator of the mTEC compartment and is activated by the engagement of particular members of the tumor necrosis factor receptors super family (TNFRSF) in mTEC and their precursors [30]. Mice displaying impaired NF-κB signaling present an abnormal medullary architecture, defective mTEC cells, including the loss of $Aire^+$ mTECs, and consequent severe autoimmune syndromes [67-70]. There are four members of TNFRSF that are expressed in mTEC and their precursors and are of particular relevance to mTEC differentiation, namely CD40 (TNFRSF5), lymphotoxin β receptor (LTβR), receptor activator of nuclear factor-κB (RANK/TNFRSF11a) and osteoprotegerin (OPG/TNFRSF11b) [70-75]. Several studies using mutant mice have shown the dependence of mTEC development on RANK, CD40, and LTβR [73, 74, 76-79]. The activation of these receptors triggers the engagement of transcription factor NF-κB via two distinct intracellular signaling pathways: the classical NF-κB pathway and the non-classical NF-κB pathway [79]. The TNF receptor-associated factor 6 (TRAF6) mediates RANK and CD40 signaling and activates the classical NF-κB pathway. Still, RANK, CD40, and LTβR signaling pathways can also activate the NF-κB complex containing RelB via non-classical NF-κB signaling mediated by NF-κB-inducing kinase (NIK). Dysfunction of TRAF6, NIK or RelB disturbs the normal development of $Aire^+$mTECs [70, 80-82], reinforcing the notion that active signaling downstream of receptors of TNFRSF is key to promote mTEC differentiation. Interestingly, RANK signaling seems to have a dominant role in mTEC development. That conclusion was evident by the analysis of mice deficient in RANKL, which indicated that RANK-mediated signaling in mTEC are activated by RANKL expressed by positively selected T cells and are essential to growth and maturation of the mTEC compartment [73, 74]. Nevertheless, CD40L is also produced by positively selected thymocytes and plays a supplementary role in the formation of the thymic medulla [74, 78]. Consistently, RANK and CD40 double deficiency further reduces

the frequency of Aire$^+$mTECs, while CD40 only partially compensate RANK absence [73, 74]. Yet, distinct hematopoietic cells that interact with mTEC and their precursors express the ligands for these receptors. The intrathymic cellular sources for RANK, CD40 and LTβR ligands (RANKL, CD40L and Lymphotoxin) and their accessibility change throughout development.

At embryonic stage, the RANKL$^+$ lymphoid tissue inducer (LTi) cells [77] and invariant Vγ5TCR$^+$ thymocytes [83], one of the first TCR$^+$ cells generated in the thymus, promote the development of the initial medullary areas by triggering maturation of mTEC progenitors. Additionally, and apart of its role in mTEC differentiation, it was recently described that LTβR plays a role in the regulation of T cell progenitor entry and seeding of the thymus [84]. Still, the identity of the LTβR ligands and the cells that express it is not yet identified. Nevertheless, the medulla expansion only occurs in the postnatal stage, together with the increase of positive selection of CD4$^+$ and CD8$^+$ thymocytes. Therefore, at this phase, the CD4$^+$SP become the major source of RANKL, CD40L and lymphotoxin [71, 74]. Furthermore, the interaction between autoantigen-specific CD4$^+$ T cells with mTECs foster their differentiation and expansion [78, 85]. Taking together, these findings suggest the existence of mTEC-restricted progenitor and a direct precursor-product relationship within medullary lineage, in which distinct intrathymic hematopoietic cells participate sequentially in mTEC expansion [72]. While RANKL$^+$ LTi cells and invariant Vγ5TCR$^+$ thymocytes regulate embryonic mTEC development, CD4$^+$SP thymocytes and autoreactive T cells provide RANKL, CD40L and Lymphotoxin for the maintenance of the mTEC niche in the postnatal thymus.

Developmental characteristics of cortical and medullary TECs

Despite the different phenotypic, functional and developmental traits, cTECs and mTECs share the expression of markers such as epithelial cell adhesion molecule 1 (EpCAM-1) and MHCII within the non-hematopoietic (CD45$^-$) thymic fraction. cTECs can be further defined on the basis of the expression of CDR-1, cytokeratin 8 (K8), Ly51 [33, 86], CD205, CD40 [32], ACK4 (also known as CCRL1) [17], the proteasome subunit β5t

[31] and high levels of IL-7 [87]. During embryogenesis, the expression of MHCII and CD40 are lower and then increases with cTEC maturation [32]. The evaluation of β5t-expressing cells through ontogeny showed that cTEC can be identified based on this marker and $\beta5t^+$ cells were detectable as early as E12.5, specifically in $CD205^+$ cTECs [31]. Moreover, the $CD205^+Ly51^+MHCII^+$ -expressing cells gradually increase with β5t-expressing TECs during ontogeny, suggesting that β5t is expressed by immature and mature cTECs [31].

Despite these advances, the differentiation steps of cTECs are still poorly characterized in comparison with mTEC, wherein a further degree of heterogeneity has been uncovered. mTECs are characterized by expression of K5 and K14, reactivity with lectin *Ulex europaeus* agglutinin (UEA) and expression of mouse thymic stroma 10 (MTS-10) and MTS-24 [33, 86]. Postnatal mTECs contain two major subpopulations that are defined based in the expression levels of MHC class II and CD80 molecules, $mTEC^{low}$ ($MHCII^{low}CD80^{low}$) and $mTEC^{hi}$ ($MHCII^{hi}CD80^{hi}$) [16]. The $mTEC^{low}$ population is nonetheless heterogeneous, containing the precursors of $mTEC^{hi}$ subpopulation [77], CCL21- expressing cells [88] and also terminally differentiated post-Aire $mTEC^{low}$ involucrin-expressing cells [71]. In particular, reaggregate thymus organ cultures (RTOC) with embryonic $mTEC^{low}$ subpopulation showed that those cells were able to give rise to $mTEC^{hi}$ [77], indicating, despite the above-mentioned heterogeneity, a direct precursor-product relationship between a fraction of $mTEC^{low}$ and $mTEC^{hi}$ subsets. Interestingly, the $Aire^+$ $mTEC^{hi}$ populations progressively lose MHCII and Aire expression becoming terminally differentiated post-Aire $mTEC^{low}$, which appear to express involucrin [89, 90]. Furthermore, $mTEC^{low}$ cells expressing the chemokine CCL21, seem to be essential for attracting positively selected thymocytes from the cortical compartment and therefore the establishment of self-tolerance of T cells [88] (**Figure 2**).

The $mTEC^{hi}$ subset is also heterogeneous in respect to the composition of cells expressing Aire [91] and Fezf2 [63]. Interestingly, while Aire expression maps only to the $mTEC^{hi}$ subset, Fezf2 expression is detectable in both $mTEC^{low}$ and $mTEC^{hi}$ subtypes. In $mTEC^{hi}$ subsets, both $Aire^-$ $Fezf2^+$ and $Aire^+$ $Fezf2^+$ populations are present [63] (**Figure 2**). Subsequently, $Aire^+$ $mTEC^{hi}$ subsets are also further subdivided into OPG-positive

(OPG$^+$) and -negative (OPG$^-$) subpopulations. OPG is an osteoclastogenesis inhibitory protein that lacks a transmembrane domain and function as a secreted decoy receptor for RANKL [92, 93]. Similarly to RANK, OPG expression is enriched in mTECs as compared with cTECs or other cell types within the thymus. Contrarily to mice deficient in RANKL-RANK signaling [73], it was also shown that the deficiency in OPG causes an increase in mTEC number and enlargement of the thymic medulla [73], indicating that OPG balances excessive RANKL-RANK signaling in mTECs. In conclusion, both mTEC^{low} and mTEC^{hi} subsets contain functionally heterogeneous relevant mature mTEC subpopulations (**Figure 2**).

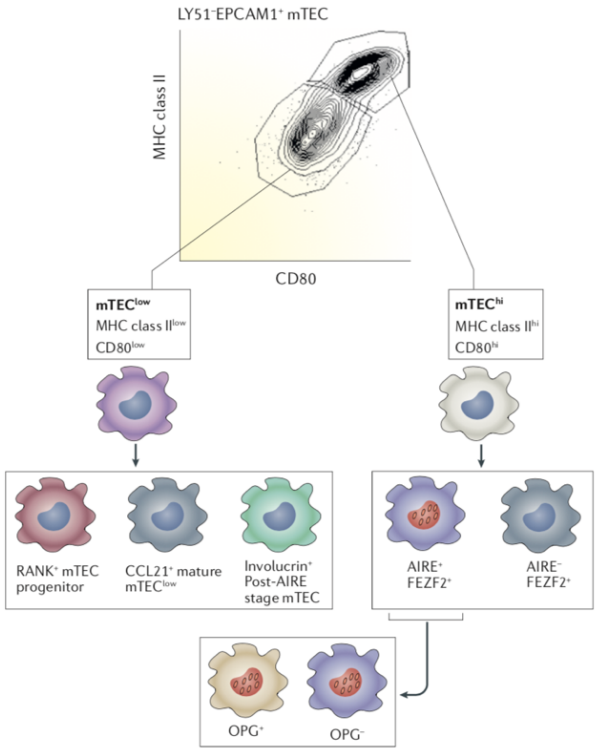

Figure 2 - **mTEC heterogeneity in the adult thymus**. Medullary thymic epithelial cells (mTECs) are defined as CD45$^-$EpCAM$^+$UEA$^+$Ly51$^-$CD205$^-$. mTECs are further subdivided in two subsets based on different levels of expression of MHCII and CD80: MHC class II^{low}CD80^{low} (mTEC^{low}) subset and an MHC class II^{hi}CD80^{hi} (mTEC^{hi}) subset. mTEC^{low} cells contain mTEC^{hi} progenitors and also post-Aire mature mTEC expressing involucrin. The mTEC^{hi} subset is also heterogeneous, with subpopulations defined by their expression AIRE and FEZF2, as well as OPG, a regulator of mTEC homeostasis. From [94].

Thymus development during embryogenesis

The unique structural organization of the thymic stroma is a dynamic process that starts during embryogenesis and proceeds during postnatal life [95]. The thymic organogenesis initiates early in embryonic development from endodermal pharyngeal pouches (PPs), specifically in the region of the third endodermal pharyngeal pouches (3PPs) in case of mice and human (**Figure 3**) [96]. Essentially, the outgrowth of 3PPs goes through patterning stages that lead to the formation of thymus in response to developmental signals such as fibroblasts growth factors (FGFs), BMP4, and Wnt ligands [95, 97, 98]. Nonetheless, the proliferative capacity of epithelial cells seems to rely on signals provided by neural crest-derived mesenchyme [99]. Actually; the thymic mesenchyme is known to regulate embryonic TEC proliferation through the provision of FGF7 and FGF10 [100, 101]. Additionally, the lack of expression of FGF-receptor 2IIIb (FGFR2IIIb) results in a severely hypoplastic thymus [102] (**Figure 3**).

Through the initiation of organogenesis, two defining processes take place in thymus development: the patterning of the rudiment into thymus- and parathyroid-specific domains, and the initiation of TEC differentiation. This initial budding is followed by outgrowth and patterning stages, such that each 3PP forms a shared primordium for two organs–the thymus and the parathyroid glands [95] (**Figure 3**). Therefore, the thymus primordia can be distinguished from the parathyroid counterpart at E11.5 in mouse by the respective restricted expression of two transcription factors, forkhead N1 (*Foxn1*) (thymus primordium) and the glial cells missing 2 (*Gcm2*) (parathyroid) [97]. Subsequently, they separate from pharyngeal endoderm and resolve into discrete organ primordia about E12.5 [103]. Foxn1 plays a critical role in thymus development, function, maintenance, and even regeneration, functioning as a master regulator of TEC differentiation [104, 105]. Foxn1 was one of the first members of the forkhead (FOX) super-family of transcription factors to be implicated in a specific developmental defect in vertebrates [106]. At E9.5, it is already evident the presence of low levels of Foxn1 expression in the pharyngeal endoderm [104]. While, higher levels of Foxn1 expression appear within the thymus primordium at E11.25 [103]. As illustrated in figure 3, this higher expression begins in the most ventral tip of the 3PP and subsequently expands to comprise the entire thymus

domain.

Some genes can affect the thymus development by influencing processes that take place prior to thymus specification. By analyses of mutant phenotypes and gene-expression patterns, several studies have identified a transcription-factor network that is required for the initial formation and early patterning of the thymus/parathyroid rudiment. Consequently, factors such homeobox A3 (*Hoxa3*) [107], paired box gene 1 (*Pax1*) [108-110], *Pax3* [111], eyes absent 1 homologue (*Eya1*) [112, 113], sine oculis-related homeobox 1 homologue (*Six1*) [113] and T-box protein 1 (*Tbx1*) [114] are co-expressed in pharyngeal endoderm. Mutations in those genes can lead to abnormal thymus development, such thymus aplasia, or hypoplasia, or failure of the thymus lobes to migrate toward the chest [108, 109, 111-117]. That is in agreement to the study developed by Su *et al.*, which showed that mutations in *Hoxa3* and *Pax1* result in defective TEC development. The most dramatic defect is a partial block at the DN to DP transition in *Hoxa3*$^{+/-}$ *Pax1*$^{-/-}$ mutants causing a marked reduction in the number of DP cells [110].

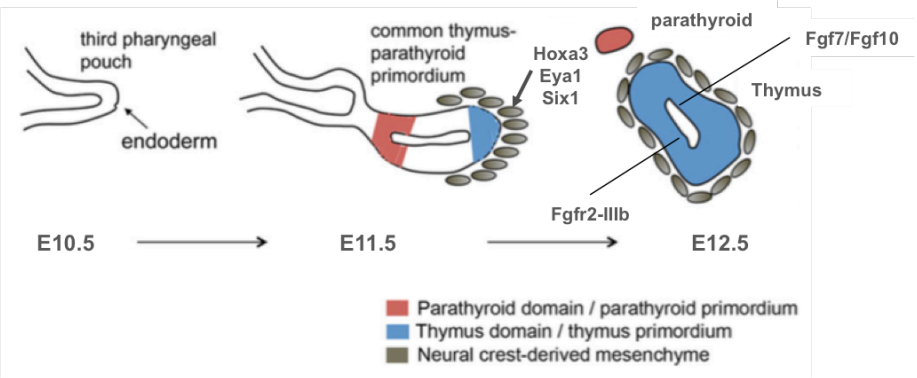

Figure 3 - Early events during thymus organogenesis. Representation of the development of a mouse embryo from day 10.5 (E10.5) until E12.5 of gestation. The gray ovals represent neural crest-derived mesenchymal cells. While red represents region of GCM2 expression, marking the parathyroid primordium, the blue represents region of FOXN1 expression, indicating the thymus primordium. Adapted from [97].

Further knowledge of TEC differentiation during embryonic stage, while the thymus is actively expanding, and that could lead to a better comprehension of TEC progenitors

(TEP) and the identification of new checkpoints of cTEC and mTEC development. Recent reports on the generation of TEPs from Parent *et al.* and Sun *et al.* used *in vitro* gene programing assays to generate TECs from human embryonic stem cells (hESCs) [118, 119]. Both studies exhibit similar results to recreate *in vitro* developmental pathways involved in *in vivo* thymus development by the combinations of Wnt3A, Retinoic Acid (RA), and BMP4, as well as inhibitors of TGF-β and canonical Wnt signaling. These findings reinforce the notion that Foxn1 and Hoxa3 transcription factors are essential regulators of TEC specification and their differentiation into mature TECs [97, 105, 117, 120].

Lineage specification of thymic epithelial cells

Initial transplantation studies in birds and mice showed that cTECs and mTECs share a common endodermal origin [121]. Subsequent studies have attempted to define the identity of TEPs. The initial analysis of cells expressing a surface glycoprotein MTS20 and MTS24 revealed that those have progenitor cells with capacity to give rise functional cTECs and mTECs [122, 123]. The study of a link between TEPs and the marker placenta-expressed transcript-1 (Plet1) protein, which is recognized by the antibody MTS24, might be questionable by subsequent studies [124]. Other study demonstrated that the both Plet-1^{+} and Plet-1^{-} cells isolated from early embryonic thymus were able to generate cTECs and mTECs [125]. Collectively, these results suggested that Plet1 might not represent a reliable marker for TEPs as that bipotency appeared to be related to a specific stage of thymus development. Rossi *et al.* showed that some embryonic-derived single cells are capable to generate cTECs and mTECs located in the respective cortical and medullary areas, by following the fate of microinjected individual EpCAM1^{+}CD45^{-} eYFP^{+} E12 TEC into wild type (WT) foster thymus [126]. Similarly Bluel *et al.* using genetic cell-tracing models demonstrated that reactivation of Foxn1 in TECs of Foxn1-deficient mice generates functional and organized thymic tissue comprising discrete cTEC and mTEC progeny [127]. These two series of experiments indicate that the two compartments derived from bipotent progenitors and share a common ancestry (**Figure**

4A) [95, 128]. Still, the heterogeneity of distinct stages of development within cTEC/mTEC lineages remains elusive.

Intriguingly, current studies indicated that cells with cTEC traits generate cTECs and mTECs [87, 129-131]. Baik *et al.* showed that $CD205^{+}$ $CD40^{-}$ cTECs [129] can mutually generate β5t/CD205-expressing cortical and Aire-expressing medullary epithelial microenvironments *in vivo* [129]. Moreover, the treatment with anti-RANK of E12.5 thymus, a time point in which mature mTEC are still absent, led the emergence of mTECs within $CD205^{-}$ and $CD205^{+}$ compartment, indicating that mTEC progenitors seem to exist within the CD205-expressing cTECs [129]. This evidence is consistent with a report from our laboratory using IL-7 reporter mouse in which YFP labels a TEC subset expressing high levels of IL-7 ($Il7^{YFP+}$) [43, 132]. The $Il7^{YFP+}$ population represents a particular subset of $CD205^{+}Ly51^{+}$ cTECs during fetal and perinatal life [43]. Taking advantage of the RTOC technique, purified $Il7^{YFP+}$ cTECs from E14.5 were able to give rise to both cTEC ($Ly51^{+}CD205^{+}$) and mTECs ($CD80^{+}$) [87] (**Figure 4B**). Additionally, by generating a β5t-driven lineage tracing mouse model, Ohigashi *et al.* confirmed that not only all cTECs but also nearly all mTECs, including mature $Aire^{+}$mTECs, derive from a progenitor expressing β5t [130]. These findings provide evidence that embryonic TEPs progress through the cortical lineage before the commitment in mTECs, leading to the idea that the cortex functions as a niche that harbors bipotent TEPs [128].

Overall, these studies suggest a possible continual contribution of TEPs residing in the cortical compartment to the generation and maintenance of both: cTECs and mTECs [128] (**Figure 4B**).

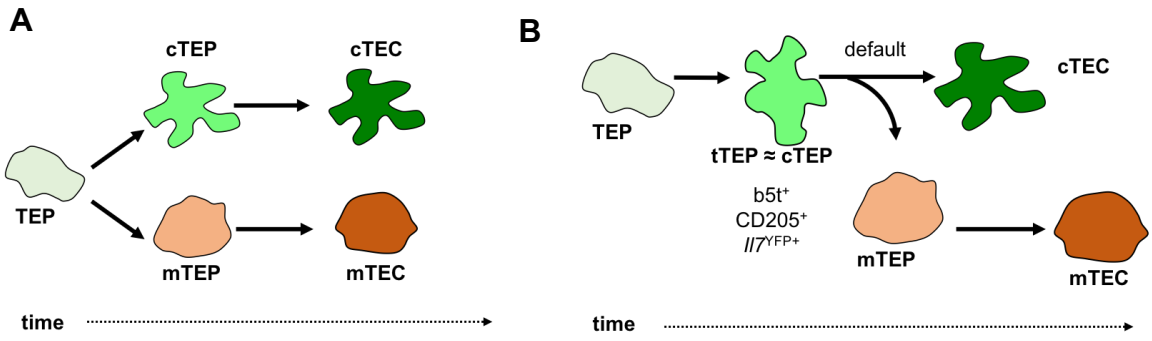

Figure 4 – **Models of thymic epithelial cell development**. **A**) Uncommitted bipotent TEC progenitors (TEPs) diverge simultaneously to lineage-committed cTEC and mTEC progenitors (cTEP and mTEP) which then progress into mature cTECs and mTECs. **B**) TEPs transverse through a transitional stage in which they express phenotypic and molecular traits associated with cortex prior to the commitment into a cTEC or mTEC fate. Adapted from [128].

Medullary thymic precursors

While the identity of cTEC unipotent progenitors (cTEP) remains elusive, several reports have identified distinct subsets that are enriched in mTEC-restricted progenitors (mTEP). As mentioned above, the generation of the mTEC lineage is an important step for induction of self-tolerance [133]. mTEC lineage–committed progenitors emerge as early as E13.5 and are characterized by expression of various cellular markers, including claudin-3 and -4 and SSEA1 [134, 135]. Other more recent study has identified specialized podoplanin (PDPN)$^+$ mTEPs, which reside at the CMJ of the postnatal thymus [136]. These findings suggested that the capacity of mTEPs is preserved beyond birth. It was also described that SSEA1$^+$ mTEPs were RANK$^-$ and appeared earlier in ontogeny than RANK$^+$ TEPs. Also, like SSEA1$^+$ mTEC stem cells, RANK$^+$SSEA1$^-$ embryonic TECs were restricted to the mTEC lineage [137]. Still, the direct analysis of precursor-product relationship between these populations remains to be determined. Nonetheless, SSEA1$^+$ mTEC stem cells, contrarily to RANK$^+$ mTEPs, were detectable in both nude mice and embryonic thymus of Relb$^{-/-}$, in which mTEC development is severely compromise [137]. Altogether, these findings are in line with the idea that specification of bipotent TECs to the mTEC lineage takes place during early thymic ontogeny, and this process results in an initial Relb-independent generation of a pool of mTEC stem cells that can create an

mTEC progeny in long term.

Moreover, embryonic mTEP populations have also been identified based on their RANK expression. Akiyama *et al.* found that RANK$^+$ cells are able to generate Aire$^+$mTECs (pMECs) via TRAF6-dependent mechanism [138]. Moreover, LTβR stimulation was found to increase levels of RANK expression in mTEPs in a Relb-dependent manner [138, 139]. Such findings match with the lack of detectable levels of RANK expression in RANK reporter mouse line when Relb is absent [137], and also with the expression of LTβR by early mTEPs [134]. Moreover, they suggest that Relb seems to operate downstream of mTEP by regulating the generation of RANK$^+$ mTEPs [138].

During these last years, we increase our knowledge of how the cortical and medullary epithelial compartments differentiate throughout development. Still, it remains unsolved, the existence of alternative stage-specific developmental pathways participating in the organization of the adult mTEC niche. Moreover, the understanding the nature of TEP and the mechanism responsible for the establishment of the embryonic thymic epithelium and its maintenance throughout postnatal life remains poorly understood. In the next chapters, I describe the work that we developed to answer some of these questions and discuss how these findings advance on our understanding of TEC biology and thymus function and homeostasis.

AIMS

In this thesis, I proposed to further characterize the lineage relationship between cTEC and mTEC in the postnatal thymus (**Results Chapter I**). Additionally, I aimed at identifying the niche of TEC progenitors (TEPs) throughout life and their relationship to the development and maintenance of cortical and medullary TEC microenvironments (**Results Chapter II**).

To reach these goals, we integrated the usage of different TEC-specific reporter mice models in immunocompetent and immunodeficient backgrounds with the analysis of TEC clonogenic assays, multiparametric flow cytometry, immunohistochemistry, gene expression profiling, *in vitro* thymic organotypic and *in vivo* thymic transplantations.

We believe that dissecting these points will provide important cellular and molecular details of value to better recognize the importance of TEPs in the maintenance of TEC niches, and consequently, in the function of thymus in T cell development and tolerance induction.

Results Chapter I

(Adapted from)

Intermediate expression of CCRL1 reveals novel subpopulations of medullary thymic epithelial cells that emerge in the postnatal thymus

Ana R. Ribeiro, Catarina Meireles, Pedro M. Rodrigues and Nuno L. Alves

European Journal of Immunology, 44(10):2918-2924 (2014

Abstract

Within the thymus, the cortical and medullary epithelial cells (cTECs and mTECs, respectively) are essential for T cell development and selection by providing the specific signals. The discrimination on cTEC/mTEC lineages downstream of common bipotent progenitors at distinct stages of development remains unclear. Analysis of the chemokine (C-C motif) receptor-like 1 (CCRL1) showed that is a late determinant of cTEC differentiation. Using CCRL1 reporter mouse we identified a subset expressing intermediate levels of CCRL1 (CCRL1^{int}) within the *Uleax europaeus* agglutinin 1 (UEA-1)$^{+}$ mTEC population that conspicuously emerge in the postnatal thymus and differentially express *Tnfrsf11a*, *Ccl21*, and *Aire*. Although, while rare in fetal and in *Rag2*$^{-/-}$ thymi, CCRL1^{int} mTECs are restored in *Rag2*$^{-/-}$ Marilyn TCR-Tg mice, indicating that the emergence of postnatal-restricted mTECs is closely related with T-cell selection. Altogether, our results indicate that alternative temporally restricted routes of new mTEC differentiation contribute to the establishment of the medullary niche in the postnatal thymus.

Introduction

The thymus is a central organ of adaptive immune system. The thymic epithelial cells (TECs) provide crucial instructive signals for the differentiation of thymocytes bearing a diverse TCR repertoire restricted to self-MHCs and tolerant to self-antigens [4]. While cortical TECs (cTECs) support T cell lineage commitment and positive selection, medullary TECs (mTECs) contribute in the elimination of autoreactive T cells and the differentiation of regulatory T cells (Treg) cells [30]. cTEC and mTEC are derived from a common bipotent progenitors existing in fetal and postnatal thymus [126, 127]. Significantly, the cTEC/mTEC maturation pathways downstream of bipotent progenitors are still unclear, as well as the requirements for the establishment of these specialized compartments at distinct stages of development.

The specification into cTEC or mTEC lineage starts early in embryonic

development [140]. At initial stages of gestation, the thymic epithelium is predominantly composed by Ly51^{+}CD205^{+} β5t^{+} cTECs [31, 32, 132], and mature mTECs, Aire^{+}mTEC, which appears around embryonic day 16 (E16) [72, 135]. The appearance of embryonic mTECs relies on cellular interactions with lymphoid tissue inducer (LTi) cells and invariant γδ T cells [77, 83], and comprises signaling through TNRF superfamily receptor activator of NF-κB (RANK) and lymphotoxin beta receptor (LT βR) expressed on TEC precursors [77, 139]. Although, despite the knowledge of distinct maturation stages in mTECs [30], the information about cTEC differentiation is still reduce. We, and others, have demonstrated that fetal TEC progenitors expressing cortical properties are able to generate mTECs [87, 129, 130]. These reports support the idea that embryonic TEC precursors progress transitionally through the cortical lineage prior to commitment to the medullary pathway, emphasizing that TEC differentiation is more complex than previously recognized [128].

The size of the medullary epithelial microenvironment continues to expand after birth, fostered by additional interactions between TECs and mature thymocytes, namely positively selected and CD4 single positive (SP4) thymocytes [30]. The concerted activation of RANK-, LTβR-, and CD40-mediated signaling on mTECs and their precursors completes the formation of the adult medullary niche [30]. It has been previously demonstrated a clonal nature for discrete embryonic mTEC islets, which progressively coalesce into larger medullary areas in the adult thymus [135, 141]. Hence, one can argue that the adult mTEC niche exclusively results from the expansion of embryonic-derived mTECs and their precursors. Still, it remains possible that alternative developmental stage-specific pathways participate in the organization of the adult mTEC niche.

In this report, we describe a novel checkpoint in cTEC differentiation, which is defined by the sequential acquisition of an atypical chemokine receptor, the (C–C motif) receptor-like 1 (CCRL1) expression. Additionally, we define unique subsets of mTECs, characterized by the intermediate CCRL1 expression, that emerge in the postnatal thymus in tight association with thymocytes that develop beyond the TCRβ selection. Our

results suggest the existence of waves of mTEC development in the embryonic and postnatal thymus.

Results and Discussion

Intermediate CCRL1 levels define distinct mTEC subtypes in the postnatal thymus

As previously described from our laboratory, in IL7^{YFP} reporter mice the expression of YFP is a surrogate of a subtype of cTECs expressing high levels of a crucial thymopoietin IL-7 (*Il7*$^{YFP+}$) [87, 132]. In CCRL1^{GFP} reporter mice, GFP expression labels cTECs in postnatal thymus [17]. The CCRL1 molecule controls the bioavailability of key chemoattractants CCL19, CCL21, and CCL25, and its expression identifies cTECs in the postnatal thymus [17]. Due to the lack of knowledge on the differentiation of CCRL1^{+} cTECs, we studied their generation using a previously created IL7^{YFP}-CCRL1^{GFP} dual reporter mice [87]. The analysis of IL7^{YFP}/CCRL1^{GFP} in immunocompetent and immunodeficient mice background showed that CCRL1^{hi} cTECs (CCRL1^{GFPhi} expressing cells) gradually increase throughout development, contributing to the expansion of TEC cellularity (Annex I). Therefore, the expression of high levels of CCRL1 can be consider as a late cTEC determinant [131].

Then, we examined the generation of mTECs relatively to the differentiation of CCRL1-expressing TECs. The primordial CD80^{+} mTECs were found within CCRL1^{-} (CCRL1^{GFPnegative}) cells (CCRL1^{-}CD80^{+}) at E15.5 (**Figure 1A**). The proportion and number of CCRL1^{-}CD80^{+} mTECs augmented throughout time (**Figure 1A and D**). Notably, a subset of CD80^{+} TECs, expressing intermediate levels of CCRL1 (CCRL1^{GFPintermediate}) (CCRL1^{int} CD80^{+}), emerged distinctly after birth (**Figure 1A**). As this subtype was virtually absent at E15.5, we compared CCRL1^{int} TECs for the expression of additional cTEC (Ly51) and mTEC (UEA binding) markers [87, 130] in E18.5 and neonatal thymus. At both periods, CCRL1^{hi} and CCRL1^{-}CD80^{+} TECs majorly identified

either Ly51^{+} cTECs or *Ulex Europaeus* Agglutinin 1 (UEA^{+}) mTECs, respectively (**Figure 1A and B**). The CCRL1^{-}CD80^{-} TECs, which represent a minor subset in the neonatal thymus, were predominantly composed of Ly51^{int} UEA^{+} TECs at this stage. CCRL1^{int} TECs at E18.5 comprised mostly Ly51^{+} UEA^{-} CD80^{-} , although few UEA^{+} CD80^{-} and scarce UEA^{+} CD80^{+} were detected (**Figure 1B and C**). Interestingly, three discrete sizeable subpopulations accumulated within neonatal CCRL1^{int} TECs, including UEA^{-} CD80^{-}, UEA^{+} CD80^{-} , and UEA^{+} CD80^{+} (**Figure 1C**). Both CD80^{-} and CD80^{+} CCRL1^{int} UEA^{+} mTEC subsets, while scarce at E18.5 (**Figure 1B and C**), totally represented approximately half and one quarter of the mTEC compartment in neonatal and young thymi, respectively (**Figure 1D**). To examine whether CD80^{+}CCRL1^{int} mTECs differentiate by the reiteration of the same pathways defined for postnatal mTECs [30, 74], we set E18.5 fetal thymic organ cultures (FTOCs). While rare in intact FTOCs, RANK, and/or CD40 stimulation induced the differentiation of CD80^{+}CCRL1^{int} mTECs (**Figure 1E**). Additionally, reaggregate thymic organ cultures (RTOCs) established with E15.5 CCRL1^{+} UEA^{-} CD80^{-} TECs, and RANK- and CD40-activated to induce mTEC differentiation, showed that a fraction of fetal CCRL1^{+} cTECs displayed CD80^{+} mTEC progenitor activity (**Figure 1F**). Next, we analyzed how the phenotypic traits of the emergent neonatal CCRL1^{int} TECs related to the expression of genes linked to cTECs (*Psmb11* and *Cstl*) and mTECs (*Tnfrsf11a* (RANK), *Ccl21*, and *Aire*) [30, 64]. Increasing *Psmb11* and *Cstl* expression was exclusively detected within CCRL1^{int}UEA^{-} and CCRL1^{hi} cells. Interestingly, a gradual increase in *Tnfrsf11a* expression was observed in CCRL1^{int} UEA^{-}, CCRL1^{int} UEA^{+} CD80^{-}, CCRL1^{int} UEA^{+} CD80^{+}, and CCRL1^{-} CD80^{+} TECs. *Ccl21*, which is expressed by postnatal immature mTECs [88], was specifically found within the CCRL1^{int} UEA^{-} CD80^{-} and CCRL1^{int} UEA^{+} CD80^{-} subsets. Lastly, *Aire* expression was equally enriched in CCRL1^{-} and CCRL1^{int} CD80^{+} mTECs (**Figure 1G**). Although fetal CCRL1^{+}UEA^{-} TECs have the potential to generate mTECs (**Figure 1F**), and the gradual increase in the expression of RANK and CCL21 within CCRL1^{int} cells might suggest a continual stepwise differentiation: CCRL1^{int} UEA^{-} – CCRL1^{int} UEA^{+} – CCRL1^{int} UEA^{+} CD80^{+}, our attempts to evaluate a direct lineage relationship between neonatal CCRL1^{int} TEC subsets have been unsuccessful, given the difficulty of establishing RTOC with perinatal TECs [125]. Thus, we can only speculate that the postnatal cTEC niche harbors

progenitors that are able to differentiate into mTECs, as shown in the fetal thymus [87, 129, 130]. Alternatively, one cannot exclude that postnatal CCRL1^{int} mTECs might differentiate from a lineage unrelated to cTECs. Collectively, our data indicate that while CCRL1^{int} UEA^{-} TECs co-express molecular traits of cTECs and mTECs, CCRL1^{int} UEA^{+} CD80^{-} and CCRL1^{int} UEA^{+} CD80^{+} cells define novel subtypes of immature and mature mTECs, respectively, that emerge postnatally.

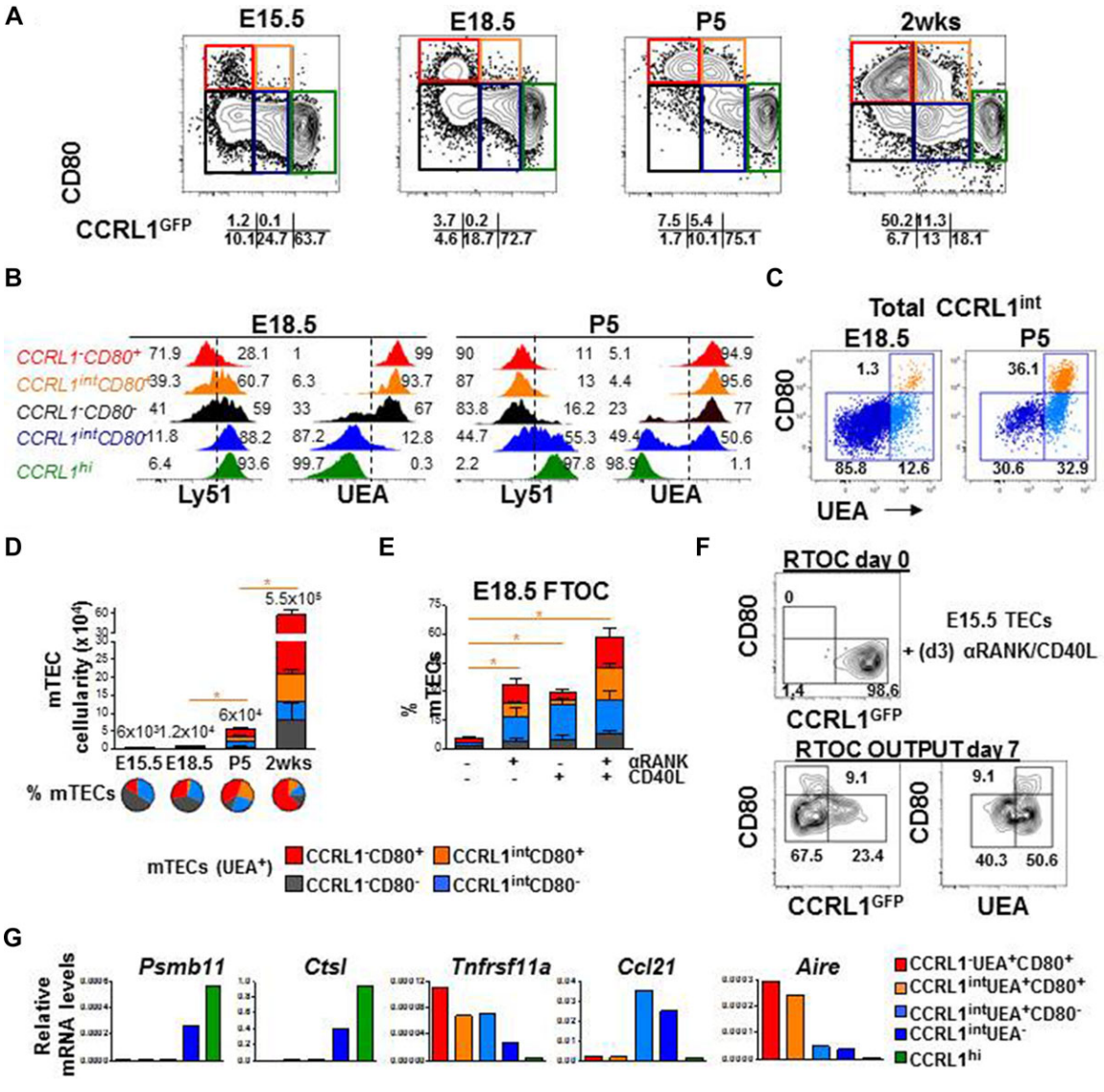

Figure 1 - **Intermediate CCRL1 expression reveals novel postnatal mTECs.** (**A**) TECs (gated as CD45^{-} EpCAM^{+}) from CCRL1^{GFP} reporter mice were analyzed for CCRL1^{GFP} and CD80 expression by FC at the indicated time points. Colored gates define different subsets and grids indicate the frequencies of each

respective one. (**B**) TEC subsets defined by the colored gates in (A) from E18.5 and postnatal day 5 (P5) thymi were analyzed for Ly51 and UEA expression by FC. Numbers in histograms indicate the frequency within each gate. Histograms are representative of three to five independent experiments. (**C**) Expression of UEA and CD80 within gated E18.5 and postnatal day 5 (P5) total CCRL1^{int} TECs was determined by FC. Numbers in plots indicate the frequency of cells found within each gate. (A–C) Plots are representative of three to five independent experiments. (**D**) Cellularity of UEA^{+} mTEC subsets from IL-7^{YFP} CCRL1^{GFP} mice. Average total mTEC cellularity is detailed above bars. Pie graphs represent the mean proportion of color-coded subsets within total UEA^{+} mTECs. *$p < 0.05$ (unpaired *t* test) (data are shown as mean + SD of 4–6 mice/group, pooled from three to five independent experiments (**E**) E18.5 FTOCs were cultured for 4 days with the indicated stimuli and then assessed for mTEC induction (UEA^{+} CD80$^{+/-}$) by FC. The proportion of subsets within UEA^{+} mTECs is color-coded. Data are shown as mean + SD of 8–10 thymic lobes/group, pooled from three independent experiments. *$p < 0.05$ (unpaired *t* test). (**F**) RTOCs established with E15.5-derived CCRL1^{+}UEA^{-}CD80^{-} TECs were stimulated with αRANK and/or CD40L and gated TECs were analyzed for the expression of the indicated markers by FC. Plots are representative of three independent experiments. (**G**) Expression of *Psmb11*, *Ctsl*, *Tnfrsf11a*, *Ccl21*, and *Aire* was assessed by qPCR in purified TEC subsets (colored columns) from postnatal day 5 (P5) IL-7^{YFP} CCRL1^{GFP} mice. Values were normalized to *18s*. Data are shown as representative of three independent experiments.

Thymic selection promotes the generation of CCRL1^{int} mTECs

The differentiation of the CCRL1^{int}CD80^{+} mTECs correlates timely with the intensification of positive thymic selection around the perinatal period [140]. Given that activation of RANK and CD40 fostered CCRL1^{int}CD80^{+} mTECs (**Figure 1C**) and the ligands for those mTEC-inductive signals are expressed by SP4 thymocytes [30], we investigated whether the appearance of CCRL1^{int}CD80^{+} mTECs depends on TEC-SP4 interactions during selection. To this end we crossed CCRL1-reporter mice onto a Marilyn- *Rag2*$^{-/-}$ TCR transgenic background, in which T cells express an I-A^{b}-restricted TCR that recognizes the male H-Y antigen [87]. As control, we co-analyzed *Rag2*$^{-/-}$ littermates, wherein mTEC differentiation is compromised due to the lack of mature thymocytes [87]. Few CD80^{+} mTECs were present in the neonatal *Rag2*$^{-/-}$ thymus, and those were majorly CCRL1^{-} (**Figure 2A-C**), resembling mTECs found in the E18.5 thymus (Figure 1). Contrarily to the normal postnatal thymus, the scarce CCRL1^{-} and CCRL1^{int}CD80^{+} subsets found in *Rag2*$^{-/-}$ mice were predominantly composed of Ly51^{+}UEA^{-} cells (**Figure 2A, B**). Strikingly, we detected a marked expansion of both CCRL1^{-}CD80^{+} and CCRL1^{int}CD80^{+} mTECs in neonatal Marilyn-*Rag2*$^{-/-}$ females (**Figure 2A-C**), recapitulating the mTEC composition of the young thymus (**Figure 1A**). Akin to the WT thymus, CCRL1^{hi} and CCRL1^{-}CD80^{+} TECs specifically identified cTECs and

mTECS, respectively, and the emergent CCRL1^{int}CD80^{+} TECs were Ly51^{lo}UEA^{+} (**Figure 2B**). One can envision that temporally restricted mTEC differentiation pathways are engaged by interactions between mTEC precursors and distinct hematopoietic cells. As shown previously [31, 72], the generation of the first embryonic mature CD80^{+} mTECs (CCRL1^{-}) precedes the development of SP4s and depends on LTβR- and RANK-mediated signaling engaged upon lympho- epithelial interaction with lymphoid tissue inducer cells and γδ T cells [77, 83, 139]. Our findings indicate that the differentiation of the postnatal-restricted CCRL1^{int}CD80^{+} mTECs results from MHC-TCR, CD40-CD40L and RANK-RANKL interactions [30, 74] between TEC precursors and TCRβ-selected thymocytes.

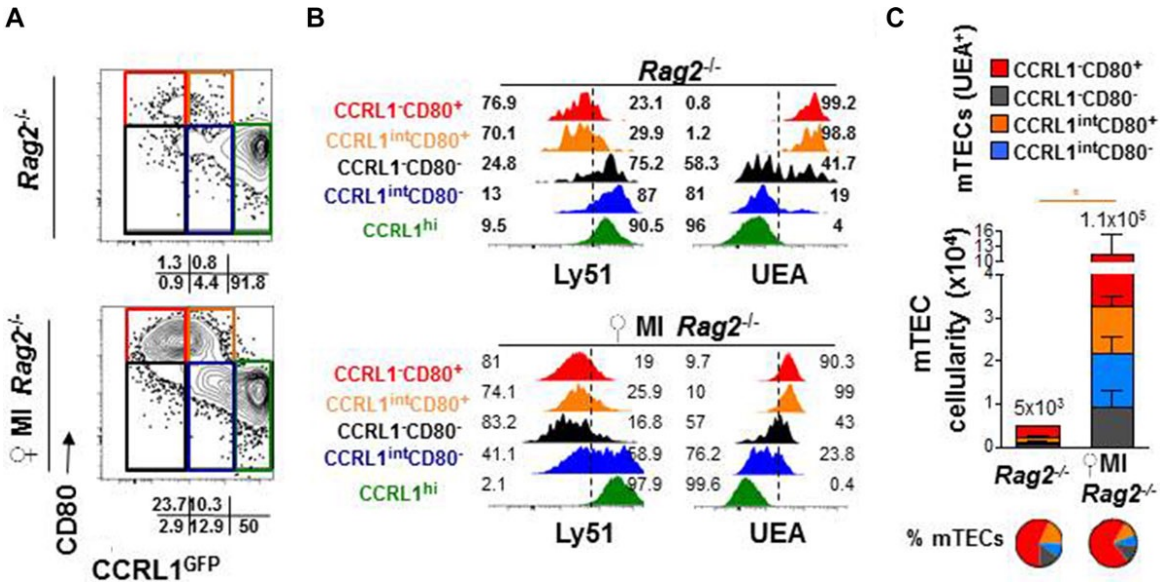

Figure 2. Thymic selection drives the emergence of the postnatal-specific CCRL1^{int}CD80^{+} TECs. (**A**) TECs (gated as CD45^{-}EpCAM^{+}) from postnatal day 5 (P5) *Rag2*$^{-/-}$ and female Marilyn- *Rag2*$^{-/-}$ mice were analyzed for CCRL1^{GFP} and CD80 expression by FC. Colored boxes define different TEC subsets and grids indicate the frequencies of each one. Plots are representative of two to three independent experiments. (**B**) Subsets defined by the colored gates in (A) from *Rag2*$^{-/-}$ and Marilyn- *Rag2*$^{-/-}$ mice were analyzed for Ly51 and UEA expression by FC. Numbers in histograms indicate the frequency within each gate. Histograms are representative of three independent experiments. (**C**) Frequency of subsets within total mTECs (pie graphs) and numbers of mTEC subsets was determined by FC. Data are shown as mean + SD of three to five samples, pooled from two independent experiments. **p* < 0.05 (unpaired *t* test).

Concluding Remarks

The neonatal life marks a period characterized by a drop in cTECs and an expansion in mTECs [17]. The identification of novel postnatal mTEC subsets supports the concept that the foundation of the adult medullary microenvironment results from alternative waves of mTEC differentiation. In this regard, recent evidence suggests that the expansion of the medulla after birth involves de novo formation of mTECs [142]. This notion implicates that fetal mTEC precursors might have limited self-renewal potential, as shown for bipotent TEC progenitors [143], and in turn the formation of the adult mTEC niche relies on additional inputs arising after birth. Still, further studies are needed to elucidate to what extent bipotent progenitors might progress through the cortical differentiation program in the adult thymus. Also, the functional relevance of the mTEC heterogeneity reported herein should be further dissected. As mTECs have a crucial role in T-cell maturation and tolerance induction, our findings have implications in therapeutics aimed at modulating TEC niches in the adult thymus.

Material and Methods

Mice

The CCRL1^{GFP} reporter mice were backcrossed onto *Rag2*$^{-/-}$ and Marilyn-*Rag2*$^{-/-}$ C57BL/6 background [87]. E0.5 was the day of vaginal plug detection. Animal experiments were performed in accordance with European guidelines.

TEC isolation and flow cytometry

TECs were isolated as described [87]. Cells were stained with anti– I-A/I-E (Alexa 780); anti-CD45.2 (PerCP-Cy5.5); anti- EpCAM (A647); anti-CD80 (A660); anti-Ly51, anti-CD205, UEA-1 (biotin), anti-EpCAM (eFluor 450) Abs, and streptavidin (PE-Cy7) (eBioscience). Flow cytometry was performed on a FACSCanto II (BD Biosciences), with

data analyzed on FlowJo software. Cell sorting was performed using the FACSAria I (BD Biosciences), with purities >95%.

Gene expression

mRNA (RNAeasy MicroKit, Quiagen) isolation and cDNA synthesis (Superscript First-Strand Synthesis System, Invitrogen) were performed as described [87]. Real-time PCR (iCycler iQ5) was performed using either TaqMan Universal PCR Master Mix and primers for *18s, Ctsl, Aire, Ccl21, Tnfrsf11a*, and *Psmb11* (Applied Biosystems); or iQ SYBR Green Supermix (Bio-Rad) and primers for *Actb* and *Ccrl1* as detailed [87]; Triplicated samples were analyzed and the Ct method was used to calculate relative levels of targets compared with *18s*/*Actb* as described [87].

FTOCs and RTOCs

FTOCs and RTOCs were established with E18.5 and E15.5 embryos, respectively, as described [87]. For FTOCs, TECs were analyzed after 4 days culturing with 1 µg/mL anti-RANK and/or with 5 µg/mL recombinant CD40L (R&D Systems). For RTOCs, 10^5 E15.5 $CCRL1^+$ UEA^- $CD80^-$ TECs were sorted and mixed with $CD4^+CD8^+$ and $CD4^+$ thymocytes at 1:1:1 ratio. After 3 days, 0.3 µg/mL anti-RANK and 1.3 µg/mL recombinant CD40L were added to the cultures. RTOC were analyzed after 7 days.

Statistical analysis

The unpaired *t* test was used to perform statistical analysis. $p < 0.05$ was considered significant.

Acknowledgments

We thank James Di Santo, Jocelyne Demengeot and Thomas Boehm for *Rag2*$^{-/-}$ *Il2rg*$^{-/-}$, Marilyn-*Rag2*$^{-/-}$ and CCRL1-reporter mice, respectively. We thank Dr. Catarina Leitão for critical reading of the manuscript and technical assistance. We thank FEDER funds through the Operational Competitiveness Programme – COMPETE and by National Funds through Fundação para a Ciência e a Tecnologia (FCT) under the project PTDC/SAU- IMU/117057/2010 funded this work. N.L.A., A.R.R., C.M. and P.M.R. are supported by FCT Investigator program and PhD fellowships.

Results Chapter II

Thymic crosstalk restrains the pool of cortical thymic epithelial cells with progenitor properties

Catarina Meireles*, Ana R. Ribeiro*, Rute D. Pinto, Catarina Leitão, Pedro M. Rodrigues and Nuno L. Alves

European Journal of Immunology, 47(6):958-969 (2017)

Abstract

Cortical (cTEC) and medullary (mTEC) thymic epithelial cells establish key microenvironments for T-cell differentiation and arise from thymic epithelial cell progenitors (TEP). However, the nature of TEPs and the mechanism controlling their stemness in the postnatal thymus remain poorly defined. Using TEC clonogenic assays as a surrogate to survey TEP activity, we found that a fraction of cTECs generates specialized clonal-derived colonies, which contain cells with sustained colony-forming capacity (*Clono*TECs). These *Clono*TECs are EpCAM^{+}MHCII^{-}Foxn1^{lo} cells that lack traits of mature cTECs or mTECs but co-express stem-cell markers, including CD24 and Sca-1. Supportive of their progenitor identity, *Clono*TECs reintegrate within native thymic microenvironments and generate cTECs or mTECs *in vivo*. Strikingly, the frequency of cTECs with the potential to generate *Clono*TECs wanes between the postnatal and young adult immunocompetent thymus, but it is sustained in alymphoid *Rag2*$^{-/-}$*Il2rg*$^{-/-}$ counterparts. Conversely, transplantation of wild-type bone marrow hematopoietic progenitors into *Rag2*$^{-/-}$*Il2rg*$^{-/-}$ mice and consequent restoration of thymocyte-mediated TEC differentiation diminishes the frequency of colony-forming units within cTECs. Our findings provide evidence that the cortical epithelium contains a reservoir of epithelial progenitors whose abundance is dynamically controlled by continual interactions with developing thymocytes across lifespan.

Introduction

The development and selection of highly diverse T cells, which are responsive against pathogens while tolerant to one's own organs, takes place in dedicated niches of the thymus. Central to this instructive process are thymic epithelial cells (TECs) that segregate into specialized cortical (cTEC) and medullary (mTEC) microenvironments [30]. While cTECs instruct the commitment of hematopoietic precursors into the T cell lineage and positively select thymocytes expressing major histocompatibility complex (MHC)-restricted T cell receptors (TCRs), mTECs contribute to the elimination of thymocytes expressing autoreactive TCR and the development of regulatory T cells [144].

Consequently, genetic alterations that affect the differentiation of TECs lead to pathologies that range from immunodeficiency to autoimmunity [30]. Since TECs are sensitive to aging and conditioning regiments linked to bone marrow transplantation or cancer therapy [123], the functionalization of thymic epithelial niches emerges as a direct approach to improve thymopoiesis in disorders associated with ineffective T-cell responses.

The two-prototypical cTEC and mTEC subsets differentiate from common bipotent TEC progenitors (TEP) that exist in the embryonic [122, 123, 126] and postnatal [127] thymus. Deciphering how bipotent TEPs self-renew and transmogrify into cTECs and mTECs has been under intense investigation. The discovery of mTEC- restricted precursors [135, 141, 145] led to the concept that TEP give rise to cortical and medullary lineages through unrelated differentiation pathways. More recently, evidence that embryonic cTEC-like progenitors have the potential to generate cTECs and mTECs [87, 129, 130] suggests that TEPs might progress through the cortical lineage prior to commitment to mTECs [128]. These findings equally implicate that TEPs nestle within the embryonic cortex. Recent studies identify distinct subsets of TECs in the postnatal thymus that contain, without exclusively marking, purportedly TEPs [146-148]. Yet, the singular identity and anatomical location of TEPs are still elusive. Moreover, whether TEC differentiation follows the same precursor-product relationships in the postnatal thymus is not airtight.

Thymic epithelial cell microenvironments turnover more rapidly than previously recognized, with an estimated replacement rate of one-two weeks to mTECs of the young adult thymus [16, 149]. These results suggest a requirement for regular differentiation of new mature TECs from their upstream progenitors. Two, not necessarily mutually exclusive, scenarios can coincide. On one hand, long-lasting TEPs must continually produce lineage- committed precursors lacking self-renewal capacity. Alternatively, the abundance of functional TEPs might drop with age, being the replenishment of cortical and medullary epithelial niches assured by downstream compartment-restricted precursors. Fate-mapping studies show that the majority of adult mTEC network arise from fetal- and newborn-derived TEPs expressing beta5t (β5t), a prototypical cTEC

marker [150, 151]. Furthermore, mTEC-restricted SSEA-1$^+$ progenitors [134, 137] and specialized podoplanin$^+$ (PDPN) mTEPs residing at the cortico-medullary junction (CMJ) [136] have been identified, both contributing to the maintenance of mTEC compartment. Together, these findings infer that the bipotent capacity of TEPs is preserved beyond birth, but might be progressively lost with age. Consequently, the maintenance of adult medullary epithelial network seems to be secured by unipotent mTEPs.

Despite recent advances, it remains unclear how changes in the bioavailability of TEPs impact on the maintenance of TEC microenvironment across life, and ultimately on thymic output. Another unexplored area pertains to the physiological causes underlying the presumed age-dependent decrease and/or senescence of TEPs. Since the amount of embryonic TEP dictates the size of functional TEC microenvironments [143], it is conceivable that the loss in the TEC network with age might be coupled to the loss in TEP stemness. Nevertheless, we lack experimental evidence that argues in favor, or against, this possibility. Herein, we identify a subset of cTECs that generates TEC colonies of clonal origin, harboring cells with progenitor traits, including continual colony-forming capacity, lack of mature TEC markers and bearing the potential to generate cTECs and mTECs. Detailed temporal analysis reveals that the abundance of cTECs with clonogenic activity decreases with the entry into the adulthood, in a process that is directly regulated by lympho–epithelial interactions.

Results

The postnatal cortical thymic epithelium contains cells with clonogenic capacity

The postnatal thymus represents a period of active growth of the TEC network, which plateaus during young adulthood followed by a progressive reduction with age [16, 131]. We conjectured that these dynamic changes in TEC niches might be coupled to a gradual exhaustion of TEPs. To seek for epithelial stemness within the postnatal thymus, we established clonogenic assays that were previously reported to select and support the

growth of stem cells from other stratified epithelial cells and the rat thymus [152, 153]. In these midscale assays, bulk postnatal cell- sorted TECs (CD45$^-$ EpCAM$^+$ MHCII$^+$) were cultivated in specialized medium onto a monolayer of feeder cells (irradiated 3T3) (Supporting Information Figure 1A). TEC-derived colonies emerged around day 6 and grew in size up to day 12, containing tightly packed cells that express the pan-epithelial marker EpCAM (Supporting Information Figure 1B and C) and cytokeratin 8 (K8) [33] (**Figure 1A**). A limitation of experiments with "bulk" cultivated TECs is that they might hinder a possible heterogeneity at the single cell level. Thus, we determined whether the clonogenic potential was a property of all, or only a fraction of postnatal-TECs. First, we performed co-culture assays with equal amounts of postnatal cell-sorted TECs isolated from mice that constitutively express Green Fluorescent Protein (GFP) or Red Fluorescent Protein (RFP) under the control of β-actin promoter. In this setting, colony-forming units could be surveyed on the basis of their live-cell fluorescence. The development of either single GFP$^+$ or single RFP$^+$ TEC-derived colonies suggested their clonal origin (**Figure 1B**). Next, combining high-speed cell sorting and high-content imaging analysis, we microscaled the assay down to single-cell level and showed that TEC colonies were clonally derived from single- sorted TECs. Interestingly, not all TECs gave origin to colonies (**Figure 1C**). Hence, serial dilution clonogenic assays offered a mean to quantify the colony-forming precursor frequency within TECs throughout normal and altered pathophysiological settings (a point addressed later in this study). Given their clonal origin, we referred to the cells that emerge from these cultures as *Clono*TECs. We also cultured postnatal-derived non-epithelial thymic stromal cells (CD45$^-$ EpCAM$^-$) under clonogenic conditions, but these lacks distinct colony-forming potential and did not generate *Clono*TECs as their CD45$^-$ EpCAM$^+$ counterparts (Supporting Information Figure 1D). Interestingly, *Clono*TECs contain a small fraction of cells with the capacity to regrow and re-establish clonal-derived colonies upon serial passages *in vitro* (**Figure 1D** and Supporting Information Figure 1E). The observations that *Clono*TECs were generated from a portion of TECs led us to investigate whether the clonogenic capacity was restricted to a subpopulation of cTECs and/or mTECs. To do so, we first purified by cell sorting cTECs (Ly51$^+$) and mTECs (UEA$^+$) from actin^{GFP} reporter mice and found that the clonogenic capacity was markedly enriched within cTECs (**Figure 1E**). Additionally,

we used CCRL1^{GFP} reporter mice, in which the combined analysis of the expression of CCRL1^{GFP} and CD80 defines discrete subsets of cTECs and mTECs in the postnatal thymus [131] (**Figure 1F**). While high levels of CCRL1^{GFP} cells (CCRL1^{hi}) identifies Ly51^{+} cTECs, intermediate levels of CCRL1^{GFP} define additional subsets of mTECs (UEA^{+} CD80^{-} and UEA^{+} CD80^{+}, as described in [131]) that arise in the postnatal thymus (**Figure 1F** and Supporting Information Figure 1F) Analysis of the discrete TEC subsets confirmed that the clonogenic capacity was mostly restricted to CCRL1^{hi} cTECs (**Figure 1F**). Limiting dilution clonogenic assays confirmed that colonies were of clonal origin and a property of a fraction of CCRL1^{hi} cTECs (Supporting Information Figure 1G). Yet, we also found residual clonogenic activity in CCRL1^{int} CD80$^{+/-}$ and CCRL1^{-} CD80^{+} expressing subsets (**Figure 1F**). Together, these results identified that most of colony-forming cells existed within cTECs (CD45^{-} EpCAM^{+} Ly51^{+} CCRL1^{hi}), suggesting that the postnatal cortical epithelial niche harbors cells with potential progenitor activity.

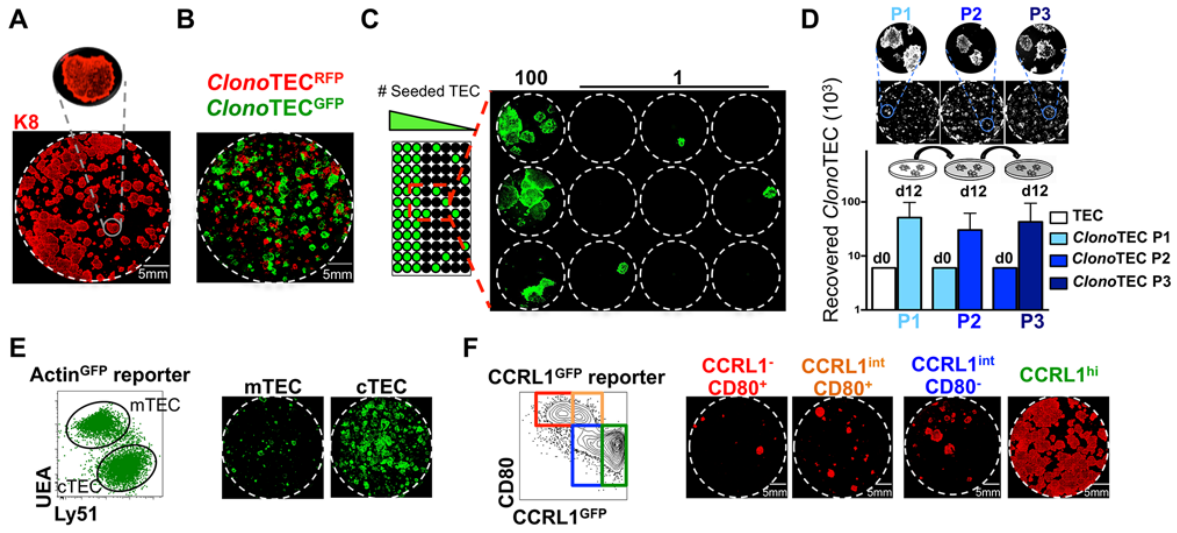

Figure 1. Colony-precursor cells are markedly restricted to the cortical thymic epithelium of the postnatal thymus. (**A**) Midscale clonogenic assays (6-well microplates) were established with cell-sorted total TECs (defined as CD45^{-}EpCAM^{+}) from postnatal day 5 (P5) thymus. After 12 days, cultures were fixed, stained with anti-cytokeratin 8 (K8) antibody and analyzed by immunofluorescence microscopy. **(B)** Cell-sorted total TECs purified from P5 Actin^{GFP} and Actin^{RFP} reporter mice were co-cultured at 1:1 ratio in midscale clonogenic assays and analyzed for the expression of GFP and RFP by fluorescence live cell imaging. **(C)** P5 Actin^{GFP} TECs were directly sorted at indicated densities into microscale clonogenic assay (96-well microplates) and the colony formation was analyzed by fluorescence live cell imaging. Green circles mark positive wells for clonogenic activity, while black circles mark wells with no activity (left).

Representative live-cell fluorescence images of indicated wells are shown (right). **(D)** *Clono*TECs contain cells with continual regrowth and colony-forming potential *in vitro*. Clonogenic assays were established with cell-sorted TECs from P5 Actin^{GFP} or Actin^{RFP} at the indicated density (6000 cells). 12 days after culture, *Clono*TECs (P1) were analyzed by flow cytometry (EpCAM$^+$ and GFP$^+$ or RFP$^+$), purified by cell sorting and re-cultured into clonogenic assays at the initial density (6000 cells) for two consecutive passages (P2 and P3). Representative scheme of the passages and live cell immunofluorescence analysis of indicated cultures at day 12 of each passage is displayed (top). The number of cells at day 0 (d0) and at day 12 (d12) from the different passages (P1-P3) is shown as mean ± SEM of a pool of 10 independent experiments. (**E**) cTECs and mTECs from P5 Actin^{GFP} were sorted and cultured under clonogenic assays. Cultures were analyzed for the expression of GFP by fluorescence live cell imaging. **(F)** TEC subsets from P5 CCRL1^{GFP} reporter mice were purified based on CCRL1^{GFP} and CD80 expression (as indicated in color gates) and cultured under clonogenic assays. Cultures were fixed, stained with anti-cytokeratin 8 (K8) antibody and analyzed by immunofluorescence microscopy. (A, B, E & F) Images represent complete individual wells from midscale clonogenic assays and are illustrative of at least three experiments. Scale bars, 5 mm.

*Clono*TECs display phenotypic and molecular traits of TEP-like cells

To determine the epithelial lineage identity of cTEC-derived *Clono*TECs that arise upon culture, we characterized them at phenotypic and molecular levels using a panel of pan-TEC, cTEC- and mTEC-restricted markers. As reference, we co-analyzed freshly isolated total TECs, cTECs and mTECs. Contrarily to *ex vivo* total TECs, *Clono*TECs lacked MHCII and expressed minute amounts of Foxn1 both at protein and mRNA levels (**Figure 2A and B**). To test whether *Clono*TECs derived from Foxn1- expressing cells that downregulated Foxn1 expression, we established clonogenic assays with cell-sorted cTECs from Foxn1^{eGFP} reporter mouse strain [30], in which nearly all TECs were marked by Foxn1^{eGFP} expression (Supporting Information Figure 2A). Notably, total, or even the highest, Foxn1^{eGFP} -expressing cTECs generated detectable colonies (containing *Clono*TECs) that lost GFP expression, as measured by live-cell fluorescence imaging and flow cytometry analyses (Supporting Information Figure 2B–D). Interestingly, *Clono*TECs expressed CD24 and Sca-1, which have been reported to identify epithelial stem cells in other anatomical sites, including breast and lung [154, 155] (**Figure 2A**). Furthermore, *Clono*TECs expressed low levels of CD205 and lacked Ly51 when compared to cTECs, and displayed little UEA binding capacity and lower levels of CD80 and lacked CD40 relatively to mTECs (**Figure 2A**). Additionally, we analyzed the molecular profile of purified *Clono*TECs for a restricted set of genes associated with cTECs (*Kitl*, *Dll4*, *Il7*, *Psmb11* (β5t), *Cxcl12* and *Ccl25*) or mTECs (*Ccl19*, *Ccl21*, *Tnfrs11a* (RANK) and *Aire*),

and found that *Clono*TECs expressed lower to undetectable levels of cortical- and medullary-associated transcripts. Collectively, these findings infer that *Clono*TECs segregate from prototypical mature TECs and typify instead a subset with TEP-like properties.

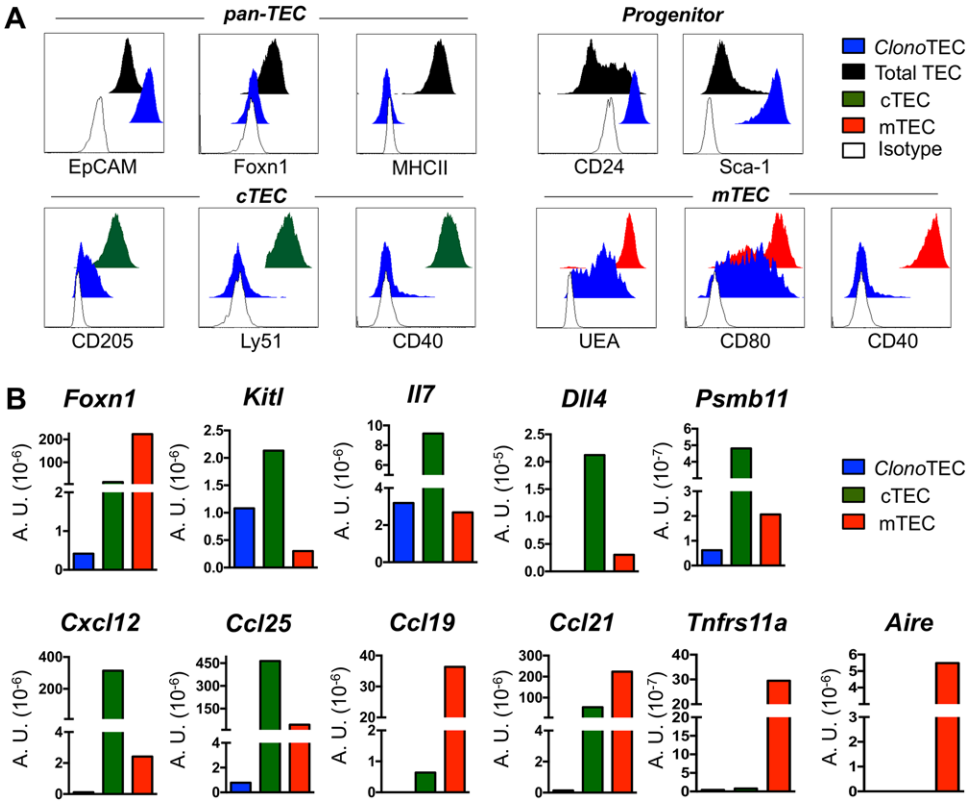

Figure 2. *Clono*TECs typify TEP-like cells. (**A**) cTEC-derived *Clono*TECs (blue) were analyzed by flow cytometry for the expression of the indicated markers. As a comparison, *ex vivo* bulk TECs (black), cTECs (dark green) or mTECs (red) isolated from postnatal day 7 thymus were co-analyzed. Isotype antibody controls for each antibody is represented (white) **(B)** *Clono*TECs, cTECs and mTECs were purified by cell sorting and analyzed by RT-qPCR for the expression of the indicated genes. Relative mRNA expression for represented target genes was normalized to *18s* and values are represented in arbitrary units (A.U.). Data are from single samples representative of two to three experiments using independent samples.

*Clono*TECs generate cTECs and mTECs *in vivo*

To define the *in vivo* lineage potential of *Clono*TECs, we combined the usage of clonogenic assays with reaggregate thymic organ cultures (RTOC) and thymic transplantation under the kidney capsule. As *Clono*TECs generated from CCRL1^{GFP}

cTEC lose GFP expression in culture (data not shown), they were not the most appropriate for fate mapping experiments. Since Ly51^{+} cTEC from Actin^{GFP} reporter mice exhibited similar clonogenic capacity to CCRL1^{GFP} cTEC from CCRL1^{GFP} reporter mice (**Figure 1**), we used purified *Clono*TECs (*Clono*TEC$^{ActinGFP+}$) generated from the first subset, in which constitutive active GFP expression provides an intrinsic label for subsequent lineage tracing *in vivo*. To reconstruct thymic epithelia microenvironments, we mixed *Clono*TEC$^{ActinGFP+}$ with dGUO-treated E14.5 thymic cells and the resulting hybrid RTOC was transplanted under the kidney capsule of WT mice to allow the ectopic formation of a thymus (Supporting Information Figure 3A). As control, dGUO-treated E14.5 thymus (*Clono*TEC$^{ActinGFP+}$ -free) were reaggregated and subjected to similar procedure. From 6 controls and 11 hybrids engrafted RTOCs, 4 and 8 ectopic thymi were respectively recovered 4 weeks post-thymic transplantation and analysed by flow cytometry and immunofluorescence microscopy. The progeny of *Clono*TEC$^{ActinGFP+}$ was distinctly present in all RTOCs as CD45-EpCAM^{+} cells, with a fraction of them expressing MHCII (Supporting Information Figure 3B). These findings indicate that *Clono*TECs contained cells competent to engage into the TEC differentiation pathway. Nevertheless, we recovered few TECs (either from embryonic or *Clono*TEC origin) from individual RTOCs for flow cytometry analysis. Thus, to gain insights about the phenotypic properties and spatial distribution of *Clono*TECs within native thymic niches, transplanted RTOCs were further analyzed by immunofluorescence microscopy. *Clono*TEC$^{ActinGFP+}$ - derived cells were found in all recovered RTOCs (Supporting Information Figure 3C-D), embedded within cortical (Ly51^{+} or K8^{+}) or medullary (UEA^{+}) microenvironments or positioned at the CMJ (intersection of K8^{+} and UEA^{+} areas) (**Figure 3A**). Although a fraction of *Clono*TEC progeny (GFP^{+}) lacked typical cTEC/mTEC markers, we found that some located within cTEC areas expressed cTEC traits, such as K8^{+} or Ly51^{+}, while others residing within mTEC areas displayed mTEC features, including UEA^{+} and MHCII^{hi} (**Figure 3A and B**). We also found rare Aire- expressing *Clono*TEC-derived cells within mTEC compartment, indicating their potential to complete mTEC maturation (**Figure 3A**). Additionally, to validate that *Clono*TEC-derived cells engaged in a TEC differentiation program, we performed similar reaggregation experiments using *Clono*TECs generated from Foxn1^{eGFP+} cTECs (Supporting Information Figure 3E). As Foxn1^{eGFP+} cTECs lose

Foxn1^{eGFP} expression *in vitro* (Supporting Information Figure 2), GFP expression provides in this case a dual label for lineage tracing and assessment of Foxn1^{eGFP} re-induction by *Clono*TECs- derived cells. We detected GFP-expressing cells only in RTOCs spiked with *Clono*TECs that derived from Foxn1^{eGFP+} cTECs (Supporting Information Figure 3F). *Clono*TECs-derived cells expressed EpCAM, with a fraction co-expressing MHCII and binding UEA (Supporting Information Figure 3G). Overall, these results indicate that cTEC-derived *Clono*TECs contain cells with the potential to generate cTECs and/or mTECs upon integration in native thymic microenvironments.

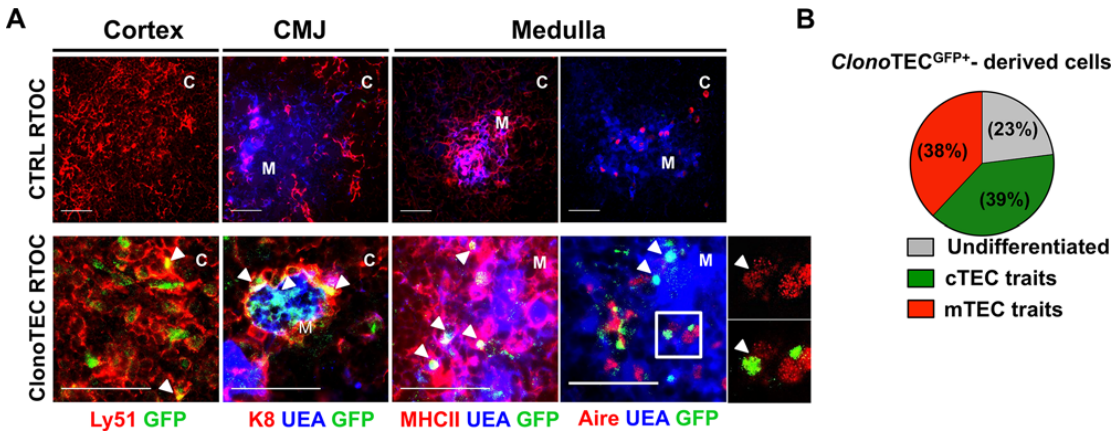

Figure 3. *Clono*TECs contain cells that are able to generate cTECs and mTECs *in vivo*. Generated cTEC^{ActinGFP}-derived *Clono*TECs^{GFP} were cell-sorted and aggregated with dGuo-treated E14.5 thymic lobes. RTOCs were transplanted into the kidney capsule of WT mice, ectopic thymi were recovered 4 weeks post-transplantation (Details in Supporting Information Figure 3A). **(A)** Immunofluorescence analysis of ectopic thymus. Control and *Clono*TECs post-transplanted RTOCs were co-analyzed for the expression of GFP, K8, Ly51, MHCII and Aire with specific antibodies and UEA binding capacity, with the indicated combinations in serial sections. Cortical (C) and medullary (M) regions were defined as either Ly51^{+} or K8^{+} areas and UEA^{+} or MHCII^{bright} areas, respectively. Triangles indicate examples of *Clono*TEC^{GFP+}-derived cells that display features of either cTEC (Ly51 or K8) or mTEC (UEA, MHCII, Aire) lineage traits. 50 µm scale is shown. Images are representative of 5 ectopic thymus containing *Clono*TEC^{GFP}. **(B)** Quantification of lineage fate distribution of *Clono*TECs. Pie graph represents the proportion of *Clono*TEC^{GFP+}-derived cells within the thymic grafts that express the above-indicated cTEC (green) or mTEC (red) markers. *Clono*TEC-derived cells (GFP^{+}) found within cTEC area (K8^{+} or Ly51^{+}) and expressing these markers were scored as cTECs. *Clono*TEC-derived cells (GFP^{+}) found within mTEC area (UEA^{+} and MHCII^{bright}) and binding UEA or expressing high levels of MHCII were scored as mTECs. *Clono*TEC-derived cells (GFP^{+}) found within cTEC and mTEC areas that lacked respective cTEC/mTEC-markers were considered as undifferentiated (gray).

The clonogenic activity of cTECs decreases with the entry into the adulthood

The observation that a fraction cTEC-derived *Clono*TECs maintains their clonogenic potential *in vitro* and generates cTECs and/or mTECs indicate that the cortical niche harbors TEC progenitors. Thus, we inferred that the measurement of the clonogenic potential of TEC subsets at neonatal, pre-puberty and young adult stages could be used as a proxy to survey alterations in TEP dynamics throughout time. In CCRL1 reporter mice, analysis of $CCRL1^{GFP}$ and CD80 expression allowed us to discriminate heterogeneous TEC subsets in the postnatal thymus [131]. While $CCRL1^{GFPhi}$ cTECs (gate D) were dominant in the neonatal period, distinct mTEC subsets (gates A, B, C), which either lacked or expressed intermediate levels of CCRL1) [131], expanded during the first weeks of age and predominated in the young adult thymus (**Figure 4A**). To determine the colony-precursor frequency within these detailed TEC subsets, we combined cell sorting, limiting dilutions in microscale clonogenic assays and high-content imaging microscopy. Given the clonal origin of TEC-derived colonies, we estimated the frequency of colony-forming cells by dividing the number of colonies by the number of sorted cells per well for each detailed subset (**Figure 4B**). We observed that clonogenic activity was highly restricted to the $CCRL1^{GFPhi}$ cTEC subset (gate D) at all time points analyzed (**Figure 4B**). Furthermore, we noticed that the clonogenic potential of $CCRL1^{GFP}$ cTECs gradually decreased from postnatal day 5 to young adult thymus (**Figure 4C**). To further evaluate the reduction in colony-forming potential of cTECs with time, we established competitive clonogenic assays with age-matched or age-mismatched cTECs isolated from $Actin^{GFP}$ and $Actin^{RFP}$ report mice. While co-culture experiments with $cTEC^{ActinGFPhi}$ and $cTEC^{ActinRFP}$ from post- natal day 5 thymus yielded a similar respective proportion of GFP^+ or RFP^+*Clono*TECs, cTECs purified from postnatal day 5 thymus showed a marked clonogenic advantage over cTECs isolated from 2-week-old counterparts (Supporting Information Figure 4). Together, our findings suggest that TEP-like cells within cTECs autonomously lose the clonogenic capacity with the entry into the adulthood.

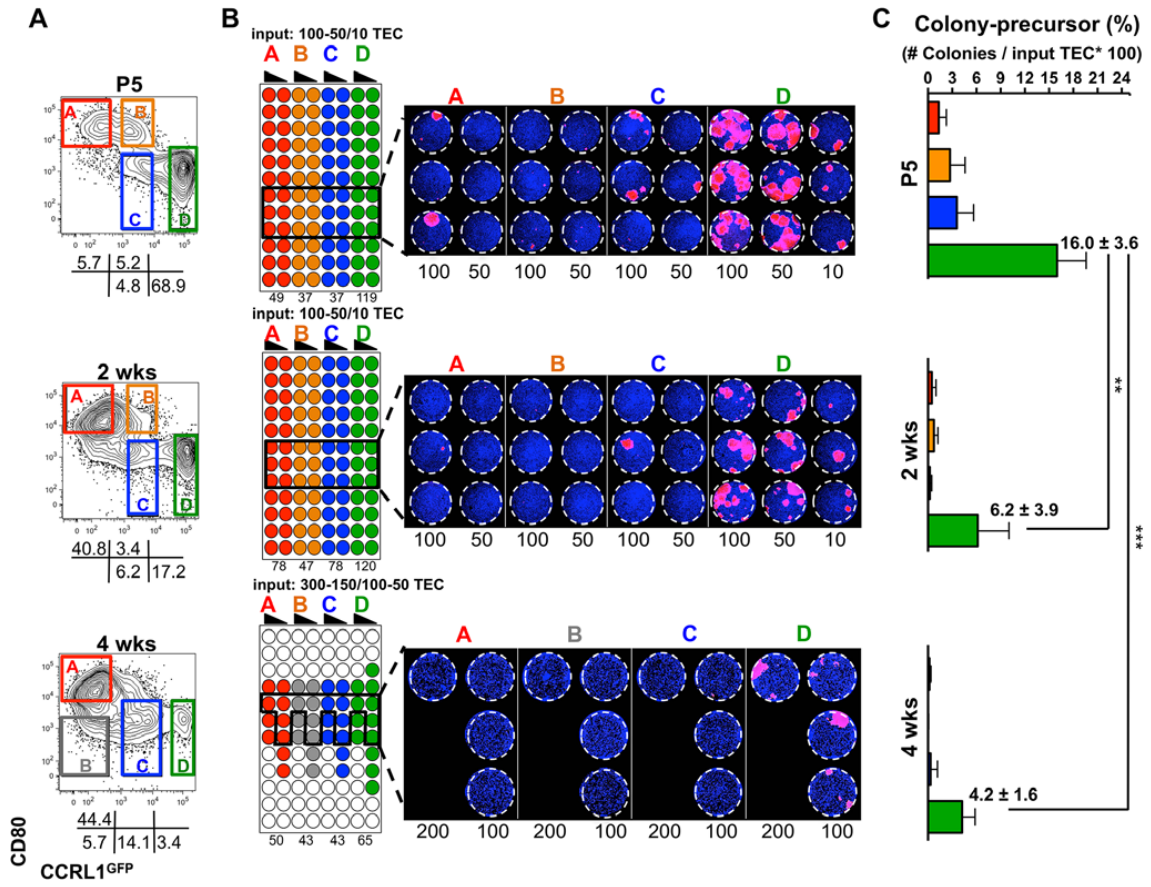

Figure 4. The pool of TEC colony-precursor cells residing within the postnatal cortex decreases during the transition from postnatal to adult life. (**A**) TECs from CCRL1^{GFP} reporter mice were analyzed by flow cytometry at indicated time-points for the expression of CCRL1^{GFP} and CD80. Proportions of indicated subsets are shown below the plots. **(B)** Colored TEC subsets (A-B-C-D) illustrated in (A) were purified by cell sorting and cultured in microscale clonogenic assay (96-well microplates) at designated cell densities (input: as represented on the top of the schematic plate). Numbers below each schematic plate represent the total amount of wells analyzed per subset (left). Representative images of full individual wells for each time point and TEC subset are shown (right). Number of plated cells (input) is shown below. 96-well plate cultures were fixed, stained with anti-cytokeratin 8 (K8) Ab and analyzed by high-content immunofluorescence microscopy. Data shown are representative of three to four experiments performed per time point. **(C)** Colony-precursor cell frequency (%) was estimated by dividing the number of colonies obtained by the number of seeded TEC (input) x 100. Data are shown as mean ± SEM of a pool of 5 (p5), 6 (2 wks) and 9 (4 wks) independent experiments. ** $p< 0.005$ *** $p< 0.001$, the two-tailed Mann–Whitney U test.

The clonogenic potential of TECs is sustained in alymphoid thymus

Just as TECs have a central function in T-cell development, thymocytes are in turn vital to TEC maturation [144]. Albeit lympho-epithelial interactions are often considered

stimulatory to TEC differentiation, and in particular to the expansion of the mTEC network, we previously conjectured that signals provided by developing thymocytes might restrain functional properties coupled to immature TECs [144]. To determine whether the loss in clonogenic potential of cTECs was directly linked to thymocyte-driven TEC differentiation, we used *Rag2*$^{-/-}$*Il2rg*$^{-/-}$ CCRL1^{GFP} -reporter mice, in which T-cell development is profoundly blocked at early stage of development. Consequently, TEC maturation is severely arrested in these mice due the lack of maturation signals delivered by lymphoid cells. Specifically, apart of virtually lacking mature CD80^{+} mTECs, *Rag2*$^{-/-}$*Il2rg*$^{-/-}$ thymus display a partial blockade in full CCRL1 and MHCII expression [131, 132] (**Figure 5A**). We performed limiting dilution clonogenic assays (as described in Figure 4) with TECs that either lack or express intermediate and higher levels of CCRL1 isolated from 2- and 6-week-old *Rag2*$^{-/-}$*Il2rg*$^{-/-}$ thymus. We found that the capacity to generate colonies was scattered among the three TEC subtypes in the 2-week-old thymus, progressively increasing within TECs expressing higher levels of CCRL1 (CCRL1^{GFPhi}) (**Figure 5B and C**). Notably, the frequency of colony-precursor cells was sustained within the three TEC subsets in the 6-week-old *Rag2*$^{-/-}$*Il2rg*$^{-/-}$ thymus (**Figure 5C**). The maintenance of the pool of cells with clonogenic capacity was also notorious when their absolute cellularity was extrapolated within the total number of TECs of the alymphoid thymi and longitudinally compared to their abundance in immunocompetent counterparts (**Figure 5D**). These results indicate that thymocyte-derived signals might negatively affect the clonogenic potential of TECs during life.

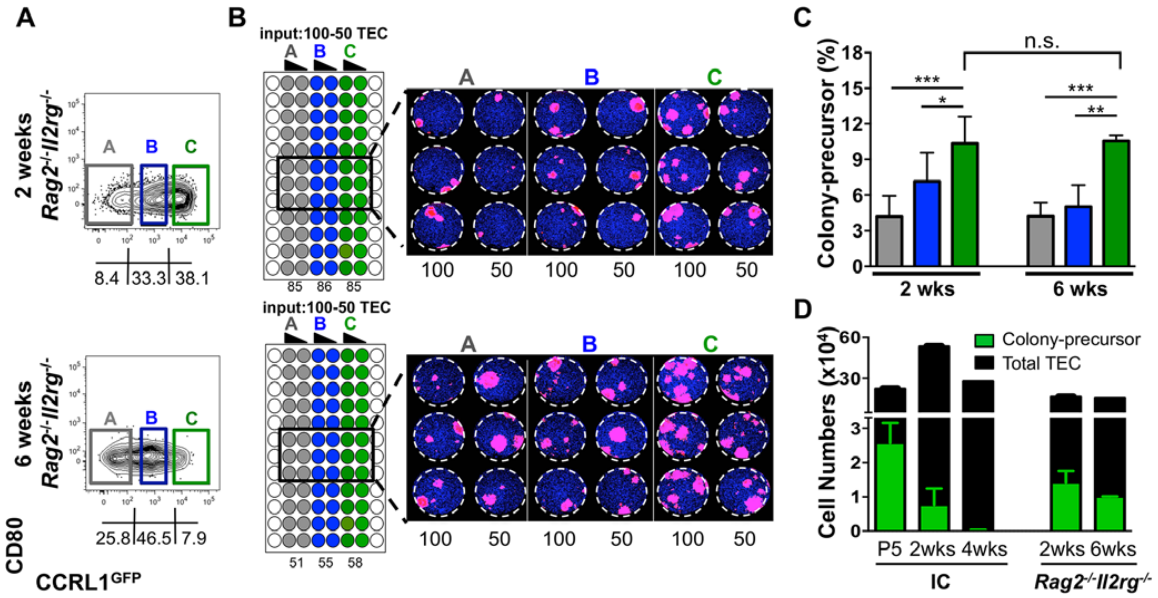

Figure 5. The pool of TEC colony-precursor cells is sustained in the adult *Rag2*$^{-/-}$*Il2rg*$^{-/-}$ thymus. (**A**) TECs from *Rag2*$^{-/-}$*Il2rg*$^{-/-}$ CCRL1^{GFP} mice were analyzed by flow cytometry at indicated time-points for the expression of CCRL1 ^{GFP} and CD80. Proportion of indicated subsets are shown below the plots. (**B**) Colored TEC subsets (A-B-C) illustrated in (A) were purified by cell sorting and cultured in microscale clonogenic assay (96-well microplates) at designated cell densities (input: as represented on the top of the schematic plate). Numbers below each schematic plate represent the total amount of wells analyzed per subset (left). Representative images of full individual wells for each time point and TEC subset are shown (right). Number of plated cells (input) is shown below. 96-well plate cultures were fixed, stained with anti-cytokeratin 8 (K8) Ab and analyzed using a high-content immunofluorescence microscopy. Data shown are representative of three to four experiments per time point. **(C)** Colony-precursor cell frequency (%) was estimated based on the number of colonies relatively to the number of seeded TECs (as in Fig. 4C). Data are shown as mean ± SEM of a pool of 6 (2 wks) and 4 (6 wks) independent experiments. *p<0.05 **p<0.005 ***p<0.001, the two-tailed Mann–Whitney U test. (**D**) Number of colony-precursor cells (green) within total TEC (black) for immunocompetent (IC) (Fig. 4) and *Rag2*$^{-/-}$*Il2rg*$^{-/-}$ (this figure) mice. The number of colony-precursor cell was estimated based on the frequency of these cells within the total TEC cellularity for a given time. IC: Data are shown as mean ± SEM of a pool of 3 (p5), 4 (2 weeks) and 3 (4 weeks) independent experiments; *Rag2*$^{-/-}$*Il2rg*$^{-/-}$: Data are shown as mean ± SEM of a pool of 3 (2 weeks) and 3 (6 weeks) independent experiments.

Since lympho–epithelial interactions are minimal in *Rag2*$^{-/-}$*Il2rg*$^{-/-}$ mice [132], we also analyzed the clonogenic potential of *Rag2*$^{-/-}$ CCRL1^{GFP} – reporter mice in which T cell development is blocked at the double negative (DN) 3 stage [156], which leads to the development of some CD80^{+} mTECs (Supporting Information Figure 5A). Similar to the results obtained in *Rag2*$^{-/-}$*Il2rg*$^{-/-}$ mice, the frequency of colony-precursor was maintained in TEC isolated from adult *Rag2*$^{-/-}$ background (Supporting Information Figure 5). These

results indicated that interactions between DN T cells – TECs are not sufficient to induce the decrease of clonogenic activity detected in normal mice.

Lympho-epithelial interactions control the clonogenic potential of TECs

To directly assess the influence of thymocyte-TEC crosstalk on TEC clonogenic capacity we reconstituted 6-week-old *Rag2*$^{-/-}$*Il2rg*$^{-/-}$ CCRL1-reporter mice with bone marrow (BM) precursors from WT mice and analyzed the frequency of colony-forming cells of recipient mice 6 weeks post-transplantation. As expected, the number of CD45^{+} cells increased and T-cell development was corrected in the thymus of WT BM-reconstituted *Rag2*$^{-/-}$*Il2rg*$^{-/-}$ CCRL1^{GFP}-reporter mice (data not shown), restoring the differentiation of CD80^{+} mTECs and the normal cTEC/mTEC segregation (**Figure 6A**). The conditioning sub-lethal irradiation protocol prior to BM transplantation and age did not alter the clonogenic activity of TECs from 12-week-old non-reconstituted *Rag2*$^{-/-}$*Il2rg*$^{-/-}$ CCRL1^{GFP} -reporter mice (**Figure 6B and C**), as the frequency of colony-forming cells in TECs that either lack or express inter- mediate and higher levels of CCRL1 was similar to the ones in unconditioned 6-week-old mice (**Figure 5C**). Strikingly, the clonogenic potential of purified cortical/medullary subsets from WT BM-reconstituted *Rag2*$^{-/-}$*Il2rg*$^{-/-}$ CCRL1-reporter mice exhibited a notorious reduction and restriction to the CCRL1^{GFPhi} TEC subset (**Figure 6B and C**), normalizing to the profile observed in young immunocompetent mice. Collectively, our findings demonstrate that continual thymic crosstalk negatively regulates TEC clonogenic activity.

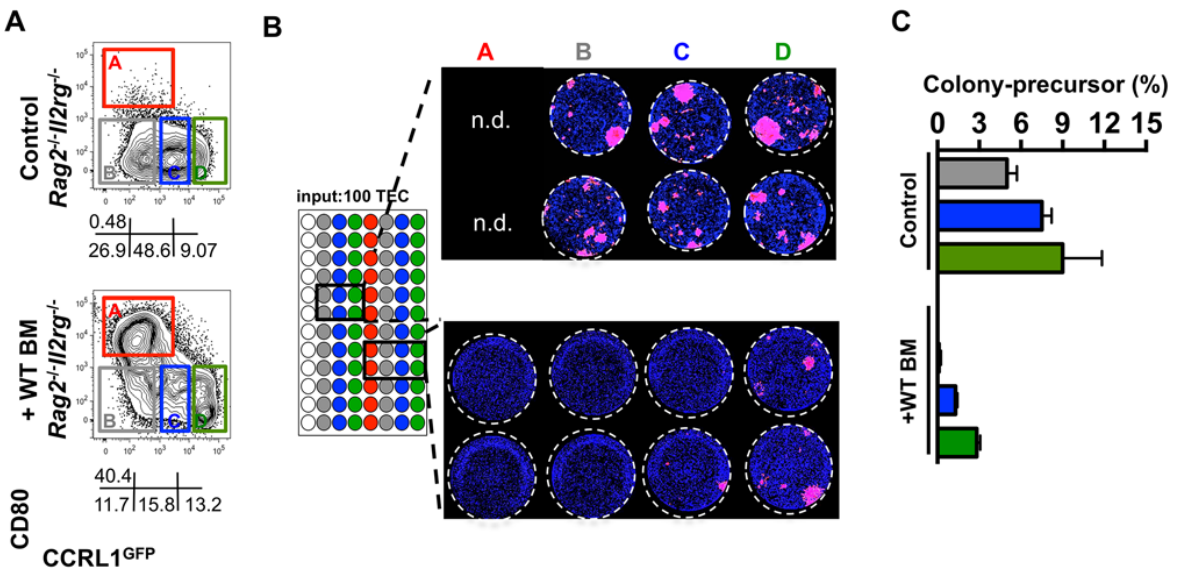

Figure 6. Thymocyte-derived signals negatively impact the pool of TEC colony-precursor cells. *Rag2*$^{-/-}$*Il2rg*$^{-/-}$ CCRL1^{GFP} mice were reconstituted with WT BM precursors (+WT BM) or left non-reconstituted (Control). **(A)** TECs from control and WT BM-reconstituted *Rag2*$^{-/-}$*Il2rg*$^{-/-}$ CCRL1^{GFP} mice were analyzed by flow cytometry for the expression of CCRL1 ^{GFP} and CD80. The proportion of indicated subsets is shown below the plots. **(B)** TEC subsets (A-B-C-D) illustrated in **(A)** were purified by cell sorting and cultured in microscale clonogenic assay (96-well microplates) at designated cell densities (input: as represented on the top of the schematic plate). Representative images of full individual wells for each time point and TEC subset (right). 96-well plate cultures were fixed, stained with anti-cytokeratin 8 (K8) Ab and analyzed using a high-content immunofluorescence microscopy. n.d. (not determined). Data are representative of two experiments. **(C)** Colony-precursor cell frequency (%) was estimated by dividing the number of colonies obtained by the number of seeded TEC (input) x 100. Data are shown as mean ± SEM of 3 control and 4 WT BM-reconstituted samples from a pool of two independent experiments.

Discussion

Comprehending the principles that underlie the maintenance of cortical and medullary thymic epithelial compartments is chief to harness thymopoiesis in the elderly and in patients with immunodeficiency disorders or autoimmunity. Therefore, the prospective isolation of TEPs within the adult thymus has emerged as a central objective in thymic biology, as it would provide means for reconstructing functionalized thymic epithelial microenvironments in therapies targeting thymus disorders. An aspect of equal importance that has been overlooked pertains to the principles that control the bioavailability and functionality of those progenitors in the adulthood. Given that TEC network expands vigorously during the period between birth and early adulthood, we

centered our attention in this temporal window with the premise that it might reveal new insights on how TEP homeostasis is balanced *in vivo*. Our temporal analysis of TEC clonogenic potential suggests that the postnatal life defines a period of intense stem cell-like activity within the thymic cortex, which gradually diminished thereafter with the entry into the adulthood as a result of lympho-epithelial interactions. These findings support the notion that the pool of TEPs and/or their replenish rate deteriorates across life, providing a possible explanation to their incapacity to sustain functional epithelial niches in the aged thymus.

Detailed phenotypic and molecular analyses show that *in vitro*- generated *Clono*TECs lacked traits that are typically associated with cortical or medullary lineages, but instead expressed markers linked to stem cells. These observations correlate with their reduced levels of Foxn1, which is central for the initiation and maintenance of the TEC program but appears dispensable for the maintenance of the thymic epithelial stem cell pool [127, 148, 157]. Using Foxn1^{eGFP} reporter thymus, we showed that *Clono*TECs derived from Foxn1-expressing cTEC lose Foxn1 expression *in vitro*, indicating that Foxn1 levels are tightly controlled by thymic microenvironmental factors. Nonetheless, our understanding on the molecular signals that initiate and sustain the expression of this master regulator of TEC identity *in vivo* requires further analysis. Importantly, the findings that a fraction of *Clono*TECs retains continual clonogenic potential *in vitro* and contain cells that can diversify into cTECs and mTECs *in vivo* reinforce their TEP-like signature. Still, the progeny of *Clono*TECs that reintegrated within thymic microenvironment was limited. Whether the low engraftment of *Clono*TECs is due to experimental impediments related to the establishment of organotypic cultures or competitive disadvantage relatively to embryonic TEP within RTOCs is unclear. For technical reasons related with the establishment of RTOCs, the proportion of *Clono*TECs within the hybrid RTOCs before thymic transplanting was reduced relatively to TECs derived from E14.5 “carrier” thymus (1:5-16:1). The abundance and/or competitive fitness of *ex vivo* embryonic TEC progenitors might under these conditions limit the integration, maintenance and the generation of a more prominent *Clono*TEC-derived progeny 4 weeks after transplantation. Moreover, and similarly to the capacity to continual establish colony-forming units, it is possible that only a fraction of *Clono*TECs developed within the ectopic thymus and

contributed to the TEC network. Future studies should address the long-term maintenance of *Clono*TECs within native thymic niches. This technical limitation seems to be common to several studies using hybrid RTOCs, which are composed of predominant embryonic thymic stromal cells mixed with adult TEC subsets purportedly enriched with TEPs [146-148]. Furthermore, due to high cell density requirements to perform RTOC experiments, we used a pool of cTEC-derived *Clono*TECs from multiple colonies. This technical impediment has precluded testing the lineage potential of cTEC-derived *Clono*TECs from individual colonies or residual mTEC-derived *Clono*TECs. Despite phenotypic similarities at a population level, possible intra- and inter-clonal heterogeneity within *Clono*TECs might also influence their engraftment and lineage potential. Hence, it is possible that *Clono*TECs contain cTEC- and mTEC-producing cells. Nonetheless, *Clono*TECs were originally generated from cells with a prototypical cTEC features, suggesting that the cortical thymic epithelium compartment harbors cTEC and/or mTEC precursors. Future refined experimental setups are required to address these possibilities at the single cell level with the purported postnatal-derived TEC progenitors, as reported earlier with embryonic cells [126]. Furthermore, apart of lineage tracing assays, it would be equally important to unravel whether postnatal-derived TEC progenitors can functionally contribute to thymopoiesis.

Using distinct experimental approaches, three recent reports have revealed the existence of TEC stem cell activity within the adult thymus. First, Ucar *et al*. reported the presence of EpCAM^{-} Foxn1^{-} cells within the thymic stroma that form under specialized *in vitro* culture system spheroids, so-called thymosphere, with the capacity to generate cTECs and mTECs [146]. We reason that cTECs with colony-forming capacity described in our report are distinct from thymosphere-generating cells. First, although the location of thymosphere-forming cell remains undetermined, *Clono*TECs arise from a fraction of cells belonging to the prototypical cTEC lineage (EpCAM^{+} Ly51^{+} CCRL1^{+}). Secondly, CD45^{-} EpCAM^{-} thymic stromal cells failed to form *Clono*TEC-containing colonies in our experimental condition. Despite being hitherto phenotypically undistinguishable from cTECs lacking clonogenic activity, *Clono*TEC- generating cTECs might encompass a subset of progenitor cells nestling in the cortical compartment that have not completed the cTEC maturation program. In this regard, Wong *et al*. documented that bipotent TEPs

exist within a fraction of UEA-1^{-}MHII^{lo} cTEC- like cells of the adult thymus [147] and Ulyanchenko *et al*. further mapped them to a fraction of Ly51^{+} MHCII^{hi} Plet1^{+} cTECs [148], inferring in agreement with our results that TEPs share to some extent a cortical-associated signature. Along this line, genetic inducible cell-fate mapping studies by Ohigashi *et al*. and Mayer *et al*. found that a large fraction of adult cTECs and mTECs develop from fetal- and newborn-derived TECs expressing β5t [150, 151]. These findings suggest that TEC differentiation in the postnatal period follows a similar process to the one defined in the embryonic life [128], in which the cortex represents a reservoir of TEPs wherefrom they can potentially differentiate into cortical and medullary epithelial lineages. However, it remains to be elucidated whether cTEC-derived *Clono*TECs and other recently identified subsets enriched in TEP-like cells, contain truly bipotent progenitors or unipotent progenitors for each lineage. It is important to underline that even with the most refined subsets and distinct assays, TEC precursors are still being described at the population level but are not yet recognized at the single-cell level. Albeit it is conceptually possible that several pools of TEP-like cells exist within the thymus, further studies are required to determine the lineage and temporal relationship between the distinct types of TEPs that are being disclosed within the postnatal thymus.

It remains unclear how TEC stem cell activity is controlled in the adult thymus. The incapacity of TEPs to undergo compensatory proliferation to maintain the mature TEC compartment [143] indicates a deficit in their stemness. The progenitor features of *Clono*TECs led us to use the colony-forming potential as a surrogate to survey the dynamics of TEP during early postnatal life and adulthood. Our findings indicate that clonogenic activity is predominantly enriched in cTECs during the first week of life. Previous observations showed that cTECs regenerate after the specific ablation of CCRL1^{hi} cTECs [17]. Nevertheless, the complete cTEC depletion was not achieved in this study and therefore resistant TEP within CCRL1-expressing subset might explain the observed regenerative capacity of cortical epithelium. The drop in the clonogenic activity of CCRL1^{hi} cTECs in the ensuing weeks might suggest that the bioavailable pool of TEPs is reduced with the entry into the adulthood. In this regard, the contribution of β5t^{+} progenitors to cTEC and mTEC lineages declines postnatally [150, 151] and TEPs isolated from the adult thymus are extremely rare cells [146, 147, 150]. The maintenance

of TEC clonogenic activity in 6- and 12-week-old alymphoid thymus suggests that aging is, not per se, a determinant in this process. In particular, we observed that clonogenic activity was enriched in CCRL1^{hi} cTEC-like subset of *Rag2*$^{-/-}$*Il2rg*$^{-/-}$ mice, indicating that TEPs might progress through, and settle within, the cortical lineage in a thymocyte-independent manner. In fact, bone marrow reconstitution experiments revealed that clonogenic potential is dynamically modulated by interactions with developing thymocytes. Similar observations were recently suggested to Cld3,4^{+}SSEA1^{+} mTEC-restricted cells, which are rare in the adult thymus and enriched in *Rag2*$^{-/-}$ mice [134]. These findings provide evidence for a negative feedback mechanism in which continual thymic crosstalk fine-tunes the homeostasis of distinct TEPs. Thymocyte-derived signals are often considered stimulatory for TEC differentiation [30]. Nonetheless, previous studies, including from our group, have shown that thymocyte-TEC crosstalk negatively regulates functional attributes coupled to cTECs, including the expression of DLL4 and IL-7 [87, 158]. Now, our findings implicate that thymocyte-derived signals might act at the root of the TEC differentiation branch, deteriorating the pool of TEPs and possibly limiting their replenishment rate. It remains how- ever opened whether these effects are mediated by direct or indirect lympho–epithelial interactions. These notions might provide a possible explanation to the failure in sustaining TEC compartments in the aged thymus [16] and the success of inducing cTEC and mTEC niches in WT BM-reconstituted adult mice that lacked previous functional lympho-epithelial crosstalk [132, 159]. Last, our data question whether the mere prospective isolation of bipotent progenitors from the adult and aged thymus represents the more desirable strategy for cellular replacement therapies in thymic disorders. Alternative approaches might focus in unraveling active mediators of stem cell activity, which will permit a more effective functionalization of TEPs isolated the adult thymus.

Material and Methods

Mice

Transgenic Actin reporter C57BL/6J mice in which the chicken β-actin promoter

respectively drives enhanced Green Fluorescent Protein (eGFP) ($Actin^{GFP}$) or Red Fluorescent Protein (RFP) ($Actin^{RFP}$) expression were purchased from Jackson Laboratory. Ccrl1:eGFP ($CCRL1^{GFP}$) [17] and $Foxn1^{eGFP}$ reporter mice [30] were kindly provided by Dr. Thomas Boehm (Germany). Ccrl1:eGFP ($CCRL1^{GFP}$) reporter mice were used as such or were backcrossed onto *Rag2*$^{-/-}$*Il2rg*$^{-/-}$ or *Rag2*$^{-/-}$ [132] C57BL/6J background. For thymic transplantation, 6-8-week-old C57BL/6J mice were used as recipients. Mice were housed under specific pathogen- free conditions and experiments were performed in accordance with institutional guidelines. For fetal studies, the day of vaginal plug detection was designated embryonic day (E) 0.5.

TEC Clonogenic assay

FACS sorted TECs were cultured onto a feeder layer of irradiated mouse embryonic NIH/3T3 (3T3) fibroblast cell line as described [152, 153]. 3T3 cells were regularly maintained in culture using Dulbecco-Vogt modification of Eagle's Medium (DMEM, Gibco–Invitrogen) supplemented with 10% fetal bovine serum (FBS) and penicillin/streptomycin. For the preparation of feeder layer, 3T3 cells were irradiated (60 Gy) one day before the experiment, seeded onto 6-well (midscale) or 96-well culture plates (microscale) coated with 0,05mg/mL of fibronectin (Sigma- Aldrich), at a density of 12.5×10^4 cells cm^{-2} or 5×10^4 cells per cm^{-2}, respectively. TEC purified by cell sorting were directly cultured onto feeder layer in a specialized medium consisting of a 3:1 mixture of DMEM and Ham's F-12 medium (Gibco–Invitrogen), supplemented with 10% FBS, hydrocortisone 0.4 µg mL^{-1}, 10^{-}6 M cholera toxin, 5 µg mL^{-1} insulin, 2×10^{-9} M 3,3',5-triiodo-L- thyronin (T3), 10 ng ml^{-1} recombinant human epidermal growth factor rhEGF, and penicillin/streptomycin (Peprotech). All cul- tures were performed at 37°C in a 7% CO_2 atmosphere for 12 days. Colonies were firstly revealed by hemacolor staining (Merck) according to the manufacturer's instructions or processed for flow cytometry or immunofluorescence microscopy analyses as described below.

TEC and ClonoTEC isolation and flow cytometry analysis

TECs were isolated as described [87]. *Clono*TEC were recovered from clonogenic assays using 0.05% trypsin-EDTA (Gibco- Invitrogen), followed by cold PBS supplemented with 10% FBS to stop the reaction. Single-cell suspensions were stained with anti-Ly51 (PE) (BD Biosciences); anti-Sca-1 (BV785); anti-CD24 (BV510) and anti-EpCAM (BV421) (BioLegend); anti–I-A/I-E (Alexa 780); anti-CD45.2 (PerCP-Cy5.5); anti-CD40 (PE); anti-CD205 (biotin); UEA-1 (biotin); anti-CD80 (APC) and streptavidin (PE-Cy7) (eBioscience); anti-FOXN1 (Alexa 647) [38] was kindly provided by Dr. Hans-Reimer Rodewald (Germany). For intracellular staining, cells were fixed and permeabilised with the Transcription Factor Staining Buffer Set (eBioscience) according to the manufacture's instructions. Flow cytometry analysis was performed with the LSRFortessa instrument (BD Biosciences) and FlowJo software. Cell sorting was performed using the FACSAria II (BD Biosciences), with sort purities >95%.

Immunofluorescence analysis

Immunofluorescence staining was performed directly either on midscale and microscale clonogenic assays or on 8-µm sections of reaggregate thymic organ cultures (RTOCs) samples. Cultures or Thymus were fixed in 4% paraformaldehyde (Electron Microscopy Sciences) and stained with rabbit anti-GFP (Thermo Fisher Scientific), rat Troma-I (kindly provided by Drs. Brulet and Kemler), rat anti–I-A/I-E, rat anti-Aire, UEA1- or Ly51-biotinilated (eBioscience); and revealed with secondary Alexa Fluor 488 anti- rabbit, Alexa Fluor 647 anti-rat, or streptavidin Alexa 555 (Invit- rogen). Nuclei were stained with DAPI (Invitrogen). Vectashield mounting medium (Vector Laboratories) was used to prepare the slides. Analysis was performed with IN Cell Analyzer 2000 (GE lifesciences) and collected images were processed with Fiji Software.

Gene expression

For quantitative PCR, mRNA from sorted cells was purified using the RNeasy Micro Kit (QIAGEN). RNA was reverse transcribed to cDNA, using the SuperScript III First-Strand Synthesis System for RT-PCR (Invitrogen) and Random Hexamers (Fermentas), and then subjected to real-time PCR using TaqMan Universal PCR Master Mix (Applied Biosystems) and primers for *18s*, *Foxn1*, *Il7*, *Psmb11*, *Tnfrsf11a*, *Aire, Kitl, Dll4, Cxcl12, Ccl25, Ccl19, Ccl21* (Applied Biosystems). All samples were analyzed as triplicates, and the Ct method was used to calculate relative levels of tar- get mRNA compared with *18s*. Procedures were done according to the manufacturer's protocols. Real-time PCR was performed in an iCycler iQ5 Real-Time PCR thermocycler (Bio-Rad). Data were analyzed using iQ5 Optical System software (Bio-Rad).

RTOC

Freshly isolated E14.5 thymic lobes were used to establish RTOCs, as described [13]. Previous to aggregation, embryonic lobes were cultured for 3 days in DMEM supplemented with 10% FBS and 360mg/L 2-deoxyguanosine (dGuo) (Sigma-Aldrich). *Clono*TEC^{GFP+} were sorted to high purity (>95%). RTOCs were established from mixtures of 50,000–150,000 Actin $^{GFP+}$ or Foxn1^{eGFP} –derived *Clono*TECs with E14.5 thymic cells at 1:16 to 1:5 ratios, and transplanted under the kidney capsule of WT mice. Ectopic thymus were recovered after 4 weeks of transplantation and analyzed by flow cytometry or immunohistochemistry.

Bone marrow chimeras

A total of 10^7 CD3-depleted bone marrow (BM) cells (MACS MicroBead, Miltenyi Biotec) from 6-week-old wild-type (WT) C57BL/6J donors were injected i.v. in 6-week-old sublethally irradiated (0.4Gy) *Rag2*$^{-/-}$*Il2rg*$^{-/-}$ CCRL1-reporter mice.

Statistical analysis

Statistical analysis of the results was made using GraphPad Prism Software. The two-tailed Mann–Whitney U test was used for analysis between groups. A 95% confidence interval was applied in the calculations, and samples with p values < 0.05 were considered significant (*).

Acknowledgements

We thank Thomas Boehm (Max Planck Institute of Immunology and Epigenetics, Freiburg, Germany) for Foxn1^{eGFP} reporter mice. We thank Dr. Hans-Reimer Rodewald (German Cancer Research Center, Heidelberg, Germany) for the anti-Foxn1 antibody. We thank Dr. Leonor Araújo for technical support and Drs. Chiara Perrod and Gema Romera-Cardenas for critical reading the manuscript. We also thank Dr. Sofia Lamas and the caretakers from the animal facility for the assistance with animal experimentation.

C.M., A.R.R., and N.L.A. conceived and designed experiments, performed experiments, analyzed the data, and wrote the manuscript. P.M.R., R.D.P., and C.L. performed experiments and analyzed data. N.L.A. conceptualized the original idea.

This work has received funding from the European Research Council (ERC) under the European Union's Horizon 2020 research and innovation programme (grant agreement No 637843 - TEC Pro), from FEDER - Fundo Europeu de Desenvolvimento Regional funds through the COMPETE 2020 - Operacional Programme for Competitiveness and Internationalisation (POCI), Portugal 2020, and by Portuguese funds through FCT - Fundação para a Ciência e a Tecnologia/Ministério da Ciência, Tecnologia e Ensino Superior in the framework of the project "Institute for Research and Innovation in Health Sciences" (POCI- 01-0145-FEDER-007274) and FEDER funds through the Operational Competitiveness Programme – COMPETE and by National Funds through FCT – Fundação para a Ciência e a Tecnologia under the project FCOMP-01-0124-FEDER-021075 (PTDC/SAU- IMU/117057/2010). N.L.A., P.M.R.,

A.R.R., C.M., and R.D.P. are supported by the Investigator program, Post-doctoral and PhD fellowships from FCT (Portugal).

Supplementary Information

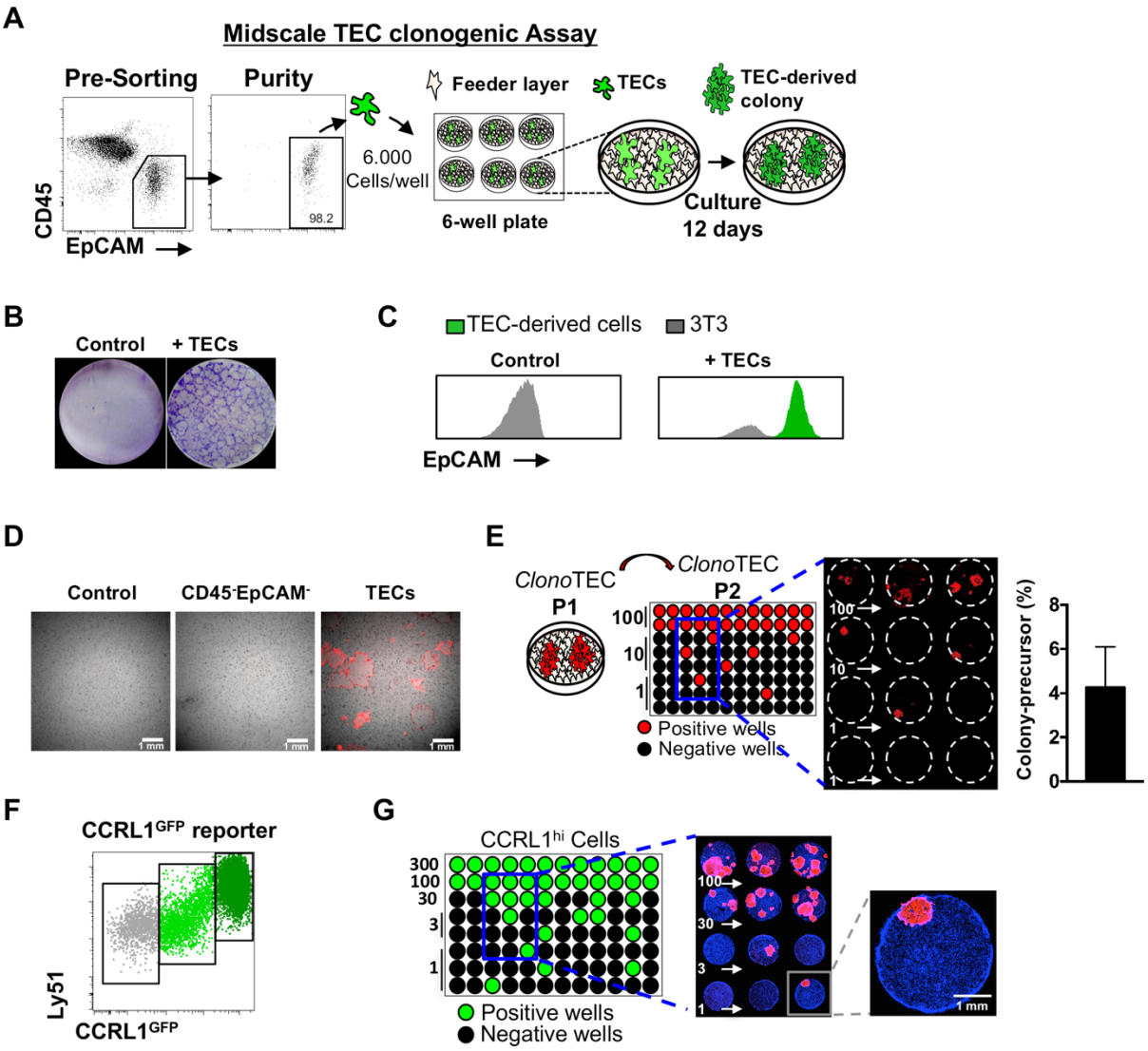

Supporting Information Figure 1. Postnatal cortical (CCRL1^{GFPhi}) thymic epithelial cells (TECs) are enriched in cells with clonogenic capacity. (A) A schematic representation of Midscale Clonogenic Assay. TECs were purified by cell sorting. Flow cytometry analysis of postnatal day 5 (P5) thymus before (Pre-sorting) and after TEC purification by cell sorting (Purity). Six thousand cell-sorted total TECs were seeded onto feeder layer (irradiated 3T3s) in clonogenic assays (as described in Material & Methods) in flat-bottomed 6-well microplates and cultured for 12 days. **(B)** Representative macroscopic images of clonogenic assays in the absence (control) or presence of TECs (+TECs). Hemacolor staining revealed TEC colonies 12 days after culture. **(C)** P5-derived colonies were analyzed by flow cytometry for EpCAM in clonogenic assays set in the absence (control) or presence of TECs (+TECs). **(D)** Six thousand cell-sorted total TECs or non-TEC stromal cells (CD45^{-}EpCAM^{-}) from P5 Actin^{RFP} mice were cultured into midscale clonogenic assay. Control cultures only with feeder cells are shown (Control). The colony formation was determined by brightfield and fluorescence live cell imaging after 12 days in culture. Images

represent complete individual wells and are illustrative of three experiments. (**E**) Clonogenic assays were established with cell-sorted TECs from P5 Actin^{RFP} at the indicated density (6.000 cells). 12 days after culture, *Clono*TECs (P1) were analyzed by flow cytometry (EpCAM^{+} RFP^{+}), purified by cell sorting and recultured into 96-well microscaled clonogenic assays at the indicated densities (100, 10 and 1 cell per well) (scheme: Red circles mark positive wells for clonogenic activity, black circles mark wells with no activity). Representative images of individual wells are shown. Graph represents the colony- precursor cell frequency (%) of *Clono*TECs from passage 1 (P1), estimated by dividing the number of colonies obtained by the number of seeded TEC (input) x 100. Images represent complete individual wells and are illustrative of three experiments. **(F**) Total TECs (CD45^{-} EpCAM^{+}) from postnatal day 5 (P5) CCRL1^{GFP} reporter mice were analyzed by flow cytometry for CCRL1^{GFP} and Ly51 expression. (**G**) P5 CCRL1^{hi} TECs were sorted at designated densities in a microscaled clonogenic assay (96-well plates) as depicted in the scheme of Microscale Clonogenic Assay. Green circles mark positive wells for clonogenic activity, while black circles mark wells with no activity. Plates were analyzed 12 days after culture for K8 expression to reveal TEC-derived colonies. Images represent complete individual wells and are illustrative of at least five experiments.

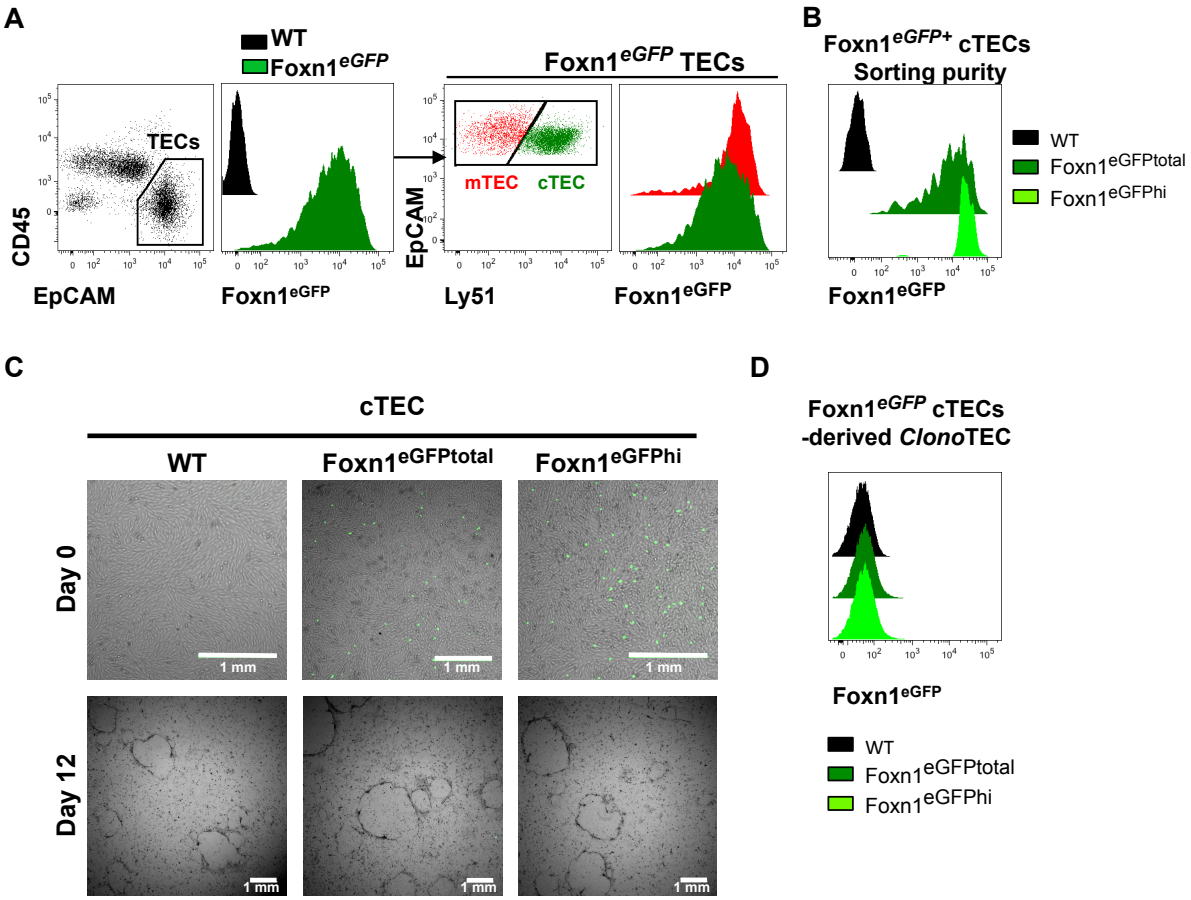

Supporting Information Figure 2. cTECs displaying clonogenic potential lose Foxn1 expression *in vitro*. (A) Left: Total TECs ($CD45^-$ $EpCAM^+$) from postnatal day 5 (P5) from $Foxn1^{eGFP}$ reporter and WT littermates were analyzed for $Foxn1^{eGFP}$ expression within TECs. Right: cTECs and mTECs from $Foxn1^{eGFP}$ reporter were analyzed for $Foxn1^{eGFP}$ expression. $Foxn1^{eGFP}$ cTECs were cell sorted to establish clonogenic assays. (**B**) Sorting purity of WT, total $Foxn1^{eGFP}$ cTEC and $Foxn1^{eGFP}$ cTECs is shown. (**C**) Representative microscopy images of clonogenic assays established with cell- sorted WT, total $Foxn1^{eGFP}$ and $Foxn1^{eGFPhi}$ cTECs analyzed at indicated time points. Images are illustrative of at least three experiments. (**D**) WT-, total $Foxn1^{eGFP}$ - and $Foxn1^{eGFPhi}$ cTEC-derived *Clono*TECs were analyzed for Foxn1 ^{eGFP} expression at day 12.

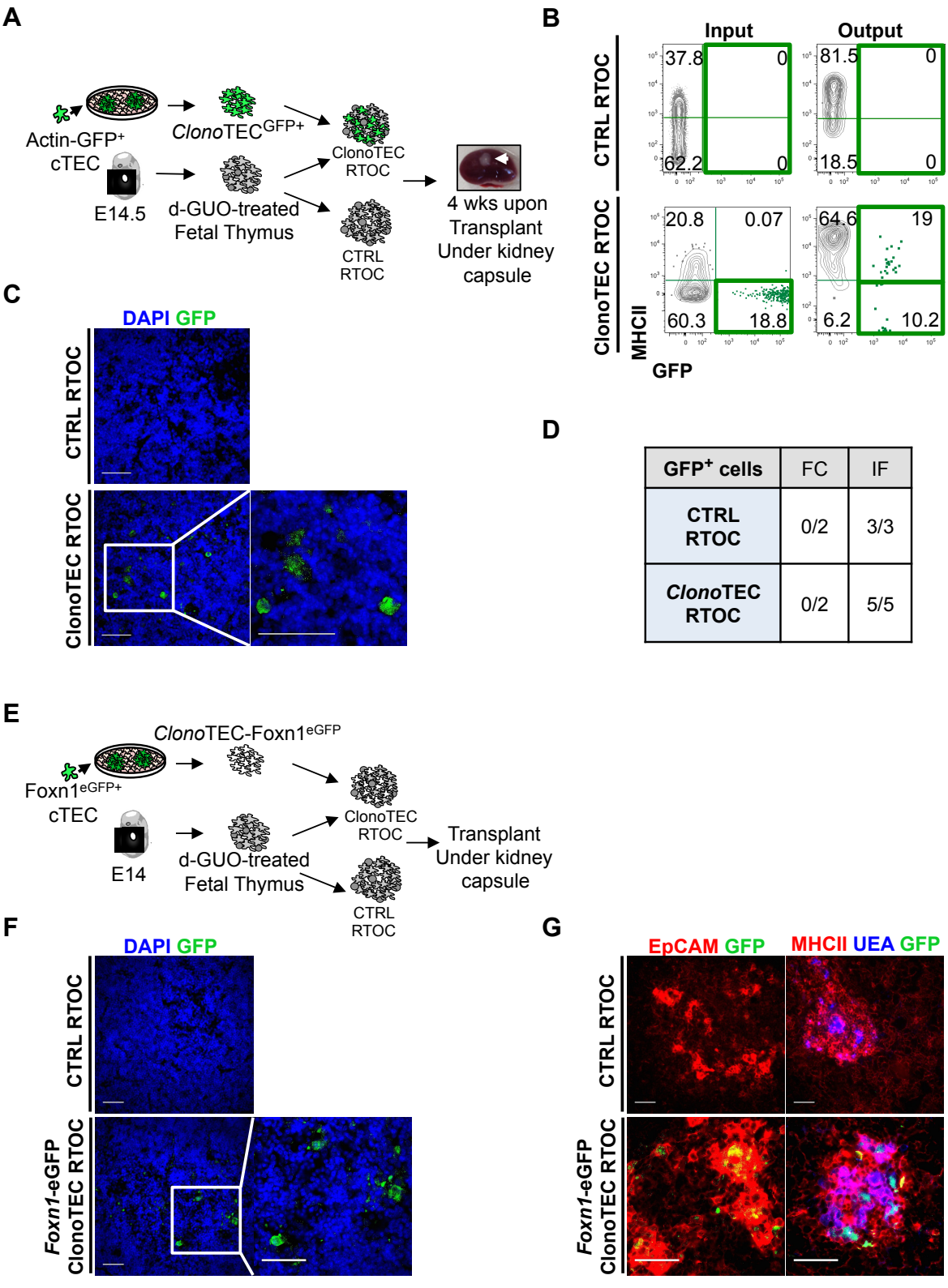

Supporting Information Figure 3 (A) A schematic representation of the lineage tracing experiment using Actin^{GFP}-derived *Clono*TECs. Briefly, cTECA^{ActinGFP}-derived *Clono*TECs^{GFP} were purified by cell sorting and

aggregated with cells from dGuo-treated E14.5 thymic lobes (*Clono*TEC RTOC) at a ratio 1:8. As control, RTOCs were established with cells from dGuo-treated E14.5 thymic lobes only. (CTRL RTOC). RTOCs were transplanted into the kidney capsule of WT mice, ectopic thymi were recovered 4 weeks post-transplantation and analyzed by flow cytometry **(B)** or fluorescent microscopy **(C)**. **(B)** TECs ($CD45^-$ $EpCAM^+$) were analyzed for the expression of MHCII and GFP before reaggregation (input) and after transplantation (output). FACS plots are representative of 3- experiments/ectopic thymus. **(C)** Immunofluorescence analysis of ectopic thymus. Control and *Clono*TECs RTOCs were screened for GFP cells (anti-GFP Ab). Square designates the zoomed area. 50µm scale is shown. Images are representative of 5 ectopic thymus containing *Clono*TEC^{GFP}. **(D)** Table represents the number of RTOCs analyzed by flow cytometry (FC) or fluorescent microscopy/immunofluorescence (IF) in which *Clono*$TECs^{GFP}$-derived GFP^+ cells were found. **(E)** A schematic representation of the lineage tracing experiment using $Foxn1^{eGFP}$-derived *Clono*TECs. Briefly, cTEC-$Foxn1^{eGFP+}$-derived *Clono*TECs were purified by cell sorting and aggregated with cells from dGuo-treated E14.5 thymic lobes. RTOCs were transplanted into the kidney capsule of WT mice, ectopic thymi were recovered 4 weeks post-transplantation and analyzed by fluorescent microscopy. **(F and G)** Immunofluorescence analysis of ectopic thymus. Control and $Foxn1^{eGFP}$ *Clono*TECs RTOCs were screened for GFP cells (anti-GFP Ab) and analyzed for the expression of EpCAM, MHCII and UEA as depicted. Square designates the zoomed area in (C). 50µm scale is shown. Images are representative of 5 ectopic thymus containing *Clono*$TECs^{GFP}$-derived cells.

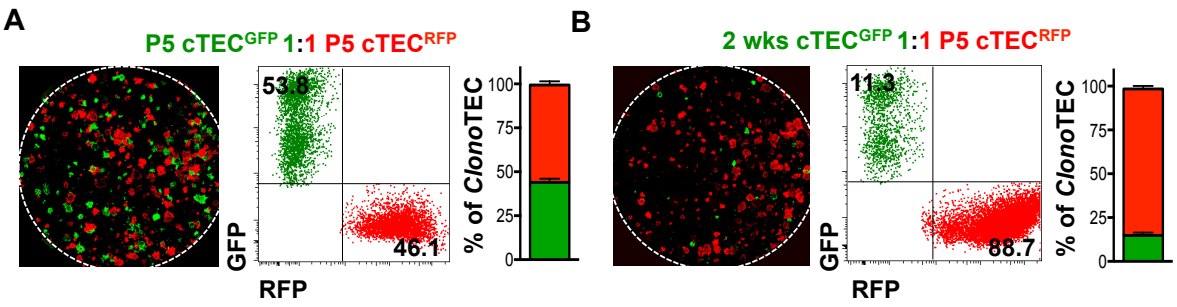

Supporting Information Figure 4. Clonogenic activity of cTECs decreases with time. (A) Age-matched postnatal day 5 (P5) or **(B)** mismatched P5 and 2-weeks-old cTECs from Actin^{GFP} and Actin^{RFP} reporter mice were co-cultured in a ratio 1:1 in midscale clonogenic assays for 12 days. *Clono*TEC^{GFP} and *Clono*TEC^{RFP} were analyzed by fluorescence microscopy and flow cytometry. The percentages of recovered cells analyzed by flow cytometry are represented in the graphs. Images represent complete individual wells and are illustrative of three experiments.

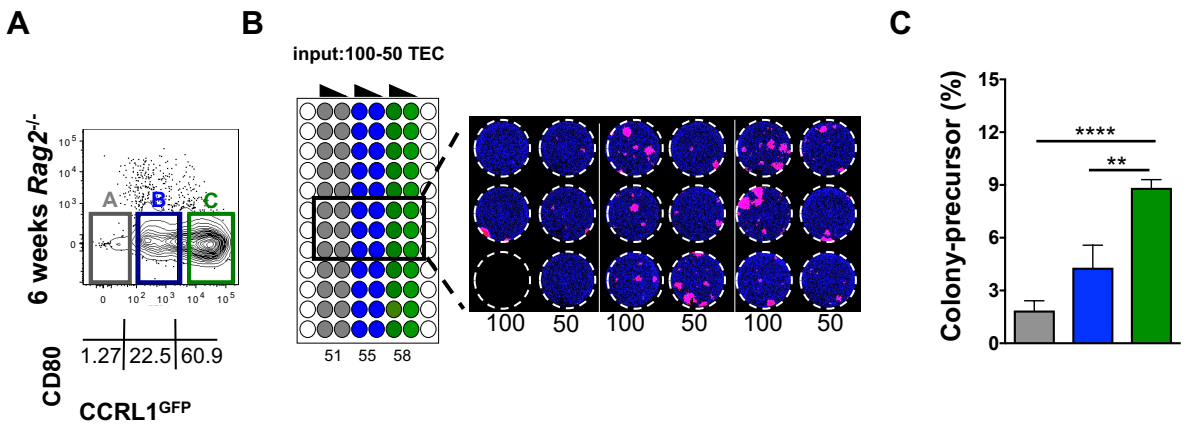

Supporting Information Figure 5. The pool of TEC colony-precursor cells is sustained in the adult *Rag2*$^{-/-}$ thymus. (A) TECs from *Rag2*$^{-/-}$ CCRL1^{GFP} mice were analyzed by flow cytometry at 6-weeks old for the expression of CCRL1 ^{GFP} and CD80. Proportion of indicated subsets are shown below the plot. (B) Colored TEC subsets (A-B-C) illustrated in (A) were purified by cell sorting and cultured in microscale clonogenic assay (96-well microplates) at designated cell densities (input: as represented on the top of the schematic plate). Numbers below each schematic plate represent the total amount of wells analyzed per subset (left). Representative images of full individual wells for each time point and TEC subset are shown (right). Number of plated cells (input) is shown below. 96-well plate cultures were fixed, stained with anti-cytokeratin 8 (K8) Ab and analyzed using a high-content immunofluorescence microscopy. Data shown are representative of three to three experiments per time point. **(C)** Colony-precursor cell frequency (%) was estimated based on the number of colonies relatively to the number of seeded TECs (as in Fig. 4C). Data are shown as mean ± SEM of a pool of 3 independent experiments. *p<0.05 **p<0.005 ***p<0.001, the two-tailed Mann–Whitney U.-

General Discussion and Future Perspectives

Thymic epithelial cells (TECs) are the major stromal component of the pre-involuted thymus and play an indispensable role in the generation of diverse and self-tolerant T cells [30, 94, 117]. As introduced before, cortical (cTEC) and medullary (mTEC) TEC lineages define functionally distinct microenvironments, which guide sequential stages of T cell development [160]. Despite this functional segregation, cTEC and mTEC arise from a bipotent TEC progenitor (TEP) [122, 123, 125, 126]. However, it is still elusive which niches are occupied by TEP and which molecular mechanisms mediate their differentiation into either cTEC or mTEC compartment. In this thesis, we first reveal a novel mTEC differentiation pathway in the postnatal thymus that appears to emerge from the cTEC compartment (**Results Chapter I**). Moreover, we show that the cTEC compartment contains a pool of specialized TEP with capacity to generate both cTEC and mTECs. Interestingly, we additionally documented that their abundance decreases through life as a result of lympho-epithelial interactions (**Results Chapter II**)**.** Our findings provide insights to better comprehend the basis of how these critical microenvironments developed throughout life. A better understanding of the checkpoints and mechanisms involved in cTEC and mTEC differentiation process will be relevant to modulate and correct intrathymic T cell production.

New Lights on the Establishment of thymic epithelial microenvironment

TECs are originally derived from the endodermal epithelium of the third pharyngeal pouch (3PP), in which the initiation of Foxn1 expression marks the onset of their differentiation program [103]. It has been shown that primordial TECs generated during embryogenesis contain bipotent TEPs able to originate cTEC and mTECs [122, 123, 126]. Still, how these embryonic progenitors relate to cTEC- or mTEC-restricted progenitors or their counterparts in the adult thymus is a matter that has been under intense scrutiny in the last years. Several studies have attempted to assess the development of the downstream progeny of bipotent TEPs. The initial description of compartment-restricted progenitors led to the idea that cTEC and mTEC differentiation splits early in their developmental pathways, and therefore the establishment of both compartments would

rely on lineage-restricted intermediate progenitors [128]. Supportive of this, initial studies demonstrated that medullary islets of the thymus have a clonal origin, suggesting that existence of mTEC-specific progenitors (mTEPs) [141]. Subsequent analysis identified cells expressing the tight junction proteins Cld3,4 in the E13 thymus as a progenitor population of Aire^{+} mTECs [135]. More recently, a further refinement of Cld3,4^{+} mTEPs has been purposed based on the expression of SSEA [134] and RANK [137]. Of note, it was described that RANK^{+} mTEPs emerge temporally downstream of SSEA-1^{+} mTEPs [137], suggesting a further degree of heterogeneity. However, the direct lineage relationship between these two subsets remains undefined.

In contrast to mTEC, we still know little about distinct developmental stages of cTECs. The progressive acquisition of CD205, β5t and IL-7 expression has been originally defined as markers of cTEC-progenitors (cTEP) in thymus ontogeny [32, 43, 132]. By crossing CCRL1-EGFP-knockin mice with IL-7-YFP transgenic mice, we observe that CCRL1 expression progressively increases in fetal cTEC development. Furthermore, the emergence of CCRL1^{hi} cells concomitantly with the increase of MHCII^{hi} and CD40^{hi} expression in cTECs, supporting the idea that CCRL1 is a late cTEC marker. Moreover, we found that the expression of CCRL1 was partially blocked in TECs from *Rag2*$^{-/-}$*Il2rg*$^{-/-}$ mice, but not in TECs from WT or *Rag2*$^{-/-}$ mice (**Results Chapter I – Figure 2**) [131]. In contrast to *Rag2*$^{-/-}$ mice, *Rag2*$^{-/-}$*Il2rg*$^{-/-}$ mice display a profound an earlier block in thymocyte development, showing that initial stages of cTEC development can occur independently of thymocyte-derived signals, but the presence of DN1-DN3 thymocytes is essential for further maturation of cTEC [32]. This observation indicates that the full acquisition of CCRL1 in cTECs seems to determine a specific step in their differentiation that is regulated by the signals provided by immature thymocytes [131].

In particular, the discrimination between β5t and Claudins expression pattern in the outer and inner layer of early thymic anlage, respectively, provided early evidence for a bimodal and unrelated TEC differentiation pathway for cTEC and mTEC [31]. However, this notion has been questioned in the last years by several independent studies from different laboratories, including our own. We have shown that embryonic TECs that co-express high levels of IL7 (Il7^{hi}) and several cortical-associated features have the

potential to differentiate into both cTECs and mTECs [87]. Moreover, studies by Baik *et al*. and Ohigashi *et al.* provide similar evidence that cTEC-like cells contain cells with cTEC/mTEC bipotent traits, either showing that in RTOC experiments in which $CD205^{+}CD40^{-}$ cTEC-like cells convert in cTEC and mTEC [129] or analyzing *in vivo* fate mapping mouse models based on β5t-cre-mediated reporter expression and demonstrating that mTEC derived from β5t-expresing cells [130]. Together, these studies disclosed a new stage in TEC developmental pathway, in which TEPs transverse thought the cTEC differentiation pathway previous to mTEC divergence. We have referred to this refined model of TEC development as "serial progression model" [128] (**Introduction – Figure 4**). This concept implicates that the cTEC compartment function as a reservoir for cells with bipotent capacity.

Using CCRL1-EGFP-knockin mouse model, we identify a novel mTEC subset that appears specifically in the postnatal thymus. Interestingly, these cells shared some features that suggest a previous cTEC history, namely the expression of intermediate levels of CCRL1. Specifically, we found a novel TEC subpopulation ($CCRL1^{int}CD80^{+}$) that was not present in embryonic stages (**Results Chapter I - Figure 1A and B**). Gene expression characterization of this new subset revealed bona-fide traits of mature mTEC, including high levels of *Aire* and *Tnfrsf11a* but insignificant amount of *Ccl21* (**Results Chapter I - Figure 1C**). Using female Marilyn-*Rag2*$^{-/-}$ mice, we additionally demonstrate that thymocytes-derived signals as RANK and CD40 are important for the development of $CCRL1^{int}$ mTECs (**Results Chapter I - Figure 2**). In conclusion, analysis of $CCRL1^{int}CD80^{+}$ subset corroborate the knowledge of the heterogeneity of mTEC lineage, which was already demonstrated by the existence of recognized subsets distinguished on the basis of the expression of MHCII, CD80, Aire, Involucrin and CCL21 (**Introduction - Figure 2**) (reviewed in [94]). While signals that determine cTEC differentiation are not yet described, the ligands expressed by positively selected thymocytes (CD40L, RANKL and LTαβ) and other hematopoietic cells are known to regulate the maturation of mTECs (reviewed in [30]). Concordantly, we show that purified $CCRL1^{+}CD80^{-}$ embryonic TECs are able to generate $UEA^{+}CD80^{+}$ mTECs, when cultured in the presence of RANK and CD40 stimulation in RTOCs. These findings indicate that cTEC $CCRL1^{+}$ compartment

could potentially harbor mTEPs (**Results Chapter I - Figure 1F**). Moreover, these results provide further experimental support for the serial progression model of TEC development, which propose that TEPs undergo a stepwise differentiation program wherein they first acquire an intermediate cTEC-like stage from which they will transmogrify into mTEC lineage (**Figure 1**).

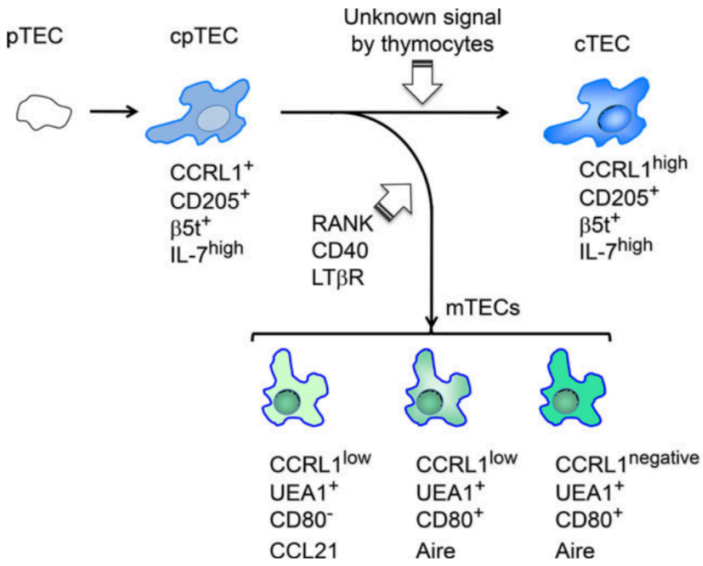

Figure 1 – Progressive development of cTECs and mTECs lineages. The progenitor TECs (pTECs) differentiate into an intermediate stage in which they express cTEC-associated molecules (cpTECs; cTEC-like progenitor TECs), including CCRL1 CD205, β5t, and high levels of IL7, prior specification into mTECs [87, 128-131]. Signals provided by developing thymocytes regulate the development of CCRL1^{high} CD205^{+} β5t^{+} IL7^{high} cTECs. TNF superfamily cytokine receptors, including RANK, CD40, and LTβR, the ligands of which are produced by positively selected thymocytes and other hematopoietic cells, regulate the development of heterogeneous subpopulations of mTECs. From [161].

Therefore, the analysis of CCRL1 expression in TECs throughout time has opened new questions that can be addressed in the future. The potential of this reporter mouse model can be used in future studies to identify the molecular signals that mediate the crosstalk between immature thymocytes and TECs to promote the differentiation of CCRL1-expressing cTECs. Knowledge in this area might provide information that will help

us to comprehend the so far poorly understood cTEC differentiation pathway. Moreover, it is important to define the molecular mechanisms that trigger the switch between the cTEC- and mTEC-genetic program and the physiological functions of CCRL1^{int}CD80^{+} mTECs subset. Despite these open questions, combining multicolor flow cytometry analysis and genetic models, we identify a novel subpopulation of mTEC in the postnatal thymus, which might implicate suggest the existence of alternative waves of mTEC differentiation to form the complete medullary compartment found in the adult thymus.

The cortical epithelium contains a pool of TEC progenitors

Mature TECs have a limited life span, which implicates that the preservation of the thymic epithelium niches depend on their continuous replenishment by TEPs [126, 127]. However, the thymus involutes with age, leading to a consequent decline in T cell production [15]. This process has been associated with the functional deterioration of instructive cTEC/mTEC microenvironments [14], possibly as a result of a drop in the bioavailability and/or function of TEPs in adult thymus. Albeit TEPs persist beyond embryonic period [127], we lack experiment evidence detailing how their pool is maintained throughout life.

Exploring selective *in vitro* clonogenic assay, we screened for progenitor activity in either cTEC or mTEC (**Results Chapter II – Figure 1E**). In line with other studies [87, 129, 130], we describe that the cTEC compartment contains cells with a higher clonogenic capability. More refined experiments with CCRL1^{GFP}-reporter validate that CCRL1^{hi} -cTEC fraction contained cells with the highest clonality capacity (**Results Chapter II – Figure 1F**). Moreover, our results show that cells deriving from these cultures (*Clono*TECs) lose cTEC and mTEC characteristics but expressed some stem-associated markers (**Results Chapter II – Figure 1 and 2**). Additionally, *Clono*TEC displayed self-renewal capacities *in vitro* and were able to integrate within cTEC or mTEC areas of the thymus, expressing either cortical or medullary traits. As such, we reason that clonogenic activity of TEC subset could be used as a surrogate tool to better understand the location and abundance of TEPs in postnatal thymus. Recent reports have shed some light on the

nature of TEPs in the adult thymus. Ucar *et al*. demonstrated that TEPs might exist within the non-TEC (EpCAM^{-}Foxn1^{-}) stromal fraction of the adult thymus. This conclusion was supported by the capacity of these cells to form spheroids under specialized *in vitro* culture conditions, so-called thymospheres, which in turn contain cells that are able to generate both cTECs and mTECs [146]. Contrary to *Clono*TECs that derived from bona-fide EpCAM^{+} TEC, thymospheres are selected from a purported TEP progenitor that resides within the non-TEC fraction. Importantly, conflicting data by Sheridan *et al*. have shown that thymospheres are mesenchymal cells with adipogenic capacity, but not with TEC potential [162]. Future studies are warranted to explain these apparently opposing findings. Using different approaches, Wong *et al* and Ulyanchenko *et al.* showed that the adult cTEC contained cells with bipotent potential. The first study identified bipotent TEPs within the UEA-1^{-}MHCII^{low} cTEC compartment [147], while the second reported a subset of Ly51^{+}MHCII^{hi}Plet1^{+} with bipotent TEP characteristics [148]. Further studies should address whether these recently identified subsets comprise different, but still developmental-related precursors. Worth noting, all these reports were done with analysis at the population level, and we still lack a unifying marker that identifies TEPs at the single-cell level.

The results described in Results Chapter I are in line with other recent observations that TEP with cortical-associated properties contribute to the formation of mTEC compartment in the postnatal thymus [150, 151]. In this case, the authors took advantage of the inducible lineage tracing mouse models driven by the temporal expression of β5t. This approach has enabled them to follow the progeny of β5t^{+} TEPs during postnatal life. Strikingly, they found that the contribution of β5t-expressing progenitors to the adult mTEC niche decreases with age. Specifically, β5t-derived *de novo* mTEC differentiation appears to be restricted to the embryo and the first week of age, with a minor penetrance in adult thymus [150, 151]. One possibility is that the growth and maintenance of the mTEC subset in the adulthood is guaranteed by mTEPs [150]. Several laboratories have been attempting to recognize mTEP in the adult thymus, but their primordial origin is still controversial. Cld3,4^{+}SSEA1^{+} cells were proposed to define a rare population of mTEPs in the adult thymus, which indicates that the pool of mTEPs might be also gradually exhausted throughout life [134]. Furthermore, fate-mapping experiments showed that

PDPN$^+$ TECs residing at cortical-medullary junction (jTECs) seem to account for the generation of almost half of the adult mTECs under steady state [136]. Altogether, these findings direct to a scenario in which the maintenance of the thymic epithelium is secure by the turnover of compartment-restricted cells. Unfortunately, these studies derived from different mouse models and markers combination, which does not allow a direct comparison. Contrarily to PDPN$^+$ TECs, the precise anatomical location of Cld3,4$^+$SSEA1$^+$ cells within the TEC microenvironment remains elusive. Addressing this point in future studies might allow us to define whether PDPN$^+$jTECs can potentially represent a transiently amplifying subset, which resides downstream of Cld3,4$^+$SSEA1$^+$ mTEPs and contributes to maintain the adult medullary network [163]. Hence, at this stage, we can only speculate one a cooperative action between bipotent progenitors and turnover of committed cells throughout life. Moreover, it will be of potential interest to monitor the dynamics of these populations under thymic regeneration settings, such as following radiation.

It is striking to note that the clonogenic potential of cTEC is maximal in the first days after birth, decreasing thereafter throughout life. This dynamic correlates with the expansion of TEC microenvironments in young thymus, and its subsequent reduction with age. To unravel the biological function of this decline, we investigated the role of thymic crosstalk in maintaining the TEP pool. We demonstrate that the decline in clonogenic capacity results from continual lympho-epithelial interactions. Still, it is unclear if these effects are mediated by direct or indirect communication between thymocytes and TECs. Intriguingly, the reduction in the clonogenic capacity of TECs is observed before the thymic involution. This notion would implicate a negative feedback loop that anticipates the subsequent progressive thymic involution that occurs with age. Whether this association is linked to a direct reduction in the number of TEPs and/or their quality has still to be determined. Nevertheless, it would be interesting to test if the transplantation of *Clono*TEC into the aged thymus will improve the thymus function in elderly. Still, additional refined experiments are required to access the exact checkpoint in thymopoiesis that leads to this negative feedback in TEP maintenance. In this regard, the analysis of TECs from mice with distinct blocks in T cell development, such TCR transgenic models can be of great value to understand the mechanisms underlying the

maintenance of TEP-derived cells. Thymus atrophy and the consequent decrease in T cell output can be partially reverted under particular conditions, such as the sex steroid ablation (SSA) [14, 16, 164], indicating that the TEC compartment possess some plasticity and regenerative capacity. It would be interesting to device future experiments to test if SSA can improve the clonogenic potential of TEC in the adult thymus.

Final remarks and future directions

The study of TEC progeny, diversification and maintenance throughout life has been under scrutiny in the past decade, delivering important advances to our current knowledge of TEC biology. In this thesis, I focused in the less understood aspect of the postnatal thymic epithelium, the TEP niche, and disclosed new concepts on how TEPs maintenance relates with cTEC and mTEC differentiation. Particularly, we provide evidence regarding the niche of TEPs in the postnatal thymus. We show that the cortical compartment harbors a pool of TEPs that decreases with age concomitantly with mTECs expansion and T cell production. The recent advances have revealed that distinct progenitors might regulate the preliminary establishment of the epithelium and its later progression or maintenance. It would be now important in the future to investigate the cellular and molecular mechanisms that underlie the homeostasis of the cTEC and TEP. Additionally, further studies are needed to understand the transcriptional and epigenetics program that contributes to TEP maintenance and/or TEC lineage differentiation. Using genome-wide analysis, e.g. RNA-seq for expression profiles or ATAC-seq for chromatin accessibility landscapes, we might define master transcriptional regulators that drive the cTEC- and mTEC- genetic program. Furthermore, integrating further advances in multi-parametric flow cytometry analysis (e.g. simultaneous analysis of 10-15 colors) would be a very helpful to define new stages on TEC differentiation, refine TEP at the single cell level and prospectively isolated them for further molecular analysis.

Altogether, I believe this thesis provide basic information that help us to understand the regulation of the thymic function throughout life. The comprehension of this is of great value since age-dependent alterations in thymopoiesis can lead to consequent

compromised T cell responses to pathogen or cancer cells or disruption in self-tolerance. Therefore, it will be of clinical relevance to apply this fundamental knowledge to potentially modulate TEC function to treat a wide range of thymic disorders, such as immunodeficiency and autoimmune disease.

REFERENCES

1. Iwasaki, A. and R. Medzhitov, *Control of adaptive immunity by the innate immune system.* Nat Immunol, 2015. **16**(4): p. 343-53.
2. Kawai, T. and S. Akira, *The role of pattern-recognition receptors in innate immunity: update on Toll-like receptors.* Nat Immunol, 2010. **11**(5): p. 373-84.
3. Mitchison, N.A., *T-cell-B-cell cooperation.* Nat Rev Immunol, 2004. **4**(4): p. 308-12.
4. Takahama, Y., *Journey through the thymus: stromal guides for T-cell development and selection.* Nat Rev Immunol, 2006. **6**(2): p. 127-35.
5. Miller, J.F., *Analysis of the thymus influence in leukaemogenesis.* Nature, 1961. **191**: p. 248-9.
6. Miller, J.F.A.P., *Effect of Neonatal Thymectomy on the Immunological Responsiveness of the Mouse.* Proceedings of the Royal Society of London. Series B. Biological Sciences, 1962. **156**(964): p. 415-428.
7. Crivellato, E., A. Vacca, and D. Ribatti, *Setting the stage: an anatomist's view of the immune system.* Trends Immunol, 2004. **25**(4): p. 210-7.
8. McCaughtry, T.M., et al., *Clonal deletion of thymocytes can occur in the cortex with no involvement of the medulla.* J Exp Med, 2008. **205**(11): p. 2575-84.
9. Stritesky, G.L., et al., *Murine thymic selection quantified using a unique method to capture deleted T cells.* Proc Natl Acad Sci U S A, 2013. **110**(12): p. 4679-84.
10. Boyd, R.L., et al., *The thymic microenvironment.* Immunol Today, 1993. **14**(9): p. 445-59.
11. Ritter, M.A. and R.L. Boyd, *Development in the thymus: it takes two to tango.* Immunol Today, 1993. **14**(9): p. 462-9.
12. Anderson, G., et al., *Thymic epithelial cells provide unique signals for positive selection of CD4+CD8+ thymocytes in vitro.* J Exp Med, 1994. **179**(6): p. 2027-31.
13. Hollander, G.A., et al., *Developmental control point in induction of thymic cortex regulated by a subpopulation of prothymocytes.* Nature, 1995. **373**(6512): p. 350-3.
14. Lynch, H.E., et al., *Thymic involution and immune reconstitution.* Trends Immunol, 2009. **30**(7): p. 366-73.

15. Chidgey, A., et al., *Impact of niche aging on thymic regeneration and immune reconstitution.* Semin Immunol, 2007. **19**(5): p. 331-40.
16. Gray, D.H., et al., *Developmental kinetics, turnover, and stimulatory capacity of thymic epithelial cells.* Blood, 2006. **108**(12): p. 3777-85.
17. Rode, I. and T. Boehm, *Regenerative capacity of adult cortical thymic epithelial cells.* Proc Natl Acad Sci U S A, 2012. **109**(9): p. 3463-8.
18. Hollander, G.A., W. Krenger, and B.R. Blazar, *Emerging strategies to boost thymic function.* Curr Opin Pharmacol, 2010. **10**(4): p. 443-53.
19. Foss, D.L., E. Donskoy, and I. Goldschneider, *The importation of hematogenous precursors by the thymus is a gated phenomenon in normal adult mice.* J Exp Med, 2001. **193**(3): p. 365-74.
20. Itoi, M., et al., *Two distinct steps of immigration of hematopoietic progenitors into the early thymus anlage.* Int Immunol, 2001. **13**(9): p. 1203-11.
21. Gordon, J. and N.R. Manley, *Mechanisms of thymus organogenesis and morphogenesis.* Development, 2011. **138**(18): p. 3865-78.
22. Jotereau, F., et al., *Cell kinetics in the fetal mouse thymus: precursor cell input, proliferation, and emigration.* J Immunol, 1987. **138**(4): p. 1026-30.
23. Godfrey, D.I., S. Stankovic, and A.G. Baxter, *Raising the NKT cell family.* Nat Immunol, 2010. **11**(3): p. 197-206.
24. Vantourout, P. and A. Hayday, *Six-of-the-best: unique contributions of gammadelta T cells to immunology.* Nat Rev Immunol, 2013. **13**(2): p. 88-100.
25. Porritt, H.E., K. Gordon, and H.T. Petrie, *Kinetics of steady-state differentiation and mapping of intrathymic-signaling environments by stem cell transplantation in nonirradiated mice.* J Exp Med, 2003. **198**(6): p. 957-62.
26. Bunting, M.D., I. Comerford, and S.R. McColl, *Finding their niche: chemokines directing cell migration in the thymus.* Immunol Cell Biol, 2011. **89**(2): p. 185-96.
27. van Ewijk, W., E.W. Shores, and A. Singer, *Crosstalk in the mouse thymus.* Immunol Today, 1994. **15**(5): p. 214-7.
28. Abramson, J. and G. Anderson, *Thymic Epithelial Cells.* Annu Rev Immunol, 2017.
29. Miller, J.F., *The golden anniversary of the thymus.* Nat Rev Immunol, 2011. **11**(7): p. 489-95.

30. Anderson, G. and Y. Takahama, *Thymic epithelial cells: working class heroes for T cell development and repertoire selection.* Trends Immunol, 2012. **33**(6): p. 256-63.
31. Ripen, A.M., et al., *Ontogeny of thymic cortical epithelial cells expressing the thymoproteasome subunit beta5t.* Eur J Immunol, 2011. **41**(5): p. 1278-87.
32. Shakib, S., et al., *Checkpoints in the development of thymic cortical epithelial cells.* J Immunol, 2009. **182**(1): p. 130-7.
33. Klug, D.B., et al., *Interdependence of cortical thymic epithelial cell differentiation and T-lineage commitment.* Proc Natl Acad Sci U S A, 1998. **95**(20): p. 11822-7.
34. Kenins, L., et al., *Intrathymic expression of Flt3 ligand enhances thymic recovery after irradiation.* J Exp Med, 2008. **205**(3): p. 523-31.
35. Rossi, F.M., et al., *Recruitment of adult thymic progenitors is regulated by P-selectin and its ligand PSGL-1.* Nat Immunol, 2005. **6**(6): p. 626-34.
36. Ara, T., et al., *A role of CXC chemokine ligand 12/stromal cell-derived factor-1/pre-B cell growth stimulating factor and its receptor CXCR4 in fetal and adult T cell development in vivo.* J Immunol, 2003. **170**(9): p. 4649-55.
37. Radtke, F., et al., *Deficient T cell fate specification in mice with an induced inactivation of Notch1.* Immunity, 1999. **10**(5): p. 547-58.
38. Hozumi, K., et al., *Delta-like 4 is indispensable in thymic environment specific for T cell development.* J Exp Med, 2008. **205**(11): p. 2507-13.
39. Feyerabend, T.B., et al., *Deletion of Notch1 converts pro-T cells to dendritic cells and promotes thymic B cells by cell-extrinsic and cell-intrinsic mechanisms.* Immunity, 2009. **30**(1): p. 67-79.
40. Koch, U., et al., *Delta-like 4 is the essential, nonredundant ligand for Notch1 during thymic T cell lineage commitment.* J Exp Med, 2008. **205**(11): p. 2515-23.
41. Peschon, J.J., et al., *Early lymphocyte expansion is severely impaired in interleukin 7 receptor-deficient mice.* J Exp Med, 1994. **180**(5): p. 1955-60.
42. von Freeden-Jeffry, U., et al., *Lymphopenia in interleukin (IL)-7 gene-deleted mice identifies IL-7 as a nonredundant cytokine.* J Exp Med, 1995. **181**(4): p. 1519-26.
43. Alves, N.L., et al., *Characterization of the thymic IL-7 niche in vivo.* Proc Natl Acad Sci U S A, 2009. **106**(5): p. 1512-7.

44. Ciofani, M., et al., *Stage-specific and differential notch dependency at the alphabeta and gammadelta T lineage bifurcation.* Immunity, 2006. **25**(1): p. 105-16.
45. Carpenter, A.C. and R. Bosselut, *Decision checkpoints in the thymus.* Nat Immunol, 2010. **11**(8): p. 666-73.
46. von Boehmer, H., *T-cell lineage fate: instructed by receptor signals?* Curr Biol, 2000. **10**(17): p. R642-5.
47. Hayday, A.C., *Gammadelta T cells and the lymphoid stress-surveillance response.* Immunity, 2009. **31**(2): p. 184-96.
48. Klein, L., et al., *Positive and negative selection of the T cell repertoire: what thymocytes see (and don't see).* Nat Rev Immunol, 2014. **14**(6): p. 377-91.
49. Klein, L., et al., *Antigen presentation in the thymus for positive selection and central tolerance induction.* Nat Rev Immunol, 2009. **9**(12): p. 833-44.
50. Nitta, T., et al., *Thymoproteasome shapes immunocompetent repertoire of CD8+ T cells.* Immunity, 2010. **32**(1): p. 29-40.
51. Murata, S., et al., *Regulation of CD8+ T cell development by thymus-specific proteasomes.* Science, 2007. **316**(5829): p. 1349-53.
52. Gommeaux, J., et al., *Thymus-specific serine protease regulates positive selection of a subset of CD4+ thymocytes.* Eur J Immunol, 2009. **39**(4): p. 956-64.
53. Hsieh, C.S., et al., *A role for cathepsin L and cathepsin S in peptide generation for MHC class II presentation.* J Immunol, 2002. **168**(6): p. 2618-25.
54. Bynoe, M.S., P. Bonorino, and C. Viret, *Control of experimental autoimmune encephalomyelitis by CD4+ suppressor T cells: peripheral versus in situ immunoregulation.* J Neuroimmunol, 2007. **191**(1-2): p. 61-9.
55. Honey, K., et al., *Cathepsin L regulates CD4+ T cell selection independently of its effect on invariant chain: a role in the generation of positively selecting peptide ligands.* J Exp Med, 2002. **195**(10): p. 1349-58.
56. Ueno, T., et al., *CCR7 signals are essential for cortex-medulla migration of developing thymocytes.* J Exp Med, 2004. **200**(4): p. 493-505.

57. Nitta, T., et al., *CCR7-mediated migration of developing thymocytes to the medulla is essential for negative selection to tissue-restricted antigens.* Proc Natl Acad Sci U S A, 2009. **106**(40): p. 17129-33.
58. Jordan, M.S., et al., *Thymic selection of CD4+CD25+ regulatory T cells induced by an agonist self-peptide.* Nat Immunol, 2001. **2**(4): p. 301-6.
59. Apostolou, I., et al., *Origin of regulatory T cells with known specificity for antigen.* Nat Immunol, 2002. **3**(8): p. 756-63.
60. Aschenbrenner, K., et al., *Selection of Foxp3+ regulatory T cells specific for self antigen expressed and presented by Aire+ medullary thymic epithelial cells.* Nat Immunol, 2007. **8**(4): p. 351-8.
61. Derbinski, J., et al., *Promiscuous gene expression in medullary thymic epithelial cells mirrors the peripheral self.* Nat Immunol, 2001. **2**(11): p. 1032-9.
62. Anderson, M.S., et al., *Projection of an immunological self shadow within the thymus by the aire protein.* Science, 2002. **298**(5597): p. 1395-401.
63. Takaba, H., et al., *Fezf2 Orchestrates a Thymic Program of Self-Antigen Expression for Immune Tolerance.* Cell, 2015. **163**(4): p. 975-87.
64. Mathis, D. and C. Benoist, *Aire.* Annu Rev Immunol, 2009. **27**: p. 287-312.
65. Finnish-German, A.C., *An autoimmune disease, APECED, caused by mutations in a novel gene featuring two PHD-type zinc-finger domains.* Nat Genet, 1997. **17**(4): p. 399-403.
66. Nagamine, K., et al., *Positional cloning of the APECED gene.* Nat Genet, 1997. **17**(4): p. 393-8.
67. Derbinski, J., et al., *Promiscuous gene expression in thymic epithelial cells is regulated at multiple levels.* J Exp Med, 2005. **202**(1): p. 33-45.
68. Derbinski, J. and B. Kyewski, *Linking signalling pathways, thymic stroma integrity and autoimmunity.* Trends Immunol, 2005. **26**(10): p. 503-6.
69. Zhu, M., et al., *NF-kappaB2 is required for the establishment of central tolerance through an Aire-dependent pathway.* J Clin Invest, 2006. **116**(11): p. 2964-71.
70. Akiyama, T., et al., *Dependence of self-tolerance on TRAF6-directed development of thymic stroma.* Science, 2005. **308**(5719): p. 248-51.

71. White, A.J., et al., *Lymphotoxin signals from positively selected thymocytes regulate the terminal differentiation of medullary thymic epithelial cells.* J Immunol, 2010. **185**(8): p. 4769-76.
72. White, A.J., et al., *Sequential phases in the development of Aire-expressing medullary thymic epithelial cells involve distinct cellular input.* Eur J Immunol, 2008. **38**(4): p. 942-7.
73. Hikosaka, Y., et al., *The cytokine RANKL produced by positively selected thymocytes fosters medullary thymic epithelial cells that express autoimmune regulator.* Immunity, 2008. **29**(3): p. 438-50.
74. Akiyama, T., et al., *The tumor necrosis factor family receptors RANK and CD40 cooperatively establish the thymic medullary microenvironment and self-tolerance.* Immunity, 2008. **29**(3): p. 423-37.
75. Shinzawa, M., et al., *Splenic extramedullary hemopoiesis caused by a dysfunctional mutation in the NF-kappaB-inducing kinase gene.* Biochem Biophys Res Commun, 2011. **414**(4): p. 773-8.
76. Boehm, T., et al., *Thymic medullary epithelial cell differentiation, thymocyte emigration, and the control of autoimmunity require lympho-epithelial cross talk via LTbetaR.* J Exp Med, 2003. **198**(5): p. 757-69.
77. Rossi, S.W., et al., *RANK signals from CD4(+)3(-) inducer cells regulate development of Aire-expressing epithelial cells in the thymic medulla.* J Exp Med, 2007. **204**(6): p. 1267-72.
78. Irla, M., et al., *Autoantigen-specific interactions with CD4+ thymocytes control mature medullary thymic epithelial cell cellularity.* Immunity, 2008. **29**(3): p. 451-63.
79. Akiyama, T., M. Shinzawa, and N. Akiyama, *TNF receptor family signaling in the development and functions of medullary thymic epithelial cells.* Front Immunol, 2012. **3**: p. 278.
80. Weih, F., et al., *Multiorgan inflammation and hematopoietic abnormalities in mice with a targeted disruption of RelB, a member of the NF-kappa B/Rel family.* Cell, 1995. **80**(2): p. 331-40.

81. Weih, F. and J. Caamano, *Regulation of secondary lymphoid organ development by the nuclear factor-kappaB signal transduction pathway.* Immunol Rev, 2003. **195**: p. 91-105.
82. Kajiura, F., et al., *NF-kappa B-inducing kinase establishes self-tolerance in a thymic stroma-dependent manner.* J Immunol, 2004. **172**(4): p. 2067-75.
83. Roberts, N.A., et al., *Rank signaling links the development of invariant gammadelta T cell progenitors and Aire(+) medullary epithelium.* Immunity, 2012. **36**(3): p. 427-37.
84. Lucas, B., et al., *Lymphotoxin beta Receptor Controls T Cell Progenitor Entry to the Thymus.* J Immunol, 2016. **197**(7): p. 2665-72.
85. Irla, M., G. Hollander, and W. Reith, *Control of central self-tolerance induction by autoreactive CD4+ thymocytes.* Trends Immunol, 2010. **31**(2): p. 71-9.
86. Gray, D.H., A.P. Chidgey, and R.L. Boyd, *Analysis of thymic stromal cell populations using flow cytometry.* J Immunol Methods, 2002. **260**(1-2): p. 15-28.
87. Ribeiro, A.R., et al., *Thymocyte selection regulates the homeostasis of IL-7-expressing thymic cortical epithelial cells in vivo.* J Immunol, 2013. **191**(3): p. 1200-9.
88. Lkhagvasuren, E., et al., *Lymphotoxin beta receptor regulates the development of CCL21-expressing subset of postnatal medullary thymic epithelial cells.* J Immunol, 2013. **190**(10): p. 5110-7.
89. Yano, M., et al., *Aire controls the differentiation program of thymic epithelial cells in the medulla for the establishment of self-tolerance.* J Exp Med, 2008. **205**(12): p. 2827-38.
90. Metzger, T.C., et al., *Lineage tracing and cell ablation identify a post-Aire-expressing thymic epithelial cell population.* Cell Rep, 2013. **5**(1): p. 166-79.
91. Gray, D., et al., *Proliferative arrest and rapid turnover of thymic epithelial cells expressing Aire.* J Exp Med, 2007. **204**(11): p. 2521-8.
92. Mizuno, A., et al., *Severe osteoporosis in mice lacking osteoclastogenesis inhibitory factor/osteoprotegerin.* Biochem Biophys Res Commun, 1998. **247**(3): p. 610-5.

93. Theill, L.E., W.J. Boyle, and J.M. Penninger, *RANK-L and RANK: T cells, bone loss, and mammalian evolution.* Annu Rev Immunol, 2002. **20**: p. 795-823.
94. Takahama, Y., et al., *Generation of diversity in thymic epithelial cells.* Nat Rev Immunol, 2017. **17**(5): p. 295-305.
95. Rodewald, H.R., *Thymus organogenesis.* Annu Rev Immunol, 2008. **26**: p. 355-88.
96. Gordon, J., et al., *Functional evidence for a single endodermal origin for the thymic epithelium.* Nat Immunol, 2004. **5**(5): p. 546-53.
97. Vaidya, H.J., A. Briones Leon, and C.C. Blackburn, *FOXN1 in thymus organogenesis and development.* Eur J Immunol, 2016. **46**(8): p. 1826-37.
98. Bleul, C.C. and T. Boehm, *BMP signaling is required for normal thymus development.* J Immunol, 2005. **175**(8): p. 5213-21.
99. Bockman, D.E. and M.L. Kirby, *Dependence of thymus development on derivatives of the neural crest.* Science, 1984. **223**(4635): p. 498-500.
100. Jenkinson, W.E., E.J. Jenkinson, and G. Anderson, *Differential requirement for mesenchyme in the proliferation and maturation of thymic epithelial progenitors.* J Exp Med, 2003. **198**(2): p. 325-32.
101. Suniara, R.K., E.J. Jenkinson, and J.J. Owen, *An essential role for thymic mesenchyme in early T cell development.* J Exp Med, 2000. **191**(6): p. 1051-6.
102. Revest, J.M., et al., *Development of the thymus requires signaling through the fibroblast growth factor receptor R2-IIIb.* J Immunol, 2001. **167**(4): p. 1954-61.
103. Gordon, J., et al., *Gcm2 and Foxn1 mark early parathyroid- and thymus-specific domains in the developing third pharyngeal pouch.* Mech Dev, 2001. **103**(1-2): p. 141-3.
104. Nehls, M., et al., *New member of the winged-helix protein family disrupted in mouse and rat nude mutations.* Nature, 1994. **372**(6501): p. 103-7.
105. Nehls, M., et al., *Two genetically separable steps in the differentiation of thymic epithelium.* Science, 1996. **272**(5263): p. 886-9.
106. Carlsson, P. and M. Mahlapuu, *Forkhead transcription factors: key players in development and metabolism.* Dev Biol, 2002. **250**(1): p. 1-23.

107. Manley, N.R. and M.R. Capecchi, *Hox group 3 paralogs regulate the development and migration of the thymus, thyroid, and parathyroid glands.* Dev Biol, 1998. **195**(1): p. 1-15.

108. Dietrich, S. and P. Gruss, *undulated phenotypes suggest a role of Pax-1 for the development of vertebral and extravertebral structures.* Dev Biol, 1995. **167**(2): p. 529-48.

109. Wallin, J., et al., *Pax1 is expressed during development of the thymus epithelium and is required for normal T-cell maturation.* Development, 1996. **122**(1): p. 23-30.

110. Su, D.M. and N.R. Manley, *Hoxa3 and pax1 transcription factors regulate the ability of fetal thymic epithelial cells to promote thymocyte development.* J Immunol, 2000. **164**(11): p. 5753-60.

111. Conway, S.J., D.J. Henderson, and A.J. Copp, *Pax3 is required for cardiac neural crest migration in the mouse: evidence from the splotch (Sp2H) mutant.* Development, 1997. **124**(2): p. 505-14.

112. Xu, P.X., et al., *Eya1 is required for the morphogenesis of mammalian thymus, parathyroid and thyroid.* Development, 2002. **129**(13): p. 3033-44.

113. Zou, D., et al., *Patterning of the third pharyngeal pouch into thymus/parathyroid by Six and Eya1.* Dev Biol, 2006. **293**(2): p. 499-512.

114. Hetzer-Egger, C., et al., *Thymopoiesis requires Pax9 function in thymic epithelial cells.* Eur J Immunol, 2002. **32**(4): p. 1175-81.

115. Su, D., et al., *Hoxa3 and pax1 regulate epithelial cell death and proliferation during thymus and parathyroid organogenesis.* Dev Biol, 2001. **236**(2): p. 316-29.

116. Nitta, T., et al., *Thymic microenvironments for T-cell repertoire formation.* Adv Immunol, 2008. **99**: p. 59-94.

117. Anderson, G., P.J. Lane, and E.J. Jenkinson, *Generating intrathymic microenvironments to establish T-cell tolerance.* Nat Rev Immunol, 2007. **7**(12): p. 954-63.

118. Parent, A.V., et al., *Generation of functional thymic epithelium from human embryonic stem cells that supports host T cell development.* Cell Stem Cell, 2013. **13**(2): p. 219-29.

119. Sun, X., et al., *Directed differentiation of human embryonic stem cells into thymic epithelial progenitor-like cells reconstitutes the thymic microenvironment in vivo.* Cell Stem Cell, 2013. **13**(2): p. 230-6.
120. Manley, N.R. and M.R. Capecchi, *The role of Hoxa-3 in mouse thymus and thyroid development.* Development, 1995. **121**(7): p. 1989-2003.
121. Le Douarin, N.M. and F.V. Jotereau, *Tracing of cells of the avian thymus through embryonic life in interspecific chimeras.* J Exp Med, 1975. **142**(1): p. 17-40.
122. Gill, J., et al., *Generation of a complete thymic microenvironment by MTS24(+) thymic epithelial cells.* Nat Immunol, 2002. **3**(7): p. 635-42.
123. Bennett, A.R., et al., *Identification and characterization of thymic epithelial progenitor cells.* Immunity, 2002. **16**(6): p. 803-14.
124. Depreter, M.G., et al., *Identification of Plet-1 as a specific marker of early thymic epithelial progenitor cells.* Proc Natl Acad Sci U S A, 2008. **105**(3): p. 961-6.
125. Rossi, S.W., et al., *Redefining epithelial progenitor potential in the developing thymus.* Eur J Immunol, 2007. **37**(9): p. 2411-8.
126. Rossi, S.W., et al., *Clonal analysis reveals a common progenitor for thymic cortical and medullary epithelium.* Nature, 2006. **441**(7096): p. 988-91.
127. Bleul, C.C., et al., *Formation of a functional thymus initiated by a postnatal epithelial progenitor cell.* Nature, 2006. **441**(7096): p. 992-6.
128. Alves, N.L., et al., *Serial progression of cortical and medullary thymic epithelial microenvironments.* Eur J Immunol, 2014. **44**(1): p. 16-22.
129. Baik, S., et al., *Generation of both cortical and Aire(+) medullary thymic epithelial compartments from CD205(+) progenitors.* Eur J Immunol, 2013. **43**(3): p. 589-94.
130. Ohigashi, I., et al., *Aire-expressing thymic medullary epithelial cells originate from beta5t-expressing progenitor cells.* Proc Natl Acad Sci U S A, 2013. **110**(24): p. 9885-90.
131. Ribeiro, A.R., et al., *The intermediate expression of CCRL1 reveals novel subpopulations of medullary thymic epithelial cells that emerge in the postnatal thymus.* Eur J Immunol, 2014.

132. Alves, N.L., et al., *Cutting Edge: a thymocyte-thymic epithelial cell cross-talk dynamically regulates intrathymic IL-7 expression in vivo.* J Immunol, 2010. **184**(11): p. 5949-53.
133. Kyewski, B. and L. Klein, *A central role for central tolerance.* Annu Rev Immunol, 2006. **24**: p. 571-606.
134. Sekai, M., Y. Hamazaki, and N. Minato, *Medullary thymic epithelial stem cells maintain a functional thymus to ensure lifelong central T cell tolerance.* Immunity, 2014. **41**(5): p. 753-61.
135. Hamazaki, Y., et al., *Medullary thymic epithelial cells expressing Aire represent a unique lineage derived from cells expressing claudin.* Nat Immunol, 2007. **8**(3): p. 304-11.
136. Onder, L., et al., *Alternative NF-kappaB signaling regulates mTEC differentiation from podoplanin-expressing presursors in the cortico-medullary junction.* Eur J Immunol, 2015. **45**(8): p. 2218-31.
137. Baik, S., et al., *Relb acts downstream of medullary thymic epithelial stem cells and is essential for the emergence of RANK(+) medullary epithelial progenitors.* Eur J Immunol, 2016. **46**(4): p. 857-62.
138. Akiyama, N., et al., *Identification of embryonic precursor cells that differentiate into thymic epithelial cells expressing autoimmune regulator.* J Exp Med, 2016. **213**(8): p. 1441-58.
139. Mouri, Y., et al., *Lymphotoxin signal promotes thymic organogenesis by eliciting RANK expression in the embryonic thymic stroma.* J Immunol, 2011. **186**(9): p. 5047-57.
140. Anderson, G., E.J. Jenkinson, and H.R. Rodewald, *A roadmap for thymic epithelial cell development.* Eur J Immunol, 2009. **39**(7): p. 1694-9.
141. Rodewald, H.R., et al., *Thymus medulla consisting of epithelial islets each derived from a single progenitor.* Nature, 2001. **414**(6865): p. 763-8.
142. Dumont-Lagace, M., et al., *Adult thymic epithelium contains nonsenescent label-retaining cells.* J Immunol, 2014. **192**(5): p. 2219-26.
143. Jenkinson, W.E., et al., *An epithelial progenitor pool regulates thymus growth.* J Immunol, 2008. **181**(9): p. 6101-8.

144. Alves, N.L., et al., *Thymic epithelial cells: the multi-tasking framework of the T cell "cradle".* Trends Immunol, 2009. **30**(10): p. 468-74.
145. Gabler, J., J. Arnold, and B. Kyewski, *Promiscuous gene expression and the developmental dynamics of medullary thymic epithelial cells.* Eur J Immunol, 2007. **37**(12): p. 3363-72.
146. Ucar, A., et al., *Adult thymus contains FoxN1(-) epithelial stem cells that are bipotent for medullary and cortical thymic epithelial lineages.* Immunity, 2014. **41**(2): p. 257-69.
147. Wong, K., et al., *Multilineage potential and self-renewal define an epithelial progenitor cell population in the adult thymus.* Cell Rep, 2014. **8**(4): p. 1198-209.
148. Ulyanchenko, S., et al., *Identification of a Bipotent Epithelial Progenitor Population in the Adult Thymus.* Cell Rep, 2016. **14**(12): p. 2819-32.
149. Nishikawa, Y., et al., *Temporal lineage tracing of Aire-expressing cells reveals a requirement for Aire in their maturation program.* J Immunol, 2014. **192**(6): p. 2585-92.
150. Ohigashi, I., et al., *Adult Thymic Medullary Epithelium Is Maintained and Regenerated by Lineage-Restricted Cells Rather Than Bipotent Progenitors.* Cell Rep, 2015. **13**(7): p. 1432-43.
151. Mayer, C.E., et al., *Dynamic spatio-temporal contribution of single beta5t+ cortical epithelial precursors to the thymus medulla.* Eur J Immunol, 2016. **46**(4): p. 846-56.
152. Senoo, M., et al., *p63 Is essential for the proliferative potential of stem cells in stratified epithelia.* Cell, 2007. **129**(3): p. 523-36.
153. Bonfanti, P., et al., *Microenvironmental reprogramming of thymic epithelial cells to skin multipotent stem cells.* Nature, 2010. **466**(7309): p. 978-82.
154. Shackleton, M., et al., *Generation of a functional mammary gland from a single stem cell.* Nature, 2006. **439**(7072): p. 84-8.
155. McQualter, J.L., et al., *Evidence of an epithelial stem/progenitor cell hierarchy in the adult mouse lung.* Proc Natl Acad Sci U S A, 2010. **107**(4): p. 1414-9.
156. Lantz, O., et al., *Gamma chain required for naive CD4+ T cell survival but not for antigen proliferation.* Nat Immunol, 2000. **1**(1): p. 54-8.

157. Nowell, C.S., et al., *Foxn1 regulates lineage progression in cortical and medullary thymic epithelial cells but is dispensable for medullary sublineage divergence.* PLoS Genet, 2011. **7**(11): p. e1002348.

158. Fiorini, E., et al., *Cutting edge: thymic crosstalk regulates delta-like 4 expression on cortical epithelial cells.* J Immunol, 2008. **181**(12): p. 8199-203.

159. Rode, I., et al., *Foxn1 Protein Expression in the Developing, Aging, and Regenerating Thymus.* J Immunol, 2015. **195**(12): p. 5678-87.

160. Blackburn, C.C. and N.R. Manley, *Developing a new paradigm for thymus organogenesis.* Nat Rev Immunol, 2004. **4**(4): p. 278-89.

161. Ohigashi, I. and Y. Takahama, *CCRL1 marks heterogeneity in cortical and medullary thymic epithelial cells.* Eur J Immunol, 2014. **44**(10): p. 2872-5.

162. Sheridan, J.M., et al., *Thymospheres Are Formed by Mesenchymal Cells with the Potential to Generate Adipocytes, but Not Epithelial Cells.* Cell Rep, 2017. **21**(4): p. 934-942.

163. Alves, N.L. and A.R. Ribeiro, *Thymus medulla under construction: Time and space oddities.* Eur J Immunol, 2016. **46**(4): p. 829-33.

164. Rodrigues, P.M., et al., *Intrathymic Deletion of IL-7 Reveals a Contribution of the Bone Marrow to Thymic Rebound Induced by Androgen Blockade.* J Immunol, 2018. **200**(4): p. 1389-1398.

ANNEX

European Journal of Immunology

SHORT COMMUNICATION

Intermediate expression of CCRL1 reveals novel subpopulations of medullary thymic epithelial cells that emerge in the postnatal thymus

Ana R. Ribeiro[1,2], *Catarina Meireles*[1,2], *Pedro M. Rodrigues*[1,2] *and Nuno L. Alves*[1]

[1] Thymus Development and Function Laboratory, Institute for Molecular and Cellular Biology, Porto, Portugal
[2] Institute for Biomedical Sciences Abel Salazar, University of Porto, Porto, Portugal

Cortical and medullary thymic epithelial cells (cTECs and mTECs, respectively) provide inductive microenvironments for T-cell development and selection. The differentiation pathway of cTEC/mTEC lineages downstream of common bipotent progenitors at discrete stages of development remains unresolved. Using IL-7/CCRL1 dual reporter mice that identify specialized TEC subsets, we show that the stepwise acquisition of chemokine (C–C motif) receptor-like 1 (CCRL1) is a late determinant of cTEC differentiation. Although cTECs expressing high CCRL1 levels (CCRL1^{hi}) develop normally in immunocompetent and *Rag2*$^{-/-}$thymi, their differentiation is partially blocked in *Rag2*$^{-/-}$*Il2rg*$^{-/-}$ counterparts. These results unravel a novel checkpoint in cTEC maturation that is regulated by the cross-talk between TECs and immature thymocytes. Additionally, we identify new *Ulex europaeus* agglutinin 1 (UEA)$^{+}$ mTEC subtypes expressing intermediate CCRL1 levels (CCRL1^{int}) that conspicuously emerge in the postnatal thymus and differentially express *Tnfrsf11a*, *Ccl21*, and *Aire*. While rare in fetal and in *Rag2*$^{-/-}$ thymi, CCRL1^{int} mTECs are restored in *Rag2*$^{-/-}$Marilyn TCR-Tg mice, indicating that the appearance of postnatal-restricted mTECs is closely linked with T-cell selection. Our findings suggest that alternative temporally restricted routes of new mTEC differentiation contribute to the establishment of the medullary niche in the postnatal thymus.

Keywords: Cortex · Medulla · Thymic epithelial cells · Thymus

Additional supporting information may be found in the online version of this article at the publisher's web-site

Introduction

Within the thymus, it is well established the role of distinct thymic epithelial cell (TEC) microenvironments in supporting the generation of functionally diverse and self-tolerant T cells [1]. While cortical TECs (cTECs) promote T-cell lineage commitment and positive selection, medullary TECs (mTECs) participate in the elimination of autoreactive T cells and the differentiation of Treg cells [2]. In particular, auto-immune regulator (Aire)$^{+}$ mTECs have an established role in tolerance induction [3]. Cortical and medullary TECs are derived from common bipotent progenitors present within the fetal and postnatal thymus [4, 5]. Importantly, the cTEC/mTEC maturation pathways downstream of bipotent progenitors, as well as the requirements for the establishment of these specialized compartments at discrete stages of development are still unresolved.

Correspondence: Ms. Ana R. Ribeiro
e-mail: ana.ribeiro@ibmc.up.pt

The cTEC/mTEC lineage specification branches early in embryonic development [6]. During initial stages of gestation, the thymic epithelium predominately comprises Ly51$^+$CD205$^+$β5t$^+$ cTECs [7–9], and mature mTECs, including Aire$^+$ mTECs, first appear around embryonic day 16 (E16) [10, 11]. The emergence of embryonic mTECs depends on cellular interactions with lymphoid tissue inducer cells and invariant γδ T cells [12, 13], and involves signaling through TNFR superfamily receptor activator of NF-κB (RANK) and lymphotoxin beta receptor (LTβR) expressed on TEC precursors [12, 14]. However, and despite the elucidation of distinct maturation stages in mTECs [2], there are still gaps in the understanding of cTEC differentiation. We, and others, have recently demonstrated that fetal TEC progenitors expressing cortical properties are able to generate mTECs [15–17]. These reports support the idea that embryonic TEC precursors progress transitionally through the cortical lineage prior to commitment to the medullary pathway, emphasising that TEC differentiation is more complex then previously recognized [18].

The size of the medullary epithelial microenvironment continues to expand after birth, fostered by additional interactions between TECs and mature thymocytes, namely positively selected and CD4 single positive (SP4) thymocytes [2]. The concerted activation of RANK-, LTβR-, and CD40-mediated signaling on mTECs and their precursors completes the formation of the adult medullary niche [2]. It has been previously demonstrated a clonal nature for discrete embryonic mTEC islets, which progressively coalesce into larger medullary areas in the adult thymus [10, 19]. Hence, one can argue that the adult mTEC niche exclusively results from the expansion of embryonic-derived mTECs and their precursors. Still, it remains possible that alternative developmental stage-specific pathways participate in the organization of the adult mTEC niche.

Here, we report a novel checkpoint in cTEC differentiation, which is defined by the sequential acquisition of chemokine (C–C motif) receptor-like 1 (CCRL1) expression and is compromised in mice with profound blocks in early T-cell development. Additionally, we define original subsets of mTECs, characterized by the intermediate CCRL1 expression, that emerge in the postnatal thymus in tight association with thymocytes that develop beyond the TCRβ selection. Our findings provide evidence for the existence of several waves of mTEC development in the embryonic and postnatal thymus.

Results and discussion

Acquisition of CCRL1 expression is a late cTEC determinant

The expression of CCRL1, an atypical chemokine receptor that controls the bioavailability of key chemoattractants CCL19, CCL21, and CCL25, identifies cTECs in the postnatal thymus [20]. Given the incomplete knowledge on the differentiation of CCRL1$^+$cTECs, we assessed their generation using previously generated IL7^{YFP}-CCRL1^{GFP} dual reporter mice [15]. While in IL7^{YFP} reporter mice, YFP expression is a surrogate of a subtype of cTECs expressing abundant levels of the crucial thymopoietin IL-7 (*Il7*$^{YFP+}$) [8, 15], in CCRL1^{GFP} reporter mice, GFP expression labels cTECs in the postnatal thymus [20]. We previously showed that postnatal *Il7*$^{YFP+}$ TECs locate within cTECs that express high CCRL1 levels (referred as CCRL1^{hi}) [15]. Here, analysis during early stages of thymic development showed that the emergence of *Il7*$^{YFP+}$, CD205$^+$, and Ly51$^+$ TECs around E12.5–13.5 [7–9] preceded the appearance of CCRL1-expressing cells (Fig. 1A and Supporting information Fig. 1B; nonreporter thymi in Supporting Information Fig. 1A). During the E12.5–15.5 period, both *Il7*$^{YFP+}$ and remaining YFP$^-$ cTECs progressively acquired the expression of CCRL1. At E18.5, and similarly to the postnatal thymus [15], *Il7*$^{YFP+}$ TECs reside within CCRL1^{hi} cells (Fig. 1A). The number of CCRL1^{hi} cTECs gradually increased throughout development, contributing to the expansion of TEC cellularity during perinatal life. TECs lacking CCRL1 and expressing intermediate CCRL1 levels (referred as CCRL1$^-$ and CCRL1^{int}, respectively) followed steadier numbers during this period (Fig. 1B). To address whether the acquisition of CCRL1 defined a late cTEC maturation stage dependent on signals provided by developing thymocytes, we crossed double reporter mice onto a *Rag2*$^{-/-}$ or *Rag*$^{-/-}$*Il2r*$^{-/-}$ background. While the majority of TECs were CCRL1^{hi} in the postnatal *Rag*$^{-/-}$ thymus, we detected an accumulation of CCRL1^{int} TECs in the *Rag2*$^{-/-}$*Il2rg*$^{-/-}$ thymus (Fig. 1C and D, nonreporter thymi in Supporting Information Fig. 1C), akin to the CCRL1 pattern observed at E15.5 (Fig. 1A). Contrarily to CCRL1, the expression of Ly51, CD205, *Psmb11* (β5t), and *Ctsl* was not impaired in TECs from *Rag2*$^{-/-}$*Il2rg*$^{-/-}$ thymi (Supporting Information Fig. 1D and E) [8, 15]. CCRL1$^-$ and CCRL1^{int} TECs in the *Rag2*$^{-/-}$*Il2rg*$^{-/-}$ thymus were distinct from immunocompetent counterparts, as in the later these subsets comprised mostly mTECs (below in Fig. 2) that are virtually absent in the *Rag2*$^{-/-}$*Il2rg*$^{-/-}$ thymus [8]. The partial blockade in CCRL1, CD40, and MHCII expression in *Rag2*$^{-/-}$*Il2rg*$^{-/-}$ mice (Supporting Information Fig. 1D) was similar to blocks in the expression of CD40 and MHCII also reported in CD3εTg26 mice [7]. Although the signals remain unidentified, our results indicate that lymphoepithelial interactions with DN1–DN3 thymocytes provide differentiation cues that control late stages in the cTEC differentiation program.

Intermediate CCRL1 levels define distinct mTEC subtypes in the postnatal thymus

We reciprocally examined the generation of mTECs relatively to the differentiation of CCRL1-expressing TECs. The primordial CD80$^+$ mTECs were found within CCRL1$^-$ cells (CCRL1$^-$CD80$^+$) at E15.5 (Fig. 2A), preceding the complete differentiation of CCRL1^{hi} cTECs around E18.5-postnatal (Fig. 1A). The proportion and number of CCRL1$^-$CD80$^+$ mTECs augmented throughout time (Fig. 2A and D). Notably, a subset of CD80$^+$ TECs, expressing intermediate levels of CCRL1 (CCRL1^{int}CD80$^+$), emerged distinctly after birth (Fig. 2A; nonreporter CD80$^+$mTECs and

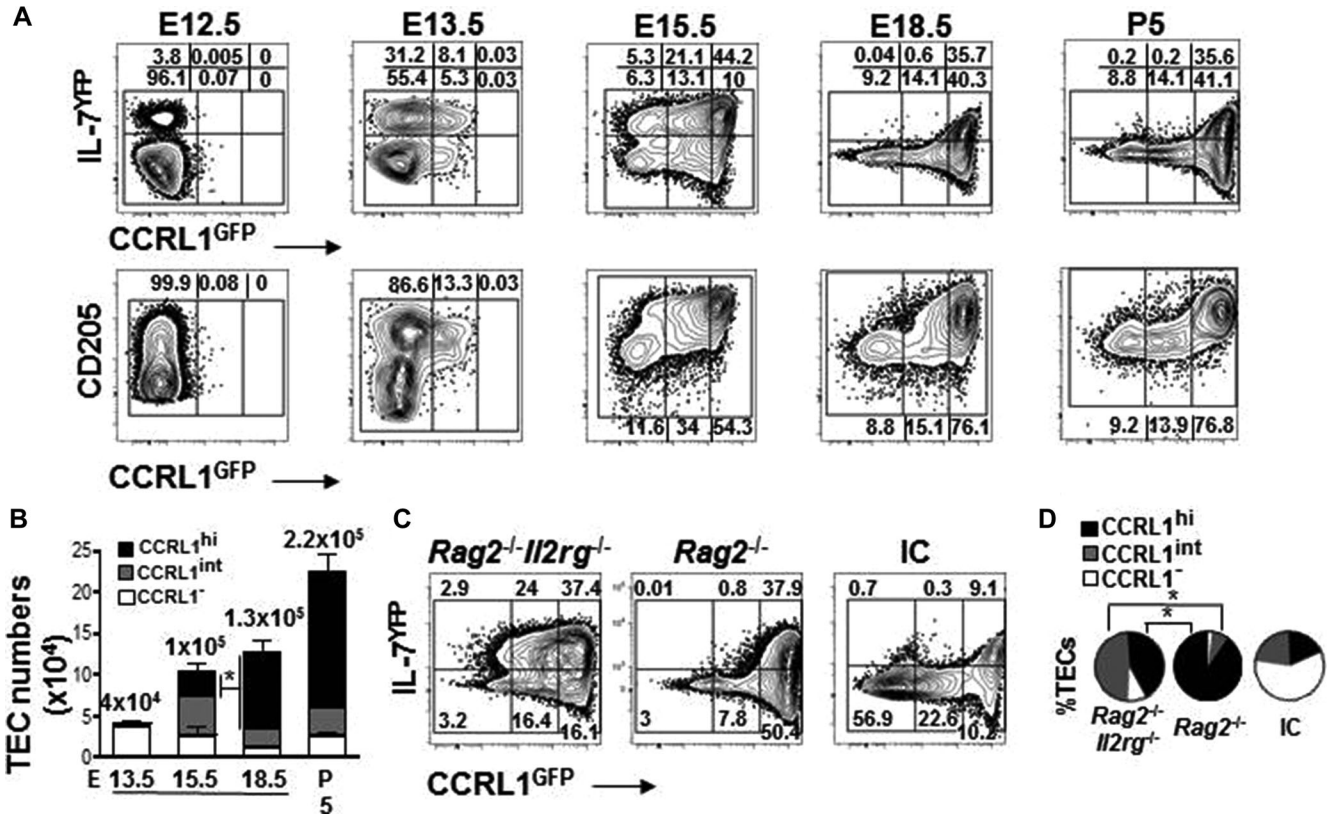

Figure 1. CCRL1 is a late cTEC determinant. (A) Total TECs (gated as CD45$^-$EpCAM$^+$) from IL-7^{YFP}CCRL1^{GFP} mice were analyzed for IL-7^{YFP} and CCRL1^{GFP} or CD205 and CCRL1^{GFP} expression by flow cytometry (FC) at the indicated time points. Numbers in plots indicate the frequency of cells found within each gate. Plots are representative of three to five independent experiments per time point. *E* represents embryonic day and *P5* represents postnatal day 5. (B) Cellularity of TECs expressing high (CCRL1^{hi}), intermediate (CCRL1^{int}), and no CCRL1 (CCRL1$^-$) was determined by the absolute thymic cell numbers and the respective frequencies of each subset obtained by FC. Numbers on top of bars indicate average TEC cellularity for each time point. Data are shown as mean + SD of 3–5 samples pooled from three to five independent experiments. $^*p < 0.05$ (unpaired *t* test). (C) TECs from 2-week-old *Rag2*$^{-/-}$, *Rag2*$^{-/-}$*Il2rg*$^{-/-}$, and immunocompetent (IC) thymi were analyzed by FC for IL-7^{YFP} and CCRL1^{GFP} expression. Numbers in plots indicate the frequency of each gate. Plots are representative of three independent experiments. (D) The mean proportion (%) of CCRL1 subsets in 2-week-old *Rag2*$^{-/-}$, *Rag2*$^{-/-}$*Il2rg*$^{-/-}$, and IC mice, determined by FC, is depicted. $^*p < 0.001$ (unpaired *t* test). Data represent means of three to five experiments ($n = 5$–6 mice/group).

Ccrl1 expression are shown in Supporting Information Fig. 2A and B, respectively). As this subtype was virtually absent at E15.5, we compared CCRL1^{int} TECs for the expression of additional cTEC (Ly51) and mTEC (UEA binding) markers [15, 17] in E18.5 and neonatal thymus. At both periods, CCRL1^{hi} and CCRL1$^-$CD80$^+$ TECs majorly identified either Ly51$^+$ cTECs or *Ulex Europaeus* Agglutinin 1 (UEA$^+$) mTECs, respectively (Fig. 2A and B). The CCRL1$^-$CD80$^-$ TECs, which represent a minor subset in the neonatal thymus, were predominantly composed of Ly51^{int}UEA$^+$ TECs at this stage. CCRL1^{int} TECs at E18.5 comprised mostly Ly51$^+$UEA$^-$CD80$^-$, although few UEA$^+$CD80$^-$ and scarce UEA$^+$CD80$^+$ were detected (Fig. 2B and C). Interestingly, three discrete sizeable subpopulations accumulated within neonatal CCRL1^{int} TECs, including UEA$^-$CD80$^-$, UEA$^+$CD80$^-$, and UEA$^+$CD80$^+$ (Fig. 2C). Both CD80$^-$ and CD80$^+$ CCRL1^{int}UEA$^+$ mTEC subsets, while scarce at E18.5 (Fig. 2B and C), totally represented approximately half and one quarter of the mTEC compartment in neonatal and young thymi, respectively (Fig. 2D). To examine whether CD80$^+$CCRL1^{int} mTECs differentiate by the reiteration of the same pathways defined for postnatal mTECs [2, 21], we set E18.5 fetal thymic organ cultures (FTOCs). While rare in intact FTOCs, RANK, and/or CD40 stimulation induced the differentiation of CD80$^+$CCRL1^{int} mTECs (Fig. 2E and Supporting Information Fig. 2C and D). Additionally, reaggregate thymic organ cultures (RTOCs) established with E15.5 CCRL1$^+$UEA$^-$CD80$^-$ TECs, and RANK- and CD40-activated to induce mTEC differentiation, showed that a fraction of fetal CCRL1$^+$ cTECs displayed CD80$^+$ mTEC progenitor activity (Fig. 2F). Next, we analyzed how the phenotypic traits of the emergent neonatal CCRL1^{int} TECs related to the expression of genes linked to cTECs (*Psmb11* and *Cstl*) and mTECs (*Tnfrsf11a* (RANK), *Ccl21*, and *Aire*) [2, 3]. Increasing *Psmb11* and *Cstl* expression was exclusively detected within CCRL1^{int}UEA$^-$ and CCRL1^{hi} cells. Interestingly, a gradual increase in *Tnfrsf11a* expression was observed in CCRL1^{int}UEA$^-$, CCRL1^{int}UEA$^+$CD80$^-$, CCRL1^{int}UEA$^+$CD80$^+$, and CCRL1$^-$CD80$^+$ TECs. *Ccl21*, which is expressed by postnatal immature mTECs [22], was specifically found within the CCRL1^{int}UEA$^-$CD80$^-$ and

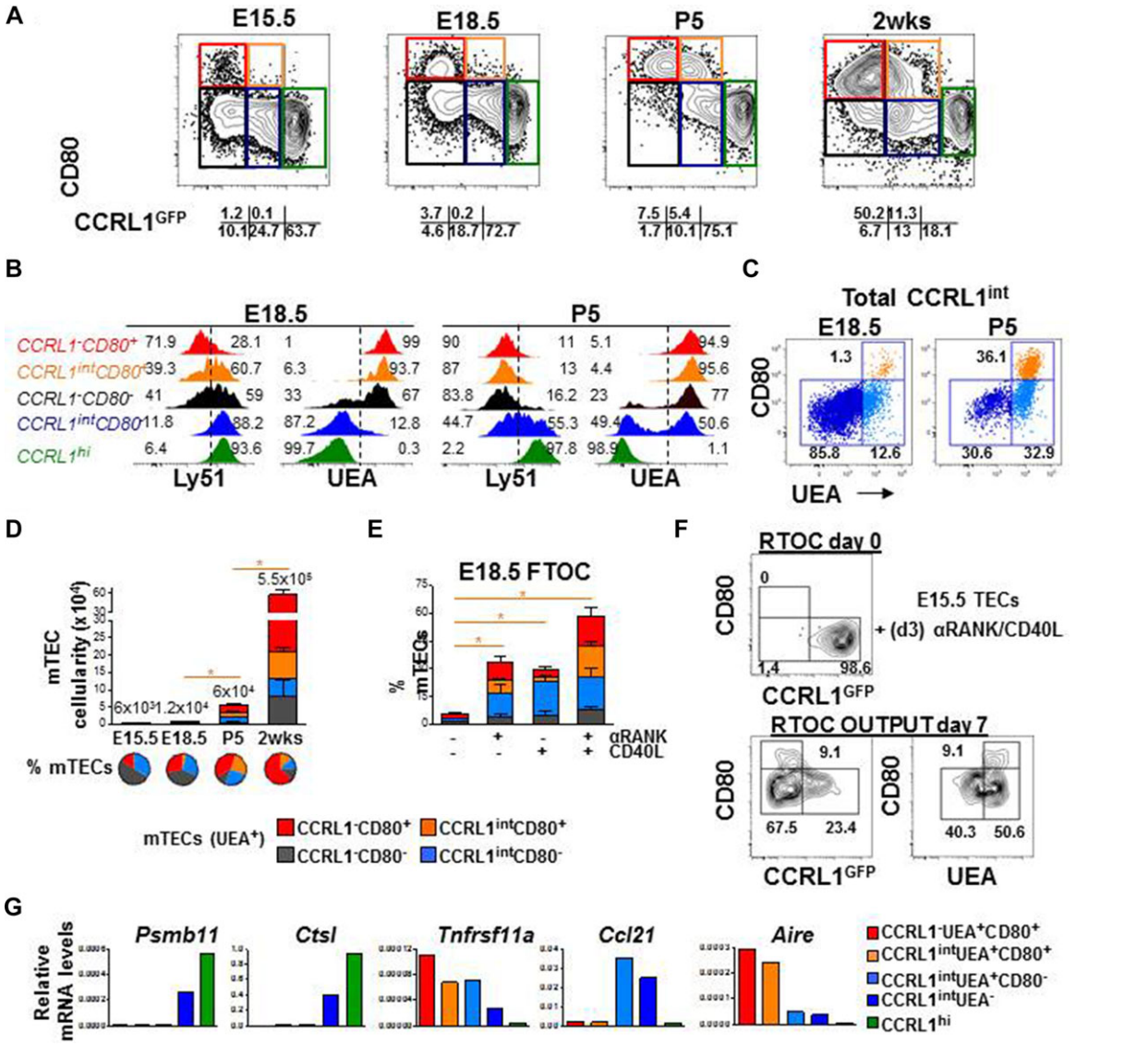

Figure 2. Intermediate CCRL1 expression reveals novel postnatal mTECs. (A) TECs (gated as CD45$^-$EpCAM$^+$) from IL-7^{YFP}CCRL1^{GFP} mice were analyzed for CCRL1^{GFP} and CD80 expression by FC at the indicated time points. Colored gates define different subsets and grids indicate the frequencies of each respective one. (B) TEC subsets defined by the colored gates in (A) from E18.5 and postnatal day 5 (P5) thymi were analyzed for Ly51 and UEA expression by FC. Numbers in histograms indicate the frequency within each gate. Histograms are representative of three to five independent experiments. (C) Expression of UEA and CD80 within gated E18.5 and postnatal day 5 (P5) total CCRL1^{int} TECs was determined by FC. Numbers in plots indicate the frequency of cells found within each gate. (A–C) Plots are representative of three to five independent experiments. (D) Cellularity of UEA$^+$ mTEC subsets from IL-7^{YFP}CCRL1^{GFP} mice was assessed as in Figure 1. Average total mTEC cellularity is detailed above bars. Pie graphs represent the mean proportion of color-coded subsets within total UEA$^+$ mTECs. *$p < 0.05$ (unpaired t test) (data are shown as mean + SD of 4–6 mice/group, pooled from three to five independent experiments (E) E18.5 FTOCs were cultured for 4 days with the indicated stimuli and then assessed for mTEC induction (UEA$^+$CD80$^{-/+}$) by FC. The proportion of subsets within UEA$^+$ mTECs is color-coded. Data are shown as mean + SD of 8–10 thymic lobes/group, pooled from three independent experiments. *$p < 0.05$ (unpaired t test). (F) RTOCs established with E15.5-derived CCRL1$^+$UEA$^-$CD80$^-$ TECs were stimulated with αRANK and/or CD40L and gated TECs were analyzed for the expression of the indicated markers by FC. Plots are representative of three independent experiments. (G) Expression of *Psmb11*, *Ctsl*, *Tnfrsf11a*, *Ccl21*, and *Aire* was assessed by qPCR in purified TEC subsets (colored columns) from postnatal day 5 (P5) IL-7^{YFP}CCRL1^{GFP} mice. Values were normalized to *18s*. Data are shown as representative of three independent experiments.

CCRL1^{int}UEA$^+$CD80$^-$ subsets. Lastly, *Aire* expression was equally enriched in CCRL1$^-$ and CCRL1^{int} CD80$^+$ mTECs (Fig. 2G). Although fetal CCRL1$^+$UEA$^-$ TECs have the potential to generate mTECs (Fig. 2F), and the gradual increase in the expression of RANK and CCL21 within CCRL1^{int} cells might suggest a continual stepwise differentiation: CCRL1^{int}UEA$^-$ – CCRL1^{int}UEA$^+$ – CCRL1^{int}UEA$^+$CD80$^+$, our attempts to evaluate a direct lineage relationship between neonatal CCRL1^{int} TEC subsets have been unsuccessful, given the difficulty of establishing RTOC with perinatal TECs [23]. Thus, we can only speculate that the postnatal cTEC niche harbors progenitors that are able to differentiate into mTECs, as shown in the fetal thymus [15–17]. Alternatively, one

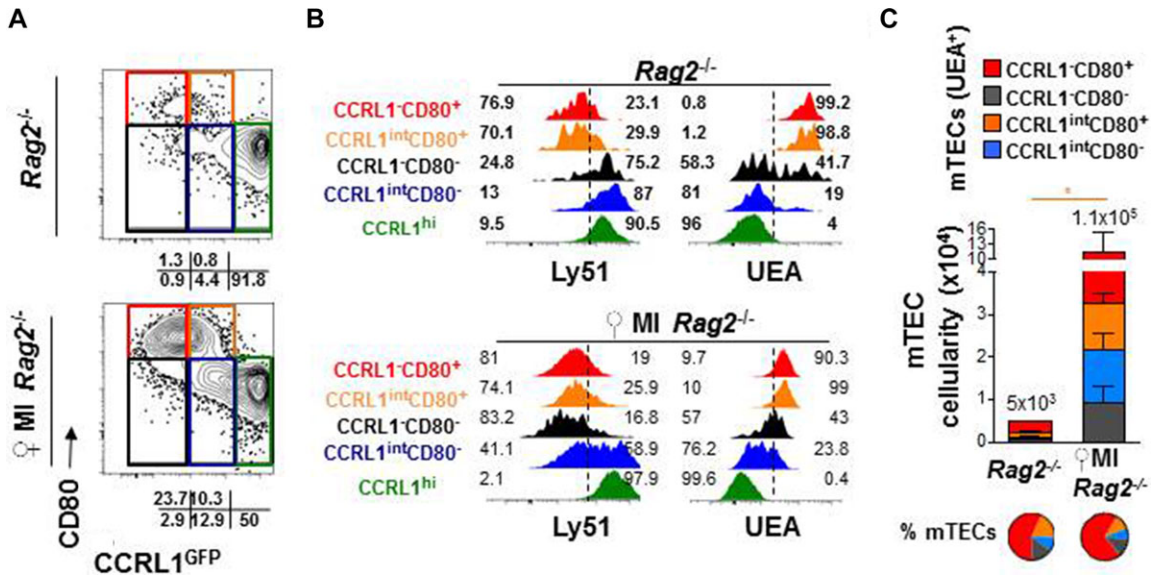

Figure 3. Thymic selection drives the emergence of the postnatal-specific CCRL1^{int}CD80^{+} TECs. (A) TECs (gated as CD45^{-}EpCAM^{+}) from postnatal day 5 (P5) *Rag2*$^{-/-}$ and female Marilyn-*Rag2*$^{-/-}$ mice were analyzed for CCRL1^{GFP} and CD80 expression by FC. Colored boxes define different TEC subsets and grids indicate the frequencies of each one. Plots are representative of two to three independent experiments. (B) Subsets defined by the colored gates in (A) from *Rag2*$^{-/-}$ and Marilyn-*Rag2*$^{-/-}$ mice were analyzed for Ly51 and UEA expression by FC. Numbers in histograms indicate the frequency within each gate. Histograms are representative of three independent experiments. (C) Frequency of subsets within total mTECs (pie graphs) and numbers of mTEC subsets was determined by FC. Data are shown as mean + SD of three to five samples, pooled from two independent experiments. $^{*}p < 0.05$ (unpaired *t* test).

cannot exclude that postnatal CCRL1^{int} mTECs might differentiate from a lineage unrelated to cTECs. Collectively, our data indicate that while CCRL1^{int}UEA^{-} TECs coexpress molecular traits of cTECs and mTECs, CCRL1^{int}UEA^{+}CD80^{-} and CCRL1^{int}UEA^{+}CD80^{+} cells define novel subtypes of immature and mature mTECs, respectively, that emerge postnatally.

Thymic selection promotes the generation of CCRL1^{int} mTECs

The differentiation of the CCRL1^{int}CD80^{+} mTECs correlates timely with the intensification of positive thymic selection around the perinatal period [6]. Given that activation of RANK and CD40 fostered CCRL1^{int}CD80^{+} mTECs (Fig. 2C) and the ligands for those mTEC-inductive signals are expressed by SP4 thymocytes [2], we investigated whether the appearance of CCRL1^{int}CD80^{+} mTECs depends on TEC-SP4 interactions during selection. To this end we crossed CCRL1-reporter mice onto a Marilyn-*Rag2*$^{-/-}$ TCR transgenic background, in which T cells express an I-A^{b}-restricted TCR that recognizes the male H-Y antigen [15]. As control, we coanalyzed *Rag2*$^{-/-}$ littermates, wherein mTEC differentiation is compromised due to the lack of mature thymocytes [15]. Few CD80^{+} mTECs were present in the neonatal *Rag2*$^{-/-}$ thymus, and those were majorly CCRL1^{-} (Fig. 3A–C), resembling mTECs found in the E18.5 thymus (Fig. 2). Contrarily to the normal postnatal thymus, the scarce CCRL1^{-} and CCRL1^{int} CD80^{-} subsets found in *Rag2*$^{-/-}$ mice were predominantly composed of Ly51^{+}UEA^{-} cells (Fig. 3A and B). Strikingly, we detected a marked expansion of both CCRL1^{-}CD80^{+} and CCRL1^{int}CD80^{+} mTECs in neonatal Marilyn-*Rag2*$^{-/-}$ females (Fig. 3A–C, nonreporter *Rag2*$^{-/-}$ and Marilyn-*Rag2*$^{-/-}$ are shown in S2E), recapitulating the mTEC composition of the young thymus (Fig. 2A). Akin to the WT thymus, CCRL1^{hi} and CCRL1^{-}CD80^{+} TECs specifically identified cTECs and mTECS, respectively, and the emergent CCRL1^{int}CD80^{+} TECs were Ly51^{lo}UEA^{+} (Fig. 3B). One can envision that temporally restricted mTEC differentiation pathways are engaged by interactions between mTEC precursors and distinct hematopoietic cells. As shown previously [10, 11], the generation of the first embryonic mature CD80^{+} mTECs (CCRL1^{-}) precedes the development of SP4s and depends on LTβR- and RANK-mediated signaling engaged upon lymphoepithelial interaction with lymphoid tissue inducer cells and γδ T cells [12–14]. Our findings indicate that the differentiation of the postnatal-restricted CCRL1^{int}CD80^{+} mTECs results from MHC-TCR, CD40-CD40L, and RANK-RANKL interactions [2, 21] between TEC precursors and TCRβ−selected thymocytes.

Concluding remarks

The neonatal life marks a period characterized by a drop in cTECs and an expansion in mTECs [20]. The identification of novel postnatal mTEC subsets supports the concept that the foundation of the adult medullary microenvironment results from alternative waves of mTEC differentiation. In this regard, recent evidence suggests that the expansion of the medulla after birth involves de novo formation of mTECs [24]. This notion implicates that fetal mTEC precursors might have limited self-renewal potential,

as shown for bipotent TEC progenitors [25], and in turn the formation of the adult mTEC niche relies on additional inputs arising after birth. Still, further studies are needed to elucidate to what extent bipotent progenitors might progress through the cortical differentiation program in the adult thymus. Also, the functional relevance of the mTEC heterogeneity reported herein should be further dissected. As mTECs have a crucial role in T-cell maturation and tolerance induction, our findings have implications in therapeutics aimed at modulating TEC niches in the adult thymus.

Materials and methods

Mice

Dual IL-7^{YFP}CCRL1^{GFP} reporter mice were backcrossed onto *Rag2*$^{-/-}$, *Rag2*$^{-/-}$*Il2rg*$^{-/-}$, and Marilyn-*Rag2*$^{-/-}$ C57BL/6 background [8, 15]. E0.5 was the day of vaginal plug detection. Animal experiments were performed in accordance with European guidelines.

TEC isolation and flow cytometry

TECs were isolated as described [15]. Cells were stained with anti– I-A/I-E (Alexa 780); anti-CD45.2 (PerCP-Cy5.5); anti-EpCAM (A647); anti-CD80 (A660); anti-Ly51, anti-CD205, UEA-1 (biotin), anti-EpCAM (eFluor 450) Abs, and streptavidin (PE-Cy7) (eBioscience). Flow cytometry was performed on a FACSCanto II, with data analyzed on FlowJo software (BD). Cell sorting was performed using the FACSAria I (BD Biosciences), with purities >95%. A 510/10-nm band pass (502LP dichroic mirror) and a 542/27-nm band pass (525LP dichroic mirror) filters were used to discriminate the GFP/YFP signals.

Gene expression

mRNA (RNAeasy MicroKit, Quiagen) isolation and cDNA synthesis (Superscript First-Strand Synthesis System, Invitrogen) were performed as described [15]. Real-time PCR (iCycler iQ5) was performed using either TaqMan Universal PCR Master Mix and primers for *18s, Ctsl, Aire, Ccl21, Tnfrsf11a*, and *Psmb11* (Applied Biosystems); or iQ SYBR Green Supermix (Bio-Rad) and primers for *Actb* and *Ccrl1* as detailed [15]; Triplicated samples were analyzed and the $\Delta\Delta$Ct method was used to calculate relative levels of targets compared with *18s/Actb* as described [15].

FTOCs and RTOCs

FTOCs and RTOCs were established with E18.5 and E15.5 embryos, respectively, as described [15]. For FTOCs, TECs were analyzed after 4 days culturing with 1 μg/mL anti-RANK and/or with 5 μg/mL recombinant CD40L (R&D Systems). For RTOCs, 10^5 E15.5 CCRL1^+UEA$^-$CD80^- TECs were sorted and mixed with CD4^+CD8^+ and CD4^+ thymocytes at 1:1:1 ratio. After 3 days, 0.3 μg/mL anti-RANK and 1.3 μg/mL recombinant CD40L were added to the cultures. RTOC were analyzed after 7 days.

Statistical analysis

The unpaired *t* test was used to perform statistical analysis. $p < 0.05$ was considered significant.

Acknowledgments: We thank James Di Santo, Jocelyne Demengeot, and Thomas Boehm for *Rag2*$^{-/-}$*Il2rg*$^{-/-}$, CCRL1-reporter, and Marilyn-*Rag2*$^{-/-}$ mice, respectively. We thank Dr. Catarina Leitão for critical reading of the manuscript and technical assistance. We thank FEDER funds through the Operational Competitiveness Programme – COMPETE and by National Funds through *Fundação para a Ciência e a Tecnologia* (FCT) under the project PTDC/SAU-IMU/117057/2010 funded this work. N.L.A., A.R.R., C.M., and P.M.R. are supported by FCT Investigator program and PhD fellowships.

Conflict of interest: The authors have no financial or commercial conflicts of interest.

References

1 **Takahama, Y.**, Journey through the thymus: stromal guides for T-cell development and selection. *Nat. Rev. Immunol.* 2006. **6**: 127–135.

2 **Anderson, G. and Takahama, Y.**, Thymic epithelial cells: working class heroes for T cell development and repertoire selection. *Trends Immunol.* 2012. **33**: 256–263.

3 **Mathis, D. and Benoist, C.**, Aire. *Annu. Rev. Immunol.* 2009. **27**: 287–312.

4 **Rossi, S. W., Jenkinson, W. E., Anderson, G. and Jenkinson, E. J.**, Clonal analysis reveals a common progenitor for thymic cortical and medullary epithelium. *Nature* 2006. **441**: 988–991.

5 **Bleul, C. C., Corbeaux, T., Reuter, A., Fisch, P., Monting, J. S. and Boehm, T.**, Formation of a functional thymus initiated by a postnatal epithelial progenitor cell. *Nature* 2006. **441**: 992–996.

6 **Anderson, G., Jenkinson, E. J. and Rodewald, H. R.**, A roadmap for thymic epithelial cell development. *Eur. J. Immunol.* 2009. **39**: 1694–1699.

7 **Shakib, S., Desanti, G. E., Jenkinson, W. E., Parnell, S. M., Jenkinson, E. J. and Anderson, G.**, Checkpoints in the development of thymic cortical epithelial cells. *J. Immunol.* 2009. **182**: 130–137.

8 **Alves, N. L., Huntington, N. D., Mention, J. J., Richard-Le Goff, O. and Di Santo, J. P.**, Cutting edge: a thymocyte-thymic epithelial cell cross-talk dynamically regulates intrathymic IL-7 expression in vivo. *J. Immunol.* 2010. **184**: 5949–5953.

9 **Ripen, A. M.**, **Nitta, T.**, **Murata, S.**, **Tanaka, K. and Takahama, Y.**, Ontogeny of thymic cortical epithelial cells expressing the thymoproteasome subunit beta5t. *Eur. J. Immunol.* 2011. **41**: 1278–1287.

10 **Hamazaki, Y.**, **Fujita, H.**, **Kobayashi, T.**, **Choi, Y.**, **Scott, H. S.**, **Matsumoto, M. and Minato, N.**, Medullary thymic epithelial cells expressing Aire represent a unique lineage derived from cells expressing claudin. *Nat. Immunol.* 2007. **8**: 304–311.

11 **White, A. J.**, **Withers, D. R.**, **Parnell, S. M.**, **Scott, H. S.**, **Finke, D.**, **Lane, P. J.**, **Jenkinson, E. J. et al.**, Sequential phases in the development of Aire-expressing medullary thymic epithelial cells involve distinct cellular input. *Eur. J. Immunol.* 2008. **38**: 942–947.

12 **Rossi, S. W.**, **Kim, M. Y.**, **Leibbrandt, A.**, **Parnell, S. M.**, **Jenkinson, W. E.**, **Glanville, S. H.**, **McConnell, F. M. et al.**, RANK signals from CD4(+)3(-) inducer cells regulate development of Aire-expressing epithelial cells in the thymic medulla. *J. Exp. Med.* 2007. **204**: 1267–1272.

13 **Roberts, N. A.**, **White, A. J.**, **Jenkinson, W. E.**, **Turchinovich, G.**, **Nakamura, K.**, **Withers, D. R.**, **McConnell, F. M. et al.**, Rank signaling links the development of invariant gammadelta T cell progenitors and Aire(+) medullary epithelium. *Immunity* 2012. **36**: 427–437.

14 **Mouri, Y.**, **Yano, M.**, **Shinzawa, M.**, **Shimo, Y.**, **Hirota, F.**, **Nishikawa, Y.**, **Nii, T. et al.**, Lymphotoxin signal promotes thymic organogenesis by eliciting RANK expression in the embryonic thymic stroma. *J. Immunol.* 2011. **186**: 5047–5057.

15 **Ribeiro, A. R.**, **Rodrigues, P. M.**, **Meireles, C.**, **Di Santo, J. P. and Alves, N. L.**, Thymocyte selection regulates the homeostasis of IL-7-expressing thymic cortical epithelial cells in vivo. *J. Immunol.* 2013. **191**: 1200–1209.

16 **Baik, S.**, **Jenkinson, E. J.**, **Lane, P. J.**, **Anderson, G. and Jenkinson, W. E.**, Generation of both cortical and Aire(+) medullary thymic epithelial compartments from CD205(+) progenitors. *Eur. J. Immunol.* 2013. **43**: 589–594.

17 **Ohigashi, I.**, **Zuklys, S.**, **Sakata, M.**, **Mayer, C. E.**, **Zhanybekova, S.**, **Murata, S.**, **Tanaka, S. et al.**, Aire-expressing thymic medullary epithelial cells originate from beta5t-expressing progenitor cells. *Proc. Natl. Acad. Sci. USA* 2013. **110**: 9885–9890.

18 **Alves, N. L.**, **Takahama, Y.**, **Ohigashi, I.**, **Ribeiro, A. R.**, **Baik, S.**, **Anderson, G. and Jenkinson, W. E.**, Serial progression of cortical and medullary thymic epithelial microenvironments. *Eur. J. Immunol.* 2014. **44**: 16–22.

19 **Rodewald, H. R.**, **Paul, S.**, **Haller, C.**, **Bluethmann, H. and Blum, C.**, Thymus medulla consisting of epithelial islets each derived from a single progenitor. *Nature* 2001. **414**: 763–768.

20 **Rode, I. and Boehm, T.**, Regenerative capacity of adult cortical thymic epithelial cells. *Proc. Natl. Acad. Sci. USA* 2012. **109**: 3463–3468.

21 **Akiyama, T.**, **Shimo, Y.**, **Yanai, H.**, **Qin, J.**, **Ohshima, D.**, **Maruyama, Y.**, **Asaumi, Y. et al.**, The tumor necrosis factor family receptors RANK and CD40 cooperatively establish the thymic medullary microenvironment and self-tolerance. *Immunity* 2008. **29**: 423–437.

22 **Lkhagvasuren, E.**, **Sakata, M.**, **Ohigashi, I. and Takahama, Y.**, Lymphotoxin beta receptor regulates the development of CCL21-expressing subset of postnatal medullary thymic epithelial cells. *J. Immunol.* 2013. **190**: 5110–5117.

23 **Rossi, S. W.**, **Chidgey, A. P.**, **Parnell, S. M.**, **Jenkinson, W. E.**, **Scott, H. S.**, **Boyd, R. L.**, **Jenkinson, E. J. et al.**, Redefining epithelial progenitor potential in the developing thymus. *Eur. J. Immunol.* 2007. **37**: 2411–2418.

24 **Dumont-Lagace, M.**, **Brochu, S.**, **St-Pierre, C. and Perreault, C.**, Adult thymic epithelium contains nonsenescent label-retaining cells. *J. Immunol.* 2014. **192**: 2219–2226.

25 **Jenkinson, W. E.**, **Bacon, A.**, **White, A. J.**, **Anderson, G. and Jenkinson, E. J.**, An epithelial progenitor pool regulates thymus growth. *J. Immunol.* 2008. **181**: 6101–6108.

Abbreviations: **Aire**: auto-immune regulator · **CCRL1**: chemokine (C–C motif) receptor-like 1 · **cTEC**: cortical TEC · **FC**: flow cytometry · **FTOC**: fetal thymic organ culture · **LTβR**: lymphotoxin beta receptor · **mTEC**: medullary TEC · **RANK**: receptor activator of NF-κB · **RTOC**: reaggregate thymic organ culture · **SP**: single positive · **TEC**: thymic epithelial cell · **UEA**: *Ulex Europaeus* Agglutinin 1

Full correspondence: Ana Rosalina Ribeiro, Institute for Molecular and Cellular Biology, Rua do Campo Alegre, 823, 4150-180 Porto, Portugal
Fax: +351-226-099-157
e-mail: ana.ribeiro@ibmc.up.pt

Additional correspondence: Dr. Nuno L. Alves, Institute for Molecular and Cellular Biology, Rua do Campo Alegre, 823, 4150–180 Porto, Portugal.
Fax: +351-226-099-157
e-mail nalves@ibmc.up.pt

Received: 20/2/2014
Revised: 6/6/2014
Accepted: 25/7/2014
Accepted article online: 28/7/2014

DOI: 10.1002/eji.201746922 Eur. J. Immunol. 2017. 47: 958–969

European Journal of Immunology

Adaptive immunity

Research Article

Thymic crosstalk restrains the pool of cortical thymic epithelial cells with progenitor properties

Catarina Meireles[*1,2,3], *Ana R. Ribeiro*[*1,2], *Rute D. Pinto*[1,2], *Catarina Leitão*[1], *Pedro M. Rodrigues*[1,2] *and Nuno L. Alves*[*1,2]

[1] Instituto de Investigação e Inovação em Saúde, Universidade do Porto, Porto, Portugal
[2] Thymus Development and Function Laboratory, Infection and Immunity Unit, Instituto de Biologia Molecular e Celular, Porto, Portugal
[3] Doctoral Program in Cell and Molecular Biology, Instituto de Ciências Biomédicas, Universidade do Porto, Porto, Portugal

Cortical (cTEC) and medullary (mTEC) thymic epithelial cells establish key microenvironments for T-cell differentiation and arise from thymic epithelial cell progenitors (TEP). However, the nature of TEPs and the mechanism controlling their stemness in the postnatal thymus remain poorly defined. Using TEC clonogenic assays as a surrogate to survey TEP activity, we found that a fraction of cTECs generates specialized clonal-derived colonies, which contain cells with sustained colony-forming capacity (*Clono*TECs). These *Clono*TECs are EpCAM+MHCII-Foxn1lo cells that lack traits of mature cTECs or mTECs but co-express stem-cell markers, including CD24 and Sca-1. Supportive of their progenitor identity, *Clono*TECs reintegrate within native thymic microenvironments and generate cTECs or mTECs in vivo. Strikingly, the frequency of cTECs with the potential to generate *Clono*TECs wanes between the postnatal and young adult immunocompetent thymus, but it is sustained in alymphoid *Rag2-/-Il2rg-/-* counterparts. Conversely, transplantation of wild-type bone marrow hematopoietic progenitors into *Rag2-/-Il2rg-/-* mice and consequent restoration of thymocyte-mediated TEC differentiation diminishes the frequency of colony-forming units within cTECs. Our findings provide evidence that the cortical epithelium contains a reservoir of epithelial progenitors whose abundance is dynamically controlled by continual interactions with developing thymocytes across lifespan.

Keywords: Lympho-epithelial interactions · Progenitor · Thymic epithelial cells · Thymocytes · Thymus

Additional supporting information may be found in the online version of this article at the publisher's web-site

Introduction

The development and selection of highly diverse T cells, which are responsive against pathogens while tolerant to one's own organs, takes place in dedicated niches of the thymus. Central to this instructive process are thymic epithelial cells (TECs) that segregate into specialized cortical (cTEC) and medullary (mTEC) microenvironments [1]. While cTECs instruct the commitment of hematopoietic precursors into the T cell lineage and positively select thymocytes expressing major histocompatibility complex (MHC)-restricted T cell receptors (TCRs), mTECs contribute to the elimination of thymocytes expressing autoreactive TCR and

Correspondence: Dr. Nuno L. Alves
e-mail: nalves@ibmc.up.pt

*Co-first author.

the development of regulatory T cells [2]. Consequently, genetic alterations that affect the differentiation of TECs lead to pathologies that range from immunodeficiency to autoimmunity [1]. Since TECs are sensitive to aging and conditioning regiments linked to bone marrow transplantation or cancer therapy [3], the functionalization of thymic epithelial niches emerges as a direct approach to improve thymopoiesis in disorders associated with ineffective T-cell responses.

The two-prototypical cTEC and mTEC subsets differentiate from common bipotent TEC progenitors (TEP) that exist in the embryonic [4–6] and postnatal [7] thymus. Deciphering how bipotent TEPs self-renew and transmogrify into cTECs and mTECs has been under intense investigation. The discovery of mTEC-restricted precursors [8–10] led to the concept that TEP give rise to cortical and medullary lineages through unrelated differentiation pathways. More recently, evidence that embryonic cTEC-like progenitors have the potential to generate cTECs and mTECs [11–13] suggests that TEPs might progress through the cortical lineage prior to commitment to mTECs [14]. These findings equally implicate that TEPs nestle within the embryonic cortex. Recent studies identify distinct subsets of TECs in the postnatal thymus that contain, without exclusively marking, purportedly TEPs [15–17]. Yet, the singular identity and anatomical location of TEPs are still elusive. Moreover, whether TEC differentiation follows the same precursor-product relationships in the postnatal thymus is not airtight.

Thymic epithelial cell microenvironments turnover more rapidly than previously recognized, with an estimated replacement rate of one-two weeks to mTECs of the young adult thymus [18, 19]. These results suggest a requirement for regular differentiation of new mature TECs from their upstream progenitors. Two, not necessarily mutually exclusive, scenarios can coincide. On one hand, long-lasting TEPs must continually produce lineage-committed precursors lacking self-renewal capacity. Alternatively, the abundance of functional TEPs might drop with age, being the replenishment of cortical and medullary epithelial niches assured by downstream compartment-restricted precursors. Fate-mapping studies show that the majority of adult mTEC network arise from fetal- and newborn-derived TEPs expressing beta5t (β5t), a prototypical cTEC marker [20, 21]. Furthermore, mTEC-restricted SSEA-1$^+$ progenitors [22, 23] and specialized podoplanin$^+$ (PDPN) mTEPs residing at the cortico-medullary junction (CMJ) [24] have been identified, both contributing to the maintenance of mTEC compartment. Together, these findings infer that the bipotent capacity of TEPs is preserved beyond birth, but might be progressively lost with age. Consequently, the maintenance of adult medullary epithelial network seems to be secured by unipotent mTEPs.

Despite recent advances, it remains unclear how changes in the bioavailability of TEPs impact on the maintenance of TEC microenvironment across life, and ultimately on thymic output. Another unexplored area pertains to the physiological causes underlying the presumed age-dependent decrease and/or senescence of TEPs. Since the amount of embryonic TEP dictates the size of functional TEC microenvironments [25], it is conceivable that the loss in the TEC network with age might be coupled to the loss in TEP stemness. Nevertheless, we lack experimental evidence that argues in favor, or against, this possibility. Herein, we identify a subset of cTECs that generates TEC colonies of clonal origin, harbouring cells with progenitor traits, including continual colony-forming capacity, lack of mature TEC markers and bearing the potential to generate cTECs and mTECs. Detailed temporal analysis reveals that the abundance of cTECs with clonogenic activity decreases with the entry into the adulthood, in a process that is directly regulated by lympho–epithelial interactions.

Results

The postnatal cortical thymic epithelium contains cells with clonogenic capacity

The postnatal thymus represents a period of active growth of the TEC network, which plateaus during young adulthood followed by a progressive reduction with age [18, 26]. We conjectured that these dynamic changes in TEC niches might be coupled to a gradual exhaustion of TEPs. To seek for epithelial stemness within the postnatal thymus, we established clonogenic assays that were previously reported to select and support the growth of stem cells from other stratified epithelial cells and the rat thymus [27, 28]. In these midscale assays, bulk postnatal cell-sorted TECs (CD45$^-$EpCAM$^+$MHCII$^+$) were cultivated in specialized medium onto a monolayer of feeder cells (irradiated 3T3) (Supporting Information Fig. 1A). TEC-derived colonies emerged around day 6 and grew in size up to day 12, containing tightly packed cells that express the pan-epithelial marker EpCAM (Supporting Information Fig. 1B and C) and cytokeratin 8 (K8) [29] (Fig. 1A). A limitation of experiments with "bulk" cultivated TECs is that they might hinder a possible heterogeneity at the single cell level. Thus, we determined whether the clonogenic potential was a property of all, or only a fraction of postnatal-TECs. First, we performed co-culture assays with equal amounts of postnatal cell-sorted TECs isolated from mice that constitutively express Green Fluorescent Protein (GFP) or Red Fluorescent Protein (RFP) under the control of β-actin promoter. In this setting, colony-forming units could be surveyed on the basis of their live-cell fluorescence. The development of either single GFP$^+$ or single RFP$^+$ TEC-derived colonies suggested their clonal origin (Fig. 1B). Next, combining high-speed cell sorting and high-content imaging analysis, we microscaled the assay down to single-cell level and showed that TEC colonies were clonally derived from single-sorted TECs. Interestingly, not all TECs gave origin to colonies (Fig. 1C). Hence, serial dilution clonogenic assays offered a mean to quantify the colony-forming precursor frequency within TECs throughout normal and altered pathophysiological settings (a point addressed later in this study). Given their clonal origin, we referred to the cells that emerge from these cultures as *Clono*TECs. We also cultured postnatal-derived non-epithelial thymic stromal cells (CD45$^-$EpCAM$^-$) under clonogenic conditions, but these lack

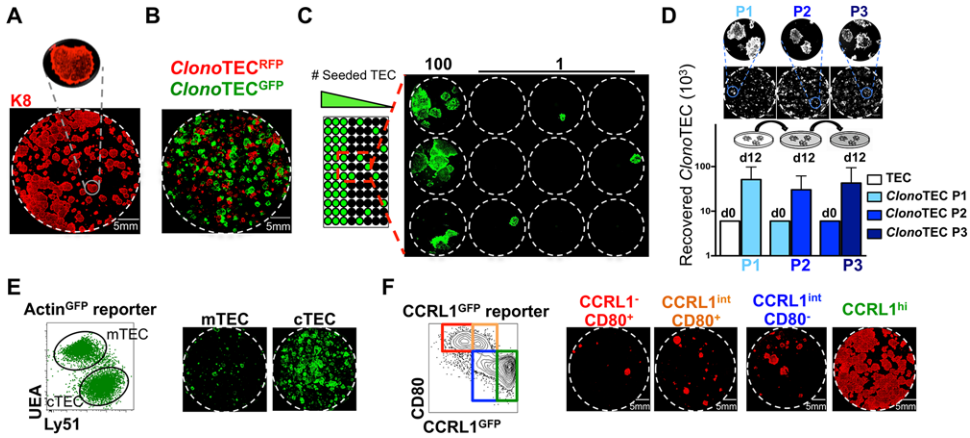

Figure 1. Colony-precursor cells are markedly restricted to the cortical thymic epithelium of the postnatal thymus. (A) Midscale clonogenic assays (6-well microplates) were established with cell-sorted total TECs (defined as CD45$^-$EpCAM$^+$) from postnatal day 5 (P5) thymus. After 12 days, cultures were fixed, stained with anti-cytokeratin 8 (K8) antibody and analyzed by immunofluorescence microscopy. **(B)** Cell-sorted total TECs purified from P5 Actin^{GFP} and Actin^{RFP} reporter mice were co-cultured at 1:1 ratio in midscale clonogenic assays and analyzed for the expression of GFP and RFP by fluorescence live cell imaging. **(C)** P5 Actin^{GFP} TECs were directly sorted at indicated densities into microscale clonogenic assay (96-well microplates) and the colony formation was analyzed by fluorescence live cell imaging. Green circles mark positive wells for clonogenic activity, while black circles mark wells with no activity (left). Representative live-cell fluorescence images of indicated wells are shown (right). **(D)** *Clono*TECs contain cells with continual regrowth and colony-forming potential in vitro. Clonogenic assays were established with cell-sorted TECs from P5 Actin^{GFP} or Actin^{RFP} at the indicated density (6000 cells). 12 days after culture, *Clono*TECs (P1) were analyzed by flow cytometry (EpCAM$^+$ and GFP$^+$or RFP$^+$), purified by cell sorting and re-cultured into clonogenic assays at the initial density (6000 cells) for two consecutive passages (P2 and P3). Representative scheme of the passages and live cell immunofluorescence analysis of indicated cultures at day 12 of each passage is displayed (top). The number of cells at day 0 (d0) and at day 12 (d12) from the different passages (P1-P3) is shown as mean ± SEM of a pool of 10 independent experiments. **(E)** cTECs and mTECs from P5 Actin^{GFP} were sorted and cultured under clonogenic assays. Cultures were analyzed for the expression of GFP by fluorescence live cell imaging. **(F)** TEC subsets from P5 CCRL1^{GFP} reporter mice were purified based on CCRL1^{GFP} and CD80 expression (as indicated in color gates) and cultured under clonogenic assays. Cultures were fixed, stained with anti-cytokeratin 8 (K8) antibody and analyzed by immunofluorescence microscopy. (A, B, E & F) Images represent complete individual wells from midscale clonogenic assays and are illustrative of at least three experiments. Scale bars, 5 mm.

distinct colony-forming potential and did not generate *Clono*TECs as their CD45$^-$EpCAM$^+$ counterparts (Supporting Information Fig. 1D). Interestingly, *Clono*TECs contain a small fraction of cells with the capacity to regrow and re-establish clonal-derived colonies upon serial passages in vitro (Fig. 1D and Supporting Information Fig. 1E). The observations that *Clono*TECs were generated from a portion of TECs led us to investigate whether the clonogenic capacity was restricted to a subpopulation of cTECs and/or mTECs. To do so, we first purified by cell sorting cTECs (Ly51$^+$) and mTECs (UEA$^+$) from actin^{GFP} reporter mice and found that the clonogenic capacity was markedly enriched within cTECs (Fig. 1E). Additionally, we used CCRL1^{GFP} reporter mice, in which the combined analysis of the expression of CCRL1^{GFP} and CD80 defines discrete subsets of cTECs and mTECs in the postnatal thymus [26] (Fig. 1F). While high levels of CCRL1^{GFP} cells (CCRL1^{hi}) identifies Ly51$^+$cTECs, intermediate levels of CCRL1^{GFP} define additional subsets of mTECs (UEA$^+$CD80$^-$ and UEA$^+$CD80$^+$, as described in [26]) that arise in the postnatal thymus (Fig. 1F and Supporting Information Fig. 1F) Analysis of the discrete TEC subsets confirmed that the clonogenic capacity was mostly restricted to CCRL1^{hi} cTECs (Fig. 1F). Limiting dilution clonogenic assays confirmed that colonies were of clonal origin and a property of a fraction of CCRL1^{hi} cTECs (Supporting Information Fig. 1G). Yet, we also found residual clonogenic activity in CCRL1^{int}CD80$^{+/-}$ and CCRL1$^-$CD80$^+$ expressing subsets (Fig. 1F). Together, these results identified that most of colony-forming cells existed within cTECs (CD45$^-$EpCAM$^+$Ly51$^+$CCRL1^{hi}), suggesting that the postnatal cortical epithelial niche harbors cells with potential progenitor activity.

*Clono*TECs display phenotypic and molecular traits of TEP-like cells

To determine the epithelial lineage identity of cTEC-derived *Clono*TECs that arise upon culture, we characterized them at phenotypic and molecular levels using a panel of pan-TEC, cTEC- and mTEC-restricted markers. As reference, we co-analyzed freshly isolated total TECs, cTECs and mTECs. Contrarily to ex vivo total TECs, *Clono*TECs lacked MHCII and expressed minute amounts of Foxn1 both at protein and mRNA levels (Fig. 2A and B). To test whether *Clono*TECs derived from Foxn1-expressing cells that downregulated Foxn1 expression, we established clonogenic assays with cell-sorted cTECs from Foxn1^{eGFP} reporter mouse strain [30], in which nearly all TECs were marked by Foxn1^{eGFP} expression (Supporting Information Figure 2A). Notably, total, or even the highest, Foxn1^{eGFP}-expressing cTECs generated detectable colonies (containing *Clono*TECs) that lost GFP expression, as measured by live-cell fluorescence imaging

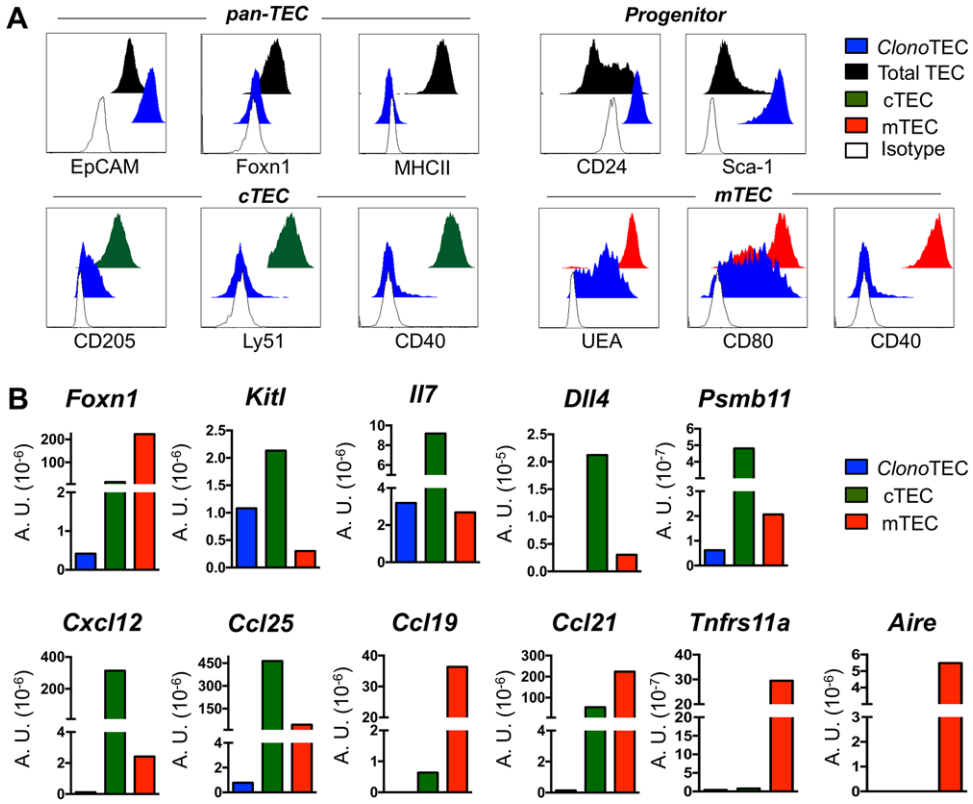

Figure 2. *Clono*TECs typify TEP-like cells. (A) cTEC-derived *Clono*TECs (blue) were analyzed by flow cytometry for the expression of the indicated markers. As a comparison, ex vivo bulk TECs (black), cTECs (dark green) or mTECs (red) isolated from postnatal day 7 thymus were co-analyzed. Isotype antibody controls for each antibody is represented (white) **(B)** *Clono*TECs, cTECs and mTECs were purified by cell sorting and analyzed by RT-qPCR for the expression of the indicated genes. Relative mRNA expression for represented target genes was normalized to *18s* and values are represented in arbitrary units (A.U.). Data are from single samples representative of two to three experiments using independent samples.

and flow cytometry analyses (Supporting Information Fig. 2B–D). Interestingly, *Clono*TECs expressed CD24 and Sca-1, which have been reported to identify epithelial stem cells in other anatomical sites, including breast and lung [31, 32] (Fig. 2A). Furthermore, *Clono*TECs expressed low levels of CD205 and lacked Ly51 when compared to cTECs, and displayed little UEA binding capacity and lower levels of CD80 and lacked CD40 relatively to mTECs (Fig. 2A). Additionally, we analyzed the molecular profile of purified *Clono*TECs for a restricted set of genes associated with cTECs (*Kitl*, *Dll4*, *Il7*, *Psmb11* (β5t), *Cxcl12* and *Ccl25*) or mTECs (*Ccl19*, *Ccl21*, *Tnfrs11a* (RANK) and *Aire*), and found that *Clono*TECs expressed lower to undetectable levels of cortical- and medullary-associated transcripts. Collectively, these findings infer that *Clono*TECs segregate from prototypical mature TECs and typify instead a subset with TEP-like properties.

*Clono*TECs generate cTECs and mTECs in vivo

To define the in vivo lineage potential of *Clono*TECs, we combined the usage of clonogenic assays with reaggregate thymic organ cultures (RTOC) and thymic transplantation under the kidney capsule. As *Clono*TECs generated from CCRL1^{GFP} cTEC lose GFP expression in culture (data not shown), they were not the most appropriate for fate mapping experiments. Since Ly51^{+}cTEC from Actin^{GFP} reporter mice exhibited similar clonogenic capacity to CCRL1^{GFP} cTEC from CCRL1^{GFP} reporter mice (Fig. 1), we used purified *Clono*TECs (*Clono*TEC$^{ActinGFP+}$) generated from the first subset, in which constitutive active GFP expression provides an intrinsic label for subsequent lineage tracing in vivo. To reconstruct thymic epithelia microenvironments, we mixed *Clono*TEC$^{ActinGFP+}$ with dGUO-treated E14.5 thymic cells and the resulting hybrid RTOC was transplanted under the kidney capsule of WT mice to allow the ectopic formation of a thymus (Supporting Information Fig. 3A). As control, dGUO-treated E14.5 thymus (*Clono*TEC$^{ActinGFP+}$-free) were reaggregated and subjected to similar procedure. From 6 control and 11 hybrid engrafted RTOCs, 4 and 8 ectopic thymi were respectively recovered 4 weeks post-thymic transplantation and analysed by flow cytometry and immunofluorescence microscopy. The progeny of *Clono*TEC$^{ActinGFP+}$ was distinctly present in all RTOCs as CD45^{-}EpCAM^{+} cells, with a fraction of them expressing MHCII (Supporting Information Fig. 3B). These findings indicate that *Clono*TECs contained cells competent to engage into

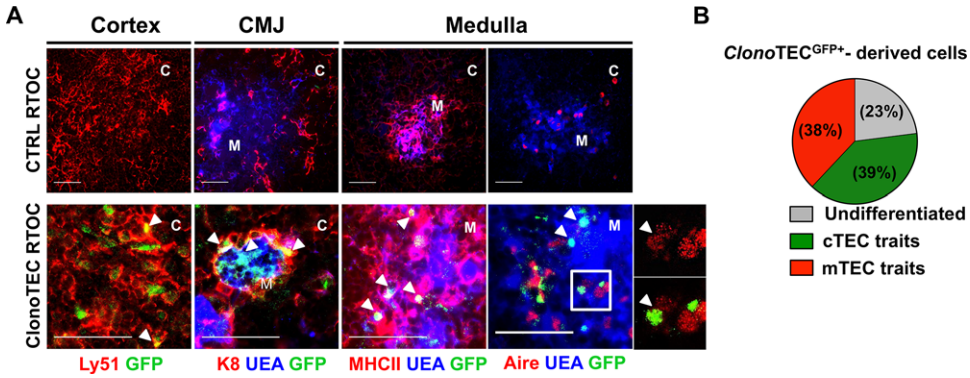

Figure 3. *Clono*TECs contain cells that are able to generate cTECs and mTECs in vivo. Generated cTEC^{ActinGFP}-derived *Clono*TECs^{GFP} were cell-sorted and aggregated with dGuo-treated E14.5 thymic lobes. RTOCs were transplanted into the kidney capsule of WT mice, ectopic thymi were recovered 4 weeks post-transplantation (Details in Supporting Information Figure 3A). **(A)** Immunofluorescence analysis of ectopic thymus. Control and *Clono*TECs post-transplanted RTOCs were co-analyzed for the expression of GFP, K8, Ly51, MHCII and Aire with specific antibodies and UEA binding capacity, with the indicated combinations in serial sections. Cortical (C) and medullary (M) regions were defined as either Ly51$^+$ or K8$^+$ areas and UEA$^+$ or MHCII^{bright} areas, respectively. Triangles indicate examples of *Clono*TEC^{GFP+}-derived cells that display features of either cTEC (Ly51 or K8) or mTEC (UEA, MHCII, Aire) lineage traits. 50 μm scale is shown. Images are representative of 5 ectopic thymus containing *Clono*TEC^{GFP}. **(B)** Quantification of lineage fate distribution of *Clono*TECs. Pie graph represents the proportion of *Clono*TEC^{GFP+}-derived cells within the thymic grafts that express the above-indicated cTEC (green) or mTEC (red) markers. *Clono*TEC-derived cells (GFP$^+$) found within cTEC area (K8$^+$ or Ly51$^+$) and expressing these markers were scored as cTECs. *Clono*TEC-derived cells (GFP$^+$) found within mTEC area (UEA$^+$ and MHCII^{bright}) and binding UEA or expressing high levels of MHCII were scored as mTECs. *Clono*TEC-derived cells (GFP$^+$) found within cTEC and mTEC areas that lacked respective cTEC/mTEC-markers were considered as undifferentiated (gray).

the TEC differentiation pathway. Nevertheless, we recovered few TECs (either from embryonic or *Clono*TEC origin) from individual RTOCs for flow cytometry analysis. Thus, to gain insights about the phenotypic properties and spatial distribution of *Clono*TECs within native thymic niches, transplanted RTOCs were further analyzed by immunofluorescence microscopy. *Clono*TEC$^{ActinGFP+}$-derived cells were found in all recovered RTOCs (Supporting Information Figure 3C-D), embedded within cortical (Ly51$^+$ or K8$^+$) or medullary (UEA$^+$) microenvironments or positioned at the CMJ (intersection of K8$^+$ and UEA$^+$ areas) (Fig. 3A). Although a fraction of *Clono*TEC progeny (GFP$^+$) lacked typical cTEC/mTEC markers, we found that some located within cTEC areas expressed cTEC traits, such as K8$^+$ or Ly51$^+$, while others residing within mTEC areas displayed mTEC features, including UEA$^+$ and MHCII^{hi} (Fig. 3A and B). We also found rare Aire-expressing *Clono*TEC-derived cells within mTEC compartment, indicating their potential to complete mTEC maturation (Fig. 3A). Additionally, to validate that *Clono*TEC-derived cells engaged in a TEC differentiation program, we performed similar reaggregation experiments using *Clono*TECs generated from Foxn1^{eGFP+} cTECs (Supporting Information Fig. 3E). As Foxn1^{eGFP+} cTECs lose Foxn1^{eGFP} expression in vitro (Supporting Information Fig. 2), GFP expression provides in this case a dual label for lineage tracing and assessment of Foxn1^{eGFP} re-induction by *Clono*TECs-derived cells. We detected GFP-expressing cells only in RTOCs spiked with *Clono*TECs that derived from Foxn1^{eGFP+} cTECs (Supporting Information Fig. 3F). *Clono*TECs-derived cells expressed EpCAM, with a fraction co-expressing MHCII and binding UEA (Supporting Information Fig. 3G). Overall, these results indicate that cTEC-derived *Clono*TECs contain cells with the potential to generate cTECs and/or mTECs upon integration in native thymic microenvironments.

The clonogenic activity of cTECs decreases with the entry into the adulthood

The observation that a fraction cTEC-derived ClonoTECs maintains their clonogenic potential in vitro and generates cTECs and/or mTECs indicate that the cortical niche harbors TEC progenitors. Thus, we inferred that the measurement of the clonogenic potential of TEC subsets at neonatal, pre-puberty and young adult stages could be used as a proxy to survey alterations in TEP dynamics throughout time. In CCRL1 reporter mice, analysis of CCRL1^{GFP} and CD80 expression allowed us to discriminate heterogeneous TEC subsets in the postnatal thymus [26]. While CCRL1^{GFPhi} cTECs (gate D) were dominant in the neonatal period, distinct mTEC subsets (gates A, B, C), which either lacked or expressed intermediate levels of CCRL1) [26], expanded during the first weeks of age and predominated in the young adult thymus (Fig. 4A). To determine the colony-precursor frequency within these detailed TEC subsets, we combined cell sorting, limiting dilutions in microscale clonogenic assays and high-content imaging microscopy. Given the clonal origin of TEC-derived colonies, we estimated the frequency of colony-forming cells by dividing the number of colonies by the number of sorted cells per well for each detailed subset (Fig. 4B). We observed that clonogenic activity was highly restricted to the CCRL1^{GFPhi} cTEC subset (gate D) at all time points analyzed (Fig. 4B). Furthermore, we noticed that the clonogenic potential of CCRL1^{GFP} cTECs gradually decreased from postnatal day 5 to

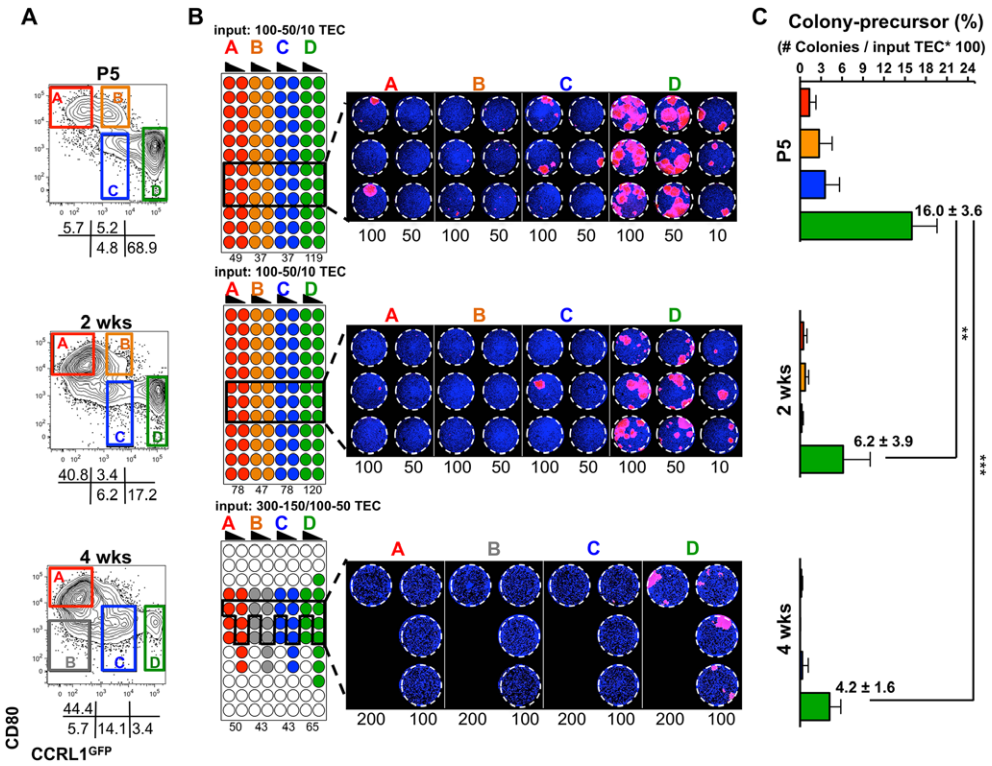

Figure 4. The pool of TEC colony-precursor cells residing within the postnatal cortex decreases during the transition from postnatal to adult life. (A) TECs from CCRL1^{GFP} reporter mice were analyzed by flow cytometry at indicated time-points for the expression of CCRL1^{GFP} and CD80. Proportions of indicated subsets are shown below the plots. **(B)** Colored TEC subsets (A-B-C-D) illustrated in (**A**) were purified by cell sorting and cultured in microscale clonogenic assay (96-well microplates) at designated cell densities (input: as represented on the top of the schematic plate). Numbers below each schematic plate represent the total amount of wells analyzed per subset (left). Representative images of full individual wells for each time point and TEC subset are shown (right). Number of plated cells (input) is shown below. 96-well plate cultures were fixed, stained with anti-cytokeratin 8 (K8) Ab and analyzed by high-content immunofluorescence microscopy. Data shown are representative of three to four experiments performed per time point. **(C)** Colony-precursor cell frequency (%) was estimated by dividing the number of colonies obtained by the number of seeded TEC (input) x 100. Data are shown as mean ± SEM of a pool of 5 (p5), 6 (2 wks) and 9 (4 wks) independent experiments. $^{**}p < 0.005$ $^{***}p < 0.001$, the two-tailed Mann–Whitney U test.

young adult thymus (Fig. 4C). To further evaluate the reduction in colony-forming potential of cTECs with time, we established competitive clonogenic assays with age-matched or age-mismatched cTECs isolated from Actin^{GFP} and Actin^{RFP} report mice. While co-culture experiments with cTEC^{ActinGFP} and cTEC^{ActinRFP} from postnatal day 5 thymus yielded a similar respective proportion of GFP$^+$ or RFP$^+$ *Clono*TECs, cTECs purified from postnatal day 5 thymus showed a marked clonogenic advantage over cTECs isolated from 2-week-old counterparts (Supporting Information Figure 4). Together, our findings suggest that TEP-like cells within cTECs autonomously lose the clonogenic capacity with the entry into the adulthood.

The clonogenic potential of TECs is sustained in alymphoid thymus

Just as TECs have a central function in T-cell development, thymocytes are in turn vital to TEC maturation [2]. Albeit lympho-epithelial interactions are often considered stimulatory to TEC differentiation, and in particular to the expansion of the mTEC network, we previously conjectured that signals provided by developing thymocytes might restrain functional properties coupled to immature TECs [2]. To determine whether the loss in clonogenic potential of cTECs was directly linked to thymocyte-driven TEC differentiation, we used *Rag2*$^{-/-}$*Il2rg*$^{-/-}$ CCRL1^{GFP}-reporter mice, in which T-cell development is profoundly blocked at early stage of development. Consequently, TEC maturation is severely arrested in these mice due the lack of maturation signals delivered by lymphoid cells. Specifically, apart of virtually lacking mature CD80$^+$ mTECs, *Rag2*$^{-/-}$*Il2rg*$^{-/-}$ thymus display a partial blockade in full CCRL1 and MHCII expression [26, 33] (Fig. 5A). We performed limiting dilution clonogenic assays (as described in Fig. 4) with TECs that either lack or express intermediate and higher levels of CCRL1 isolated from 2- and 6-week-old *Rag2*$^{-/-}$*Il2rg*$^{-/-}$ thymus. We found that the capacity to generate colonies was scattered among the three TEC subtypes in the 2-week-old thymus, progressively increasing within TECs expressing higher levels of CCRL1 (CCRL1^{GFPhi}) (Fig. 5B and C). Notably, the frequency of colony-precursor cells was sustained within the three TEC subsets in the 6-week-old *Rag2*$^{-/-}$*Il2rg*$^{-/-}$ thymus (Fig. 5C). The maintenance of the pool of cells with clonogenic capacity was also

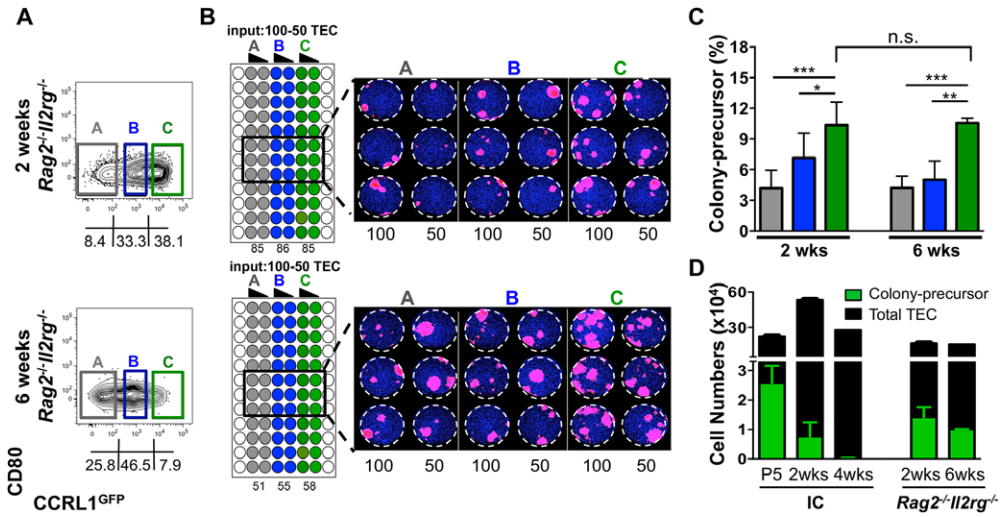

Figure 5. The pool of TEC colony-precursor cells is sustained in the adult *Rag2*$^{-/-}$*Il2rg*$^{-/-}$ thymus. (A) TECs from *Rag2*$^{-/-}$*Il2rg*$^{-/-}$ CCRL1^{GFP} mice were analyzed by flow cytometry at indicated time-points for the expression of CCRL1^{GFP} and CD80. Proportion of indicated subsets are shown below the plots. (B) Colored TEC subsets (A-B-C) illustrated in (A) were purified by cell sorting and cultured in microscale clonogenic assay (96-well microplates) at designated cell densities (input: as represented on the top of the schematic plate). Numbers below each schematic plate represent the total amount of wells analyzed per subset (left). Representative images of full individual wells for each time point and TEC subset are shown (right). Number of plated cells (input) is shown below. 96-well plate cultures were fixed, stained with anti-cytokeratin 8 (K8) Ab and analyzed using a high-content immunofluorescence microscopy. Data shown are representative of three to four experiments per time point. **(C)** Colony-precursor cell frequency (%) was estimated based on the number of colonies relatively to the number of seeded TECs (as in Fig. 4C). Data are shown as mean ± SEM of a pool of 6 (2 wks) and 4 (6 wks) independent experiments. $^{*}p<0.05$ $^{**}p<0.005$ $^{***}p<0.001$, the two-tailed Mann–Whitney U test. **(D)** Number of colony-precursor cells (green) within total TEC (black) for immunocompetent (IC) (Fig. 4) and *Rag2*$^{-/-}$*Il2rg*$^{-/-}$ (this figure) mice. The number of colony-precursor cell was estimated based on the frequency of these cells within the total TEC cellularity for a given time. IC: Data are shown as mean ± SEM of a pool of 3 (p5), 4 (2 weeks) and 3 (4 weeks) independent experiments; *Rag2*$^{-/-}$*Il2rg*$^{-/-}$: Data are shown as mean ± SEM of a pool of 3 (2 weeks) and 3 (6 weeks) independent experiments.

notorious when their absolute cellularity was extrapolated within the total number of TECs of the alymphoid thymi and longitudinally compared to their abundance in immunocompetent counterparts (Fig. 5D). These results indicate that thymocyte-derived signals might negatively affect the clonogenic potential of TECs during life.

Lympho-epithelial interactions control the clonogenic potential of TECs

To directly assess the influence of thymocyte-TEC crosstalk on TEC clonogenic capacity we reconstituted 6-week-old *Rag2*$^{-/-}$*Il2rg*$^{-/-}$ CCRL1-reporter mice with bone marrow (BM) precursors from WT mice and analyzed the frequency of colony-forming cells of recipient mice 6 weeks post-transplantation. As expected, the number of CD45^{+} cells increased and T-cell development was corrected in the thymus of WT BM-reconstituted *Rag2*$^{-/-}$*Il2rg*$^{-/-}$ CCRL1^{GFP}-reporter mice (data not shown), restoring the differentiation of CD80^{+} mTECs and the normal cTEC/mTEC segregation (Fig. 6A). The conditioning sub-lethal irradiation protocol prior to BM transplantation and age did not alter the clonogenic activity of TECs from 12-week-old non-reconstituted *Rag2*$^{-/-}$*Il2rg*$^{-/-}$ CCRL1^{GFP} -reporter mice (Fig. 6B and C), as the frequency of colony-forming cells in TECs that either lack or express intermediate and higher levels of CCRL1 was similar to the ones in unconditioned 6-week-old mice (Fig. 5C). Strikingly, the clonogenic potential of purified cortical/medullary subsets from WT BM-reconstituted *Rag2*$^{-/-}$*Il2rg*$^{-/-}$ CCRL1-reporter mice exhibited a notorious reduction and restriction to the CCRL1^{GFPhi} TEC subset (Fig. 6B and C), normalizing to the profile observed in young immunocompetent mice. Collectively, our findings demonstrate that continual thymic crosstalk negatively regulates TEC clonogenic activity.

Discussion

Comprehending the principles that underlie the maintenance of cortical and medullary thymic epithelial compartments is chief to harness thymopoiesis in the elderly and in patients with immunodeficiency disorders or autoimmunity. Therefore, the prospective isolation of TEPs within the adult thymus has emerged as a central objective in thymic biology, as it would provide means for reconstructing functionalized thymic epithelial microenvironments in therapies targeting thymus disorders. An aspect of equal importance that has been overlooked pertains to the principles that control the bioavailability and functionality of those progenitors in the adulthood. Given that TEC network expands vigorously during the period between birth and early adulthood, we centred our attention in this temporal window with the premise that it might reveal new insights on how TEP homeostasis is balanced in vivo.

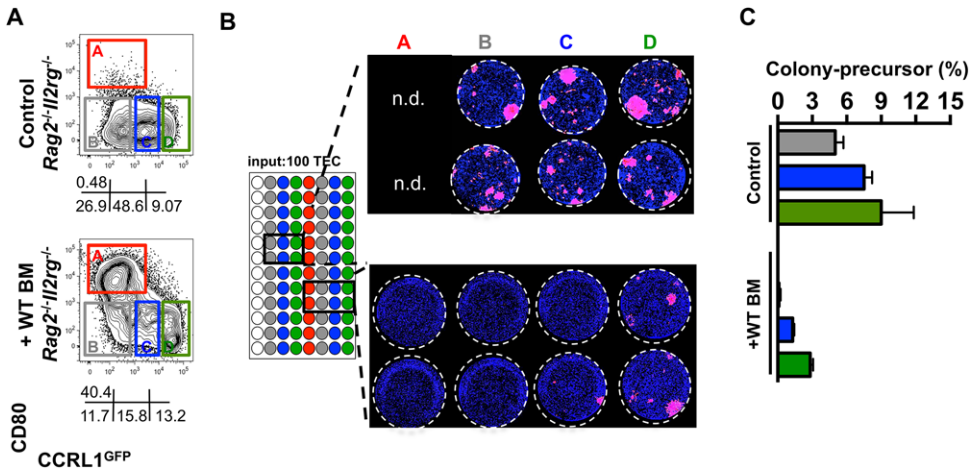

Figure 6. Thymocyte-derived signals negatively impact the pool of TEC colony-precursor cells. *Rag2*$^{-/-}$*Il2rg*$^{-/-}$ CCRL1^{GFP} mice were reconstituted with WT BM precursors (+WT BM) or left non-reconstituted (Control). **(A)** TECs from control and WT BM-reconstituted *Rag2*$^{-/-}$*Il2rg*$^{-/-}$ CCRL1^{GFP} mice were analyzed by flow cytometry for the expression of CCRL1^{GFP} and CD80. The proportion of indicated subsets is shown below the plots. **(B)** TEC subsets (A-B-C-D) illustrated in **(A)** were purified by cell sorting and cultured in microscale clonogenic assay (96-well microplates) at designated cell densities (input: as represented on the top of the schematic plate). Representative images of full individual wells for each time point and TEC subset (right). 96-well plate cultures were fixed, stained with anti-cytokeratin 8 (K8) Ab and analyzed using a high-content immunofluorescence microscopy. n.d. (not determined). Data are representative of two experiments. **(C)** Colony-precursor cell frequency (%) was estimated by dividing the number of colonies obtained by the number of seeded TEC (input) x 100. Data are shown as mean ± SEM of 3 control and 4 WT BM-reconstituted samples from a pool of two independent experiments.

Our temporal analysis of TEC clonogenic potential suggests that the postnatal life defines a period of intense stem cell-like activity within the thymic cortex, which gradually diminished thereafter with the entry into the adulthood as a result of lympho-epithelial interactions. These findings support the notion that the pool of TEPs and/or their replenish rate deteriorates across life, providing a possible explanation to their incapacity to sustain functional epithelial niches in the aged thymus.

Detailed phenotypic and molecular analyses show that in vitro-generated *Clono*TECs lacked traits that are typically associated with cortical or medullary lineages, but instead expressed markers linked to stem cells. These observations correlate with their reduced levels of Foxn1, which is central for the initiation and maintenance of the TEC program but appears dispensable for the maintenance of the thymic epithelial stem cell pool [7, 15, 34]. Using Foxn1^{eGFP} reporter thymus, we showed that *Clono*TECs derived from Foxn1-expressing cTEC lose Foxn1 expression in vitro, indicating that Foxn1 levels are tightly controlled by thymic microenvironmental factors. Nonetheless, our understanding on the molecular signals that initiate and sustain the expression of this master regulator of TEC identity in vivo requires further analysis. Importantly, the findings that a fraction of *Clono*TECs retains continual clonogenic potential in vitro and contain cells that can diversify into cTECs and mTECs in vivo reinforce their TEP-like signature. Still, the progeny of *Clono*TECs that reintegrated within thymic microenvironment was limited. Whether the low engraftment of *Clono*TECs is due to experimental impediments related to the establishment of organotypic cultures or competitive disadvantage relatively to embryonic TEP within RTOCs is unclear. For technical reasons related with the establishment of RTOCs, the proportion of *Clono*TECs within the hybrid RTOCs before thymic transplanting was reduced relatively to TECs derived from E14.5 "carrier" thymus (1:5-16:1). The abundance and/or competitive fitness of ex vivo embryonic TEC progenitors might under these conditions limit the integration, maintenance and the generation of a more prominent *Clono*TEC-derived progeny 4 weeks after transplantation. Moreover, and similarly to the capacity to continual establish colony-forming units, it is possible that only a fraction of *Clono*TECs developed within the ectopic thymus and contributed to the TEC network. Future studies should address the long-term maintenance of *Clono*TECs within native thymic niches. This technical limitation seems to be common to several studies using hybrid RTOCs, which are composed of predominant embryonic thymic stromal cells mixed with adult TEC subsets purportedly enriched with TEPs [15–17]. Furthermore, due to high cell density requirements to perform RTOC experiments, we used a pool of cTEC-derived *Clono*TECs from multiple colonies. This technical impediment has precluded testing the lineage potential of cTEC-derived *Clono*TECs from individual colonies or residual mTEC-derived *Clono*TECs. Despite phenotypic similarities at a population level, possible intra- and inter-clonal heterogeneity within *Clono*TECs might also influence their engraftment and lineage potential. Hence, it is possible that *Clono*TECs contain cTEC- and mTEC-producing cells. Nonetheless, *Clono*TECs were originally generated from cells with a prototypical cTEC features, suggesting that the cortical thymic epithelium compartment harbors cTEC and/or mTEC precursors. Future refined experimental setups are required to address these possibilities at the single cell level with the purported postnatal-derived TEC progenitors, as reported earlier with embryonic cells [6]. Furthermore, apart of

lineage tracing assays, it would be equally important to unravel whether postnatal-derived TEC progenitors can functionally contribute to thymopoiesis.

Using distinct experimental approaches, three recent reports have revealed the existence of TEC stem cell activity within the adult thymus. First, Ucar et al. reported the presence of EpCAM$^-$ Foxn1$^-$ cells within the thymic stroma that form under specialized in vitro culture system spheroids, so-called thymosphere, with the capacity to generate cTECs and mTECs [15]. We reason that cTECs with colony-forming capacity described in our report are distinct from thymosphere-generating cells. First, although the location of thymosphere-forming cell remains undetermined, *Clono*TECs arise from a fraction of cells belonging to the prototypical cTEC lineage (EpCAM$^+$Ly51$^+$CCRL1$^+$). Secondly, CD45$^-$EpCAM$^-$ thymic stromal cells failed to form *Clono*TEC-containing colonies in our experimental condition. Despite being hitherto phenotypically undistinguishable from cTECs lacking clonogenic activity, *Clono*TEC-generating cTECs might encompass a subset of progenitors cells nestling in the cortical compartment that have not completed the cTEC maturation program. In this regard, Wong et al. documented that bipotent TEPs exist within a fraction of UEA-1$^-$MHII^{lo} cTEC-like cells of the adult thymus [16] and Ulyanchenko et al. further mapped them to a fraction of Ly51$^+$MHCII^{hi}Plet1$^+$ cTECs [17], inferring in agreement with our results that TEPs share to some extent a cortical-associated signature. Along this line, genetic inducible cell-fate mapping studies by Ohigashi et al. and Mayer et al. found that a large fraction of adult cTECs and mTECs develop from fetal- and newborn-derived TECs expressing β5t [20, 21]. These findings suggest that TEC differentiation in the postnatal period follows a similar process to the one defined in the embryonic life [14], in which the cortex represents a reservoir of TEPs wherefrom they can potentially differentiate into cortical and medullary epithelial lineages. However, it remains to be elucidated whether cTEC-derived *Clono*TECs and other recently identified subsets enriched in TEP-like cells, contain truly bipotent progenitors or unipotent progenitors for each lineage. It is important to underline that even with the most refined subsets and distinct assays, TEC precursors are still being described at the population level, but are not yet recognized at the single-cell level. Albeit it is conceptually possible that several pools of TEP-like cells exist within the thymus, further studies are required to determine the lineage and temporal relationship between the distinct types of TEPs that are being disclosed within the postnatal thymus.

It remains unclear how TEC stem cell activity is controlled in the adult thymus. The incapacity of TEPs to undergo compensatory proliferation to maintain the mature TEC compartment [25] indicates a deficit in their stemness. The progenitor features of *Clono*TECs led us to use the colony-forming potential as a surrogate to survey the dynamics of TEP during early postnatal life and adulthood. Our findings indicate that clonogenic activity is predominantly enriched in cTECs during the first week of life. Previous observations showed that cTECs regenerate after the specific ablation of CCRL1^{hi} cTECs [35]. Nevertheless, the complete cTEC depletion was not achieved in this study and therefore resistant TEP within CCRL1-expressing subset might explain the observed regenerative capacity of cortical epithelium. The drop in the clonogenic activity of CCRL1^{hi} cTECs in the ensuing weeks might suggest that the bioavailable pool of TEPs is reduced with the entry into the adulthood. In this regard, the contribution of β5t$^+$ progenitors to cTEC and mTEC lineages declines postnatally [20, 21] and TEPs isolated from the adult thymus are extremely rare cells [15, 16, 20]. The maintenance of TEC clonogenic activity in 6- and 12-week-old alymphoid thymus suggests that aging is, not per se, a determinant in this process. In particular, we observed that clonogenic activity was enriched in CCRL1^{hi} cTEC-like subset of *Rag2*$^{-/-}$*Il2rg*$^{-/-}$ mice, indicating that TEPs might progress through, and settle within, the cortical lineage in a thymocyte-independent manner. In fact, bone marrow reconstitution experiments revealed that clonogenic potential is dynamically modulated by interactions with developing thymocytes. Similar observations were recently suggested to Cld3,4$^+$SSEA1$^+$ mTEC-restricted cells, which are rare in the adult thymus and enriched in *Rag2*$^{-/-}$ mice [23]. These findings provide evidence for a negative feedback mechanism in which continual thymic crosstalk fine-tunes the homeostasis of distinct TEPs. Thymocyte-derived signals are often considered stimulatory for TEC differentiation [1]. Nonetheless, previous studies, including from our group, have shown that thymocyte-TEC crosstalk negatively regulates functional attributes coupled to cTECs, including the expression of DLL4 and IL-7 [13, 36]. Now, our findings implicate that thymocyte-derived signals might act at the root of the TEC differentiation branch, deteriorating the pool of TEPs and possibly limiting their replenishment rate. It remains however opened whether these effects are mediated by direct or indirect lympho–epithelial interactions. These notions might provide a possible explanation to the failure in sustaining TEC compartments in the aged thymus [18] and the success of inducing cTEC and mTEC niches in WT BM-reconstituted adult mice that lacked previous functional lympho-epithelial crosstalk [33, 37]. Last, our data question whether the mere prospective isolation of bipotent progenitors from the adult and aged thymus represents the more desirable strategy for cellular replacement therapies in thymic disorders. Alternative approaches might focus in unraveling active mediators of stem cell activity, which will permit a more effective functionalization of TEPs isolated the adult thymus.

Materials and methods

Mice

Transgenic Actin reporter C57BL/6J mice in which the chicken β-actin promoter respectively drives enhanced Green Fluorescent Protein (eGFP) (Actin^{GFP}) or Red Fluorescent Protein (RFP) (Actin^{RFP}) expression were purchased from Jackson Laboratory. Ccrl1:eGFP (CCRL1^{GFP}) [35] and Foxn1^{eGFP} reporter mice [30] were kindly provided by Dr. Thomas Boehm (Germany). Ccrl1:eGFP (CCRL1^{GFP}) reporter mice were used as such or were backcrossed onto *Rag2*$^{-/-}$ *Il2rg*$^{-/-}$ [33] C57BL/6J background.

For thymic transplantation, 6-8-week-old C57BL/6J mice were used as recipients. Mice were housed under specific pathogen–free conditions and experiments were performed in accordance with institutional guidelines. For fetal studies, the day of vaginal plug detection was designated embryonic day (E) 0.5.

TEC Clonogenic assay

FACS sorted TECs were cultured onto a feeder layer of irradiated mouse embryonic NIH/3T3 (3T3) fibroblast cell line as described [27, 28]. 3T3 cells were regularly maintained in culture using Dulbecco-Vogt modification of Eagle's Medium (DMEM, Gibco–Invitrogen) supplemented with 10% fetal bovine serum (FBS) and penicillin/streptomycin. For the preparation of feeder layer, 3T3 cells were irradiated (60 Gy) one day before the experiment, seeded onto 6-well (midscale) or 96-well culture plates (microscale) coated with 0,05mg/mL of fibronectin (Sigma-Aldrich), at a density of 12.5×10^4 cells cm^{-2} or 5×10^4 cells per cm^{-2},respectively. TEC purified by cell sorting were directly cultured onto feeder layer in a specialized medium consisting of a 3:1 mixture of DMEM and Ham's F-12 medium (Gibco–Invitrogen), supplemented with 10% FBS, hydrocortisone 0.4 $\mu g\ mL^{-1}$, 10^{-6} M cholera toxin, 5 $\mu g\ mL^{-1}$ insulin, 2×10^{-9} M 3,3′,5-triiodo-L-thyronin (T3), 10 ng ml^{-1} recombinant human epidermal growth factor rhEGF, and penicillin/streptomycin (Peprotech). All cultures were performed at 37°C in a 7% CO_2 atmosphere for 12 days. Colonies were firstly revealed by hemacolor staining (Merck) according to the manufacturer's instructions or processed for flow cytometry or immunofluorescence microscopy analyses as described below.

TEC and *Clono*TEC isolation and flow cytometry analysis

TECs were isolated as described [13]. *Clono*TEC were recovered from clonogenic assays using 0.05% trypsin-EDTA (Gibco-Invitrogen), followed by cold PBS supplemented with 10% FBS to stop the reaction. Single-cell suspensions were stained with anti-Ly51 (PE) (BD Biosciences); anti-Sca-1 (BV785); anti-CD24 (BV510) and anti-EpCAM (BV421) (BioLegend); anti–I-A/I-E (Alexa 780); anti-CD45.2 (PerCP-Cy5.5); anti-CD40 (PE); anti-CD205 (biotin); UEA-1 (biotin); anti-CD80 (APC) and streptavidin (PE-Cy7) (eBioscience); anti-FOXN1 (Alexa 647) [38] was kindly provided by Dr. Hans-Reimer Rodewald (Germany). For intracellular staining, cells were fixed and permeabilised with the Transcription Factor Staining Buffer Set (eBioscience) according to the manufacture's instructions. Flow cytometry analysis was performed with the LSRFortessa instrument (BD Biosciences) and FlowJo software. Cell sorting was performed using the FACSAria II (BD Biosciences), with sort purities >95%.

Immunofluorescence analysis

Immunofluorescence staining was performed directly either on midscale and microscale clonogenic assays or on 8-μm sections of reaggregate thymic organ cultures (RTOCs) samples. Cultures or Thymus were fixed in 4% paraformaldehyde (Electron Microscopy Sciences) and stained with rabbit anti-GFP (Thermo Fisher Scientific), rat Troma-I (kindly provided by Drs. Brulet and Kemler), rat anti–I-A/I-E, rat anti-Aire, UEA1- or Ly51-biotinilated (eBioscience); and revealed with secondary Alexa Fluor 488 anti-rabbit, Alexa Fluor 647 anti-rat, or streptavidin Alexa 555 (Invitrogen). Nuclei were stained with DAPI (Invitrogen). Vectashield mounting medium (Vector Laboratories) was used to prepare the slides. Analysis was performed with IN Cell Analyzer 2000 (GE lifesciences) and collected images were processed with Fiji Software.

Gene expression

For quantitative PCR, mRNA from sorted cells was purified using the RNeasy Micro Kit (QIAGEN). RNA was reverse transcribed to cDNA, using the SuperScript III First-Strand Synthesis System for RT-PCR (Invitrogen) and Random Hexamers (Fermentas), and then subjected to real-time PCR using TaqMan Universal PCR Master Mix (Applied Biosystems) and primers for *18s*, *Foxn1*, *Il7*, *Psmb11*, *Tnfrsf11a*, *Aire, Kitl, Dll4, Cxcl12, Ccl25, Ccl19, Ccl21* (Applied Biosystems). All samples were analyzed as triplicates, and the $\Delta\Delta$Ct method was used to calculate relative levels of target mRNA compared with *18s*. Procedures were done according to the manufacturer's protocols. Real-time PCR was performed in an iCycler iQ5 Real-Time PCR thermocycler (Bio-Rad). Data were analyzed using iQ5 Optical System software (Bio-Rad).

RTOC

Freshly isolated E14.5 thymic lobes were used to establish RTOCs, as described [13]. Previous to aggregation, embryonic lobes were cultured for 3 days in DMEM supplemented with 10% FBS and 360mg/L 2-deoxyguanosine (dGuo) (Sigma-Aldrich). *Clono*TEC^{GFP+} were sorted to high purity (>95%). RTOCs were established from mixtures of 50,000–150,000 Actin^{GFP+} or Foxn1^{eGFP} –derived *Clono*TECs with E14.5 thymic cells at 1:16 to 1:5 ratios, and transplanted under the kidney capsule of WT mice. Ectopic thymus were recovered after 4 weeks of transplantation and analyzed by flow cytometry or immunohistochemistry.

Bone marrow chimeras

A total of 10^7 CD3-depleted bone marrow (BM) cells (MACS MicroBead, Miltenyi Biotec) from 6-week-old wild-type (WT) C57BL/6J donors were injected i.v. in 6-week-old sublethally irradiated (0.4Gy) *Rag2*$^{-/-}$ *Il2rg*$^{-/-}$ CCRL1-reporter mice.

Statistical analysis

Statistical analysis of the results was made using GraphPad Prism Software. The two-tailed Mann–Whitney U test was used for analysis between groups. A 95% confidence interval was applied in the calculations, and samples with p values < 0.05 were considered significant (*).

Acknowledgements: We thank Thomas Boehm (Max Planck Institute of Immunology and Epigenetics, Freiburg, Germany) for Foxn1^{eGFP} reporter mice. We thank Dr. Hans-Reimer Rodewald (German Cancer Research Center, Heidelberg, Germany) for the anti-Foxn1 antibody. We thank Dr. Leonor Araújo for technical support and Drs. Chiara Perrod and Gema Romera-Cardenas for critical reading the manuscript. We also thank Dr. Sofia Lamas and the caretakers from the animal facility for the assistance with animal experimentation.

C.M., A.R.R., and N.L.A. conceived and designed experiments, performed experiments, analyzed the data, and wrote the manuscript. P.M.R., R.D.P., and C.L. performed experiments and analyzed data. N.L.A. conceptualized the original idea.

This work has received funding from the European Research Council (ERC) under the European Union's Horizon 2020 research and innovation programme (grant agreement No 637843 - TEC_Pro), from FEDER - Fundo Europeu de Desenvolvimento Regional funds through the COMPETE 2020 - Operacional Programme for Competitiveness and Internationalisation (POCI), Portugal 2020, and by Portuguese funds through FCT - Fundação para a Ciência e a Tecnologia/Ministério da Ciência, Tecnologia e Ensino Superior in the framework of the project "Institute for Research and Innovation in Health Sciences" (POCI-01-0145-FEDER-007274) and FEDER funds through the Operational Competitiveness Programme – COMPETE and by National Funds through FCT – Fundação para a Ciência e a Tecnologia under the project FCOMP-01-0124-FEDER-021075 (PTDC/SAU-IMU/117057/2010). N.L.A., P.M.R., A.R.R., C.M., and R.D.P. are supported by the Investigator program, Post-doctoral and PhD fellowships from FCT (Portugal).

Conflict of interest: The authors declare no commercial or financial conflict of interest.

References

1 **Anderson, G. and Takahama, Y.**, Thymic epithelial cells: working class heroes for T cell development and repertoire selection. *Trends Immunol.* 2012. **33**: 256–263.

2 **Alves, N. L., Huntington, N. D., Rodewald, H. R. and Di Santo, J. P.**, Thymic epithelial cells: the multi-tasking framework of the T cell "cradle". *Trends Immunol.* 2009. **30**: 468–474.

3 **Boehm, T. and Swann, J. B.**, Thymus involution and regeneration: two sides of the same coin? *Nat. Rev. Immunol.* 2013. **13**: 831–838.

4 **Bennet, A. R., Farley, A., Blair, N. F., Gordon, J., Sharp, L. and Blackburn, C. C.**, Identification and characterization of thymic epithelial progenitor cells. *Immunity* 2002. **16**: 803–814.

5 **Gill, J., Malin, M., Hollander, G. A. and Boyd, R. L.**, Generation of a complete thymic microenvironment by MTS24(+) thymic epithelial cells. *Nat. Immunol.* 2002. **3**: 635–642.

6 **Rossi, S. W., Jenkinson, W. E., Anderson, G. and Jenkison, E. J.**, Clonal analysis reveals a common progenitor for thymic cortical and medullary epithelium. *Nature* 2006. **441**: 988–991.

7 **Bleul, C. C., Corbeaux, T., Reuter, A., Fisch, P., Monting, J. S. and Boehm, T.**, Formation of a functional thymus initiated by a postnatal epithelial progenitor cell. *Nature* 2006. **441**: 992–996.

8 **Rodewald, H. R., Paul, S., Haller, C., Bluethmann, H. and Blum, C.**, Thymus medulla consisting of epithelial islets each derived from a single progenitor. *Nature* 2001. **414**: 763–768.

9 **Hamazaki, Y., Fujita, H., Kobayashi, T., Choi, Y., Scott, H. S., Matsumoto, M. and Minato, N.**, Medullary thymic epithelial cells expressing Aire represent a unique lineage derived from cells expressing claudin. *Nat. Immunol.* 2007. **8**: 304–311.

10 **Gabler, J., Arnold, J. and Kyewski, B.**, Promiscuous gene expression and the developmental dynamics of medullary thymic epithelial cells. *Eur. J. Immunol.* 2007. **37**: 3363–3372.

11 **Ohigashi, I., Zuklys, S., Sakata, M., Mayer, C. E., Zhanybekova, S., Murata, S., Tanaka, S. et al.**, Aire-expressing thymic medullary epithelial cells originate from beta5t-expressing progenitor cells. *Proc. Natl. Acad. Sci. USA* 2013. **110**: 9885–9890.

12 **Baik, S., Jenkinson, E. J., Lane, P. J., Anderson, G. and Jenkinson, W. E.**, Generation of both cortical and Aire(+) medullary thymic epithelial compartments from CD205(+) progenitors. *Eur. J. Immunol.* 2013. **43**: 589–594.

13 **Ribeiro, A. R., Rodrigues, P. M., Meireles, C., Di Santo, J. P. and Alves, N. L.**, Thymocyte selection regulates the homeostasis of IL-7-expressing thymic cortical epithelial cells in vivo. *J. Immunol.* 2013. **191**: 1200–1209.

14 **Alves, N. L., Takahama, Y., Ohigashi, I., Ribeiro, A. R., Baik, S., Anderson, G. and Jenkinson, W. E.**, Serial progression of cortical and medullary thymic epithelial microenvironments. *Eur. J. Immunol.* 2014. **44**: 16–22.

15 **Ucar, A., Ucar, O., Klug, P., Matt, S., Brunk, F., Hofmann, T. G. and Kyewski, B.**, Adult thymus contains FoxN1(-) epithelial stem cells that are bipotent for medullary and cortical thymic epithelial lineages. *Immunity* 2014. **41**: 257–269.

16 **Wong, K., Lister, N. L., Barsanti, M., Lim, J. M., Hammet, M. V., Khong, D. M., Siatskas, C. et al.**, Multilineage potential and self-renewal define an epithelial progenitor cell population in the adult thymus. *Cell Rep.* 2014. **8**: 1198–1209.

17 **Ulyanchenko, S., O'neill, K. E., Medley, T., Farley, A. M., Vaidya, H. J., Cook, A. M., Blair, N. F. et al.**, Identification of a Bipotent Epithelial Progenitor Population in the Adult Thymus. *Cell Rep.* 2016. **14**: 2819–2832.

18 **Gray, D. H., Seach, N., Ueno, T., Milton, M. K., Liston, A., Lew, A. M., Goodnow, C. C. et al.**, Developmental kinetics, turnover, and stimulatory capacity of thymic epithelial cells. *Blood* 2006. **108**: 3777–3785.

19 **Nishikawa, Y., Nishijima, H., Matsumoto, M., Morimoto, J., Hirota, F., Takashi, S., Luche, H. et al.**, Temporal lineage tracing of Aire-expressing

cells reveals a requirement for Aire in their maturation program. *J. Immunol.* 2014. **192**: 2585–2592.

20 **Ohigashi, I., Zuklys, S., Sakata, M., Mayer, C. E., Hamazaki, Y., Minato, N., Hollander, G. A. et al.**, Adult thymic medullary epithelium is maintained and regenerated by lineage-restricted cells rather than bipotent progenitors. *Cell Rep.* 2015. **13**: 1432–1443.

21 **Mayer, C. E., Zuklys, S., Zhanybekova, S., Ohigashi, I., The, H. Y., Sansom, S. N., Shikama-Dorn, N. et al.**, Dynamic spatio-temporal contribution of single beta5t+ cortical epithelial precursors to the thymus medulla. *Eur. J. Immunol.* 2016. **46**: 847–856.

22 **Baik, S., Sekai, M., Hamazaki, Y., Jenkinson, W. E. and Anderson, G.**, Relb acts downstream of medullary thymic epithelial stem cells and is essential for the emergence of RANK medullary epithelial progenitors. *Eur. J. Immunol.* 2016. **46**: 857–862.

23 **Sekai, M., Hamazaki, Y. and Minato, N.**, Medullary thymic epithelial stem cells maintain a functional thymus to ensure lifelong central T cell tolerance. *Immunity* 2014. **41**: 753–761.

24 **Onder, L., Nindl, V., Scandella, E., Chai, Q., Cheng, H. W., Caviezel-Firner, S., Novkovic, M. et al.**, Alternative NF-kappaB signaling regulates mTEC differentiation from podoplanin-expressing presursors in the corticomedullary junction. *Eur. J. Immunol.* 2015. **45**: 2218–2231.

25 **Jenkinson, W. E., Bacon, A., White, A. J., Anderson, G. and Jenkinson, E. J.**, An epithelial progenitor pool regulates thymus growth. *J. Immunol.* 2008. **181**: 6101–6108.

26 **Ribeiro, A. R., Meireles, C., Rodrigues, P. M. and Alves, N. L.**, Intermediate expression of CCRL1 reveals novel subpopulations of medullary thymic epithelial cells that emerge in the postnatal thymus. *Eur. J. Immunol.* 2014. **44**: 2918–2924.

27 **Senoo, M., Pinto, F., Crum, C. P. and Mckeon, F.**, p63 Is essential for the proliferative potential of stem cells in stratified epithelia. *Cell* 2007. **129**: 523–536.

28 **Bonfanti, P., Claudinot, S., Amici, A. W., Farley, A., Blackburn, C. C. and Barrandon, Y.**, Microenvironmental reprogramming of thymic epithelial cells to skin multipotent stem cells. *Nature* 2010. **466**: 978–982.

29 **Klug, D. B., Carter, C., Crouch, E., Roop, D., Conti, C. J. and Richie, R.**, Interdependence of cortical thymic epithelial cell differentiation and T-lineage commitment. *Proc. Natl. Acad. Sci. U S A* 1998. **95**: 11822–11827.

30 **Terszowski, G., Muller, S. M., Bleul, C. C., Blum, C., Schirmbeck, R., Reimann, J., Pasquier, L. D. et al.**, Evidence for a functional second thymus in mice. *Science* 2006. **312**, 284–287.

31 **Shackleton, M., Vaillant, F., Simpson, K. J., Stingl, J., Smyth, G. K., Asselin-Labat, M. L., Wu, L. et al.**, Generation of a functional mammary gland from a single stem cell. *Nature* 2006. **439**: 84–88.

32 **Mcqualter, J. L., Yuen, K., Williams, B. and Bertoncello, I.**, Evidence of an epithelial stem/progenitor cell hierarchy in the adult mouse lung. *Proc. Natl. Acad. Sci. U S A* 2010. **107**: 1414–1419.

33 **Alves, N. L., Huntington, N. D., Mention, J. J., Richard-Le Goff, O. and Di Santo, J. P.**, Cutting Edge: a thymocyte-thymic epithelial cell cross-talk dynamically regulates intrathymic IL-7 expression in vivo. *J. Immunol.* 2010. **184**: 5949–5953.

34 **Nowell, C. S., Bredenkamp, N., Tetelin, S., Jin, X., Tischner, C., Vaidya, H., Sheridan, J. M. et al.**, Foxn1 regulates lineage progression in cortical and medullary thymic epithelial cells but is dispensable for medullary sublineage divergence. *PLoS Genet.* 2011. **7**: e1002348.

35 **Rode, I. and Boehm, T.**, Regenerative capacity of adult cortical thymic epithelial cells. *Proc. Natl. Acad. Sci. U S A* 2012. **109**: 3463–3468.

36 **Fiorini, E., Ferrero, I., Merck, E., Favre, S., Pierres, M., Luther, S. A. and Macdonald, H. R.**, Cutting edge: thymic crosstalk regulates delta-like 4 expression on cortical epithelial cells. *J. Immunol.* 2008. **181**: 8199–8203.

37 **Roberts, N. A., Desanti, G. E., Withers, D. R., Scott, H. R., Jenkinson, W. E., Lane, P. J., Jenkison, E. J. et al.**, Absence of thymus crosstalk in the fetus does not preclude hematopoietic induction of a functional thymus in the adult. *Eur. J. Immunol.* 2009. **39**: 2395–2402.

38 **Rode, I., Martins, V. C., Kubleck, G., Maltry, N., Tessmer, C. and Rodewald, H. R.**, Foxn1 protein expression in the developing, aging, and regenerating thymus. *J. Immunol.* 2015. **195**: 5678–5687.

Abbreviations: **Aire**: Auto-immune regulator · **CCRL1**: Chemokine (C-C motif) receptor-like 1 · **CMJ**: cortico-medullary junction · **cTEC**: cortical TEC · **dGUO**: deoxyguanosine · **EpCAM**: Epithelial cell adhesion molecule · **LTβR**: Lymphotoxin eta receptor · **MHC**: Major Histocompatibility Complex · **mTEC**: medullary TECs · **RANK**: Receptor activator of NF-κB · **RTOC**: reaggregate thymic organ culture · **TCR**: T cell receptor · **TEC**: Thymic epithelial cell · **TEP**: Thymic Epithelial Progenitor · **WT**: wild-type

Full correspondence: Dr. Nuno L. Alves, Instituto de Investigação e Inovação em Saúde (**I3S**), Instituto de Biologia Molecular e Celular (**IBMC**), Rua Alfredo Allen, 4200-135 Porto
e-mail: nalves@ibmc.up.pt

Received: 3/1/2017
Revised: 24/2/2017
Accepted: 14/3/2017
Accepted article online: 20/3/2017

